THE FUNCTIONAL ANALYSIS OF MITOCHONDRIAL FISSION ADAPTORS IN YEAST AND HUMAN

by

Qian Guo

A dissertation submitted to the faculty of
The University of Utah
in partial fulfillment of the requirements for the degree of

Doctor of Philosophy

Department of Biochemistry

The University of Utah

December 2012

The University of Utah Graduate School

STATEMENT OF DISSERTATION APPROVAL

The dissertation of **Qian Guo**

has been approved by the following supervisory committee members:

Janet M. Shaw	, Chair	**10/22/2012** Date Approved
Markus Babst	, Member	**10/22/2012** Date Approved
Michael S. Kay	, Member	**10/22/2012** Date Approved
Jared Rutter	, Member	**10/22/2012** Date Approved
Dennis R. Winge	, Member	**10/22/2012** Date Approved

and by **Wesley I. Sundquist and Christopher P. Hill**, Chair of the Department of **Biochemistry**

and by Charles A. Wight, Dean of The Graduate School.

ABSTRACT

The mitochondrion is an essential organelle in eukaryotic cells and organisms. This compartment is responsible for many important cellular activities. In many cell types, healthy mitochondria are branched and form tubular networks that spread evenly throughout the cytoplasm. The balance of mitochondrial fission, fusion and movement is required to maintain this morphology and proper mitochondrial functions. Recent studies suggest that disruption of mitochondria dynamics is associated with metabolic and neurodegenerative diseases. This dissertation interrogates the function of mitochondrial fission adaptors using *Saccharomyces cerevisiae* as a model system and research tool.

Mitochondrial fission is mediated by protein complexes that encircle and divide mitochondrial tubules. In budding yeast, fission requires the membrane-anchored protein Fis1 and the dynamin-related GTPase Dnm1. Dnm1 is recruited to mitochondria via interactions with the adaptor proteins Caf4 and Mdv1, which bind directly to the mitochondrial outer membrane protein Fis1. Unlike Mdv1, a function for Caf4 in fission has not been established. In Chapter 2, I demonstrate that Caf4 is a bona fide adaptor that assembles at mitochondrial division sites. Fission complexes may contain Caf4 alone or both Caf4 and Mdv1 without compromising fission function. Furthermore, despite correspondence between Caf4 and Mdv1 expression levels, functional and phylogenetic

analyses indicate that Caf4 mitochondrial fission activity has diverged from that of Mdv1.

In mammals, mitochondrial fission is mediated by the dynamin-related GTPase Drp1, which is recruited to mitochondrial surface by additional membrane-associated adaptor proteins (hFis1, Mff and MiDs). In Chapter 3, a yeast strain lacking all fission proteins is used to identify whether these adaptors is able to participate in both membrane scission and GTPase recruitment. While hFis1 is dispensable for fission, membrane-anchored Mff or MiDs paired with Drp1 are sufficient to divide mitochondria. In addition, Drp1 coassembled with MiDs in vitro forms a heteropolymer that alters Drp1 homopolymer structure with a narrower diameter. It is the first demonstration that an adaptor protein alters the architecture of a mitochondrial dynamin GTPase polymer in a manner that could facilitate membrane constriction and severing activity. Altogether, these studies advance our understanding of the multiple adaptors that function in yeast and mammalian mitochondrial fission complexes.

TABLE OF CONTENTS

LIST OF FIGURES

Figure

LIST OF TABLES

Table

CHAPTER 1

INTRODUCTION

The mitochondrion

The mitochondrion is a double-membrane organelle that only exists in eukaryotes. The origin of this organelle can be traced back to a single ancestor, the α-proteobacterium, that entered a eukaryotic cell and established itself as an endosymbiont (Gray et al., 1999). As the descendent of an independent organism, the mitochondrion contains its own chromosome and protein synthetic machinery (Henze and Martin, 2003). Mitochondrial biogenesis depends on the growth and division of the existing organelle and transport of a portion of the mitochondrion to the daughter cell during division (McConnell et al., 1990).

Mitochondria have two membranes, an outer membrane (OM) and an inner membrane (IM), which enclose the intermembrane space (IMS) and matrix, respectively (Palade, 1953). The matrix houses the mitochondrial genome (mtDNA), mitochondrial ribosomes and the majority of mitochondrial proteins (Okamoto and Shaw, 2005; Williamson and Fennell, 1979). The mtDNA encodes RNAs and proteins that are required for mitochondrial protein synthesis, oxidative phosphorylation and ATP production (Alberts, 2002). The surface area of the inner membrane is larger than that of the outer membrane. Consequently, the inner membrane forms folds called cristae, which contain the multisubunit respiratory complexes. ATP production depends on the proton gradient potential across the inner membrane. The intermembrane space lies between the outer and inner mitochondrial membrane and contains ions that are similar to those in the cytoplasm but not the matrix. This is due to the fact that the outer membrane contains channels formed by porin, which allow small molecules to travel between the cytoplasm and the intermembrane space.

The mitochondrion has been named the ‘power house’ of the cell due to its ability to combine oxygen with the breakdown products of glucose and fatty acids to generate ATP (Andersson et al., 2003). Mitochondria also have roles in fatty-acid β oxidation, amino acid and lipid biosynthesis, steroid generation and calcium signaling (Attardi and Schatz, 1988). In recent years, mitochondrial dynamics has become the focus of much research in the field (McBride et al., 2006). In addition, new findings indicate that mitochondrial dysfunction is linked to several neurodegenerative diseases (Costa et al., 2010; Manczak et al., 2011; Nakamura et al., 2011).

Mitochondrial dynamics

Mitochondria were first described as bean-shaped, double-membraned organelles by high-resolution electron microscopy (Palade, 1953). It was also reported that mitochondria undergo frequent changes in shape and distribution (Lewis and Lewis, 1914). However, it was the use of fluorescent probes and real-time imaging that allowed researchers to recognize that mitochondria are very dynamic structures, forming interconnected tubular networks or individual, small rods or spheres, depending on the cell type. These studies also revealed that mitochondrial morphology and distribution are regulated by a combination of fission, fusion and directed organelle movement. All three processes are critical to maintain proper mitochondrial function(Okamoto and Shaw, 2005).

Mitochondrial fission

An increase in mitochondrial copy number requires an increase in mitochondrial biomass followed by mitochondrial fission. These fission events increase the number of mitochondria in a cell and decrease the size of each unit. Decreasing mitochondrial size facilitates mitochondrial movement over long distances (i.e., down neuronal axons) and mitochondrial partitioning during division(Gorsich and Shaw, 2004; Li et al., 2004; Pilling et al., 2006; Taguchi et al., 2007). Generally, successful mitochondrial fission requires two types of proteins, a membrane-anchoring protein and a mitochondrial dynamin-related protein (Chan, 2012). In some cases, the recruitment also involves an adaptor protein that links the anchor to the dynamin. One end of the membrane-anchoring protein is embedded in the outer membrane while the rest of the protein forms a cytoplasmic platform for recruitment of the dynamin-related protein (Okamoto and Shaw, 2005). The mitochondrial dynamin-related protein is a GTPase that self-oligomerizes to form spirals around the mitochondrial tubule at the potential fission site (Ingerman et al., 2005; Sesaki and Jensen, 1999). GTP hydrolysis promotes conformational changes in the mitochondrial dynamin and reduces the diameter of the dynamin ring (Legesse-Miller et al., 2003). The resulting constriction is believed to be the force that completes mitochondrial fission. The exact molecular mechanism by which the mitochondrial dynamin severs the mitochondrial compartment is not clear.

When mitochondrial division is properly regulated, the mtDNA, RNAs and proteins contained in the organelle are distributed between two compartments (Rapaport et al., 1998). However, mtDNA, RNAs and proteins are not always distributed evenly. It has been reported that the mitochondrial membrane potential is lower in some

mitochondria after division, presumably because the mtDNA and/or other organelle components have been damaged (Kim et al., 2007; Lyamzaev et al., 2004). These mitochondria are less functional and are removed by a process of selective degradation called mitophagy (Gomes et al., 2011; Rambold et al., 2011; Twig et al., 2008). Excessive fission is also damaging and can cause loss of mtDNA and mitochondrial dysfunction (Rapaport et al., 1998). Suppression of fission triggers mitochondria to form interconnected nets in yeast and continuous tubules in mammalian cells, which alters mitochondrial mobility and can cause defects in cell division (Gorsich and Shaw, 2004; Okamoto and Shaw, 2005; Taguchi et al., 2007).

Mitochondrial fusion

In an early report, Lewis and Lewis stated "… we find in the living that granules can be seen to fuse together into rods or chains, and these to elongate into threads, which in turn anastomose with each other and may unite into a complicated network…" (Lewis and Lewis, 1914). We now know that Lewis was observing mitochondrial fusion events, which increase organelle size and allow mitochondrial content mixing and exchange (Azpiroz and Butow, 1993; Nunnari et al., 1997; Rambold et al., 2011). The fusion process starts with membrane docking followed by outer membrane fusion and then inner membrane fusion (Okamoto and Shaw, 2005).

Fzo1 is a GTPase that is required for mitochondrial outer membrane fusion in yeast (Hoppins et al., 2007; Rapaport et al., 1998). Fzo1 is embedded in the outer membrane through its C-terminal membrane anchor. Ugo1 also resides on the mitochondria outer membrane with its N-terminus in the cytoplasm and its C-terminus in

the intermembrane space (Sesaki and Jensen, 2001). Ugo1 contains motifs that are similar to mitochondrial carrier proteins in the inner membrane. However, instead of functioning as a carrier protein, Ugo1 binds to Fzo1. It has been reported that in the presence of GTP, Fzo1 dimerizes and forms Ugo1 promoted oligomers on adjacent mitochondria, which induces mitochondrial tethering (Anton et al., 2011). After GTP hydrolysis, the F-box protein Mdm30 is thought to promote Fzo1 complex ubiquitylation and degradation to complete MOM fusion (Cohen et al., 2011). A second GTPase, Mgm1, functions on the inner membrane to both promote fusion and maintain cristae folds. Mgm1 has both long and short isoforms (l-Mgm1 and s-Mgm1) (Detmer and Chan, 2007). The N-terminus of l-Mgm1 is anchored to the inner membrane facing the intermembrane space (Sesaki et al., 2003). Protease cleavage produces s-Mgm1, which also resides the intermembrane space (Herlan et al., 2003). A study indicated that l-Mgm1 provides a structural role, while s-Mgm1 utilizes its GTPase activity to mediate inner membrane fusion (Abutbul-Ionita et al., 2012). An independent study suggested that s-Mgm1 is able to tether opposing inner membranes and undergoes conformational changes that could potentially promote inner membrane fusion (Zick et al., 2009).

In mammals including humans, there are two Fzo1 homologs, Mfn1 and Mfn2, which form homo-oligomeric or hetero-oligomeric complexes to tether adjacent mitochondrial outer membranes (Chan, 2012; Chen et al., 2005; Chen et al., 2003). In vitro studies have led to the suggestion that a conformational change driven by GTP hydrolysis is necessary to complete membrane fusion (Ishihara et al., 2004; Koshiba et al., 2004). Functional disruption of the mammalian Mgm1 homolog, Opa1, does not affect mitochondrial outer membrane fusion but causes severe inner membrane fusion defects,

suggesting that the function of the Mgm1/Opa1 GTPases in inner membrane fusion is conserved (Song et al., 2009).

Movement

Time-lapse microscopy studies reveal that mitochondria travel within the cell cytoplasm (Li et al., 2004; Pilling et al., 2006). There are two types of movement, anterograde movement (away from the nucleus) and retrograde movement (toward the nucleus) (Frederick and Shaw, 2007). In many mammalian cell types, mitochondrial movement is dependent on microtubules. Anterograde movement is facilitated by Kinesin-1, a motor protein that forms complexes with an adaptor protein called Milton (Fransson et al., 2006; Gorska-Andrzejak et al., 2003). This complex interacts with a mitochondrial membrane-anchored GTPase called Miro (Fransson et al., 2006). Retrograde movement, on the other hand, is performed by a dynein motor. Although it is not yet clear, retrograde transport may also require Miro to attach dynein to mitochondria as well (Russo et al., 2009). The situation is different in some yeast and plants, where mitochondria move along actin filaments using a myosin motor protein instead (Fehrenbacher et al., 2004; Zheng et al., 2009).

In mammalian cells, mitochondrial movement is particularly important during cell division due to the fact that mitochondria cannot be synthesized *de novo* and must be generated from existing organelles in the mother cell (McConnell et al., 1990). Additionally, the size and functional status of the organelle appears to be a factor affecting mitochondrial movement (Campello et al., 2006; Chen et al., 2003; Hollenbeck and Saxton, 2005; Li et al., 2004; Verstreken et al., 2005). For example, a highly

polarized cell like a neuron has a long axon extension connecting the cell body to the synaptic terminal. Different parts of the neuron have distinct needs for ATP and other mitochondrial functions. Transport of mitochondria from the cell body to the nerve terminal enables nerve cells to perform their normal functions in synaptic vesicle release and recycling. Mitochondria that are smaller in size must be generated by fission from the tubular network in the cell body before they can be moved down the axon to the synapse (Chen et al., 2003; Li et al., 2004; Verstreken et al., 2005). Conversely, damaged mitochondria are moved toward the cell body where they can potentially fuse with other mitochondria or be degraded via mitophagy (Miller and Sheetz, 2004). Mitochondrial movement is also important in cells that divide asymmetrically like the budding yeast Sacc*haromyces cerevisiae*. In this case, mitochondria from the mother cell move along polarized actin filaments to the bud (anterograde) via the actin-based motor protein Myo2 (Bretscher, 2003). Mmr1 (a mitochondrial outer membrane protein) together with Ypt11 (a Rab-like GTPase) function as Myo2 adaptors that link mitochondria to Myo2 for movement on actin (Itoh et al., 2004; Itoh et al., 2002). Consistent with this idea, over expression of Mmr1 and Ypt11 drives excess mitochondria into buds (Frederick et al., 2008).

Mitochondrial fission in yeast

S. cerevisiae is an ideal model organism to explore biological and physiological processes. The cells of most organisms are not able to survive when mtDNA is mutated or lost because there is not enough ATP synthesized in the absence of oxidative phosphorylation. However, yeast cells that retain a mitochondrial compartment but lose

mtDNA are still able to propagate when provided with a fermentable carbon source such as glucose. As a result, even yeast with severe defects in mitochondrial size, number, movement and function can be studied. Moreover, conditional alleles can be generated that allow the study of essential genes and proteins that is necessary for mitochondrial dynamics.

Mitochondria in yeast form a tubular network that is located close to the plasma membrane and extends throughout the cell (Okamoto and Shaw, 2005). This network is constantly undergoing fission and fusion events. Mutations in genes required for fission cause a distinctive defect in mitochondrial morphology. When fission is blocked, fusion continues and mitochondria form an interconnected often net-like organelle that often collapses to one side of the cell (Bleazard et al., 1999; Otsuga et al., 1998; Sesaki and Jensen, 1999). Aside from the mitochondrial morphology defect, mitotically dividing haploid and diploid fission mutants seem very healthy. These cells grow at rates that are similar to wild-type cells and display normal respiratory activity. In addition, the net-like mitochondria are shuttled to daughter cells efficiently. When fission is blocked in diploid cells undergoing sporulation, however, mitochondria are not always distributed into all four meiotic progeny, resulting in nonviable spores (Gorsich and Shaw, 2004). Thus, mitochondrial fission is required for yeast fitness in the wild where sporulation is a necessary part of the life cycle.

Yeast fission proteins

There are four known proteins that function in yeast mitochondrial fission, Fis1, Mdv1, Caf4 and Dnm1. These proteins coassemble on the mitochondrial outer membrane

where they form complexes that divide mitochondrial tubules (Okamoto and Shaw, 2005). Fis1 (fission protein) is a membrane-anchor protein (Mozdy et al., 2000). It has a C-terminal trans-membrane domain that inserts into the outer mitochondrial membrane and an N-terminal TPR-like (tetratricopeptide repeat) domain exposed to the cytoplasm (Suzuki et al., 2005). Fis1 is uniformly localized on the mitochondrial surface. When Fis1 is expressed without its transmembrane segment, the TPR domain of the protein relocalizes to the cytoplasm and can no longer mediate fission. Structural studies show that the Fis1 TPR domain contains a hydrophobic concave groove (Suzuki et al., 2005; Zhang and Chan, 2007; Zhang et al., 2012). Mutations in this groove disrupt assembly of fission complexes (Karren et al., 2005).

Dnm1 is a dynamin-related protein that assembles from the cytoplasm into punctate structures on the mitochondrial surface (Bleazard et al., 1999; Mozdy et al., 2000; Otsuga et al., 1998). In time-lapse imaging studies, some of these structures are located at sites where mitochondrial fission occurs. Classical dynamin and dynamin-related proteins are large GTPases that participate in many different membrane-remodeling processes (Praefcke and McMahon, 2004). During endocytosis, classical dynamin functions to sever the necks of clathrin coated pits at the plasma membrane and release clathrin-coated vesicles. Dynamin has six domains, a GTPase domain, a middle domain, a PH (Pleckstrin-homology) domain, a GED (GTPase effector domain) domain and a PRD (prolin-rich domain) domain. Studies show that all of these domains are crucial for dynamin function. Cryo-EM and crystal structures indicate that dynamin-GTP is recruited to the membrane of liposomes by binding of its PH domain directly to lipids in the bilayer (Faelber et al., 2011; Ford et al., 2011; Mears et al., 2007). The recuited

dynamin self-assembles into spirals that encircle the neck of the clathrin-coated pit. GTP hydrolysis causes conformational changes in the dynamin spiral that constrict and sever the membrane. In vitro studies confirmed that dynamin is sufficient to constrict and sever membranes, although this process is likely regulated by additional accessory proteins in vivo. Similar to dynamin, yeast Dnm1 contains an N-terminal GTPase domain, a middle domain and a C-terminal GED. In Dnm1, the PH domain is replaced by the Insert B domain, and the PRD is absent. Cryo-EM study suggests that, like dynamin, Dnm1 also forms a spiral that tubulates liposomes. Upon GTP binding and hydrolysis, the diameter of the Dnm1 spiral inner lumen decreases from ~80 nm to ~25 nm. Dnm1 spirals dissemble after GTP hydrolysis (Mears et al., 2010). Although the two proteins share common properties, there are some differences. Unlike dynamin, the Dnm1 structure appears to form via a 'two-start' helix, which results in a larger Dnm1 spiral with different spacing (pitch) between the rungs of the spiral. In contrast to dynamin, which directly contacts the lipid bilayer, there is a gap between the Dnm1 spiral and the lipid surface. This finding suggests that Dnm1 may not interact with lipid.

Recruitment of Dnm1 onto the mitochondrial surface requires an adaptor protein called Mdv1, which bridges the interaction between Fis1 and Dnm1 (Cerveny and Jensen, 2003; Cerveny et al., 2001; Mozdy et al., 2000; Naylor et al., 2006; Tieu and Nunnari, 2000; Tieu et al., 2002). Mdv1 (mitochondrial division) contains an N-terminal extension (NTE), a coiled-coil domain (CC) and a C-terminal WD40 domain (WD40) predicted to form a beta-propeller. Fluorescence microscopy studies showed two localization patterns for Mdv1. First, the protein localized uniformly on the mitochondrial surface because of its interaction with Fis1. Second, Mdv1 also formed puncta on the surface of

mitochondrial tubules that colocalized with Dnm1. Although it has not been clearly demonstrated, these puncta are thought to be co-assemblies of Mdv1 and Dnm1 in the spirals that surround mitochondrial tubules.

Structural studies indicated that the NTE of Mdv1 forms a clamp around the outer surface of the Fis1 TPR domain (Zhang and Chan, 2007). In addition, a study by Koirala et al. showed that Mdv1 forms a dimer via a long, antiparallel coiled-coil in the middle of the protein (Koirala et al., 2010). A subsequent co-structure revealed that the antiparallel coiled-coil domain of Mdv1 sits on top of, and interacts with, residues in the adjacent Fis1 TPR domain (Zhang et al., 2012). Thus, this complex on the mitochondrial outer membrane consists of two Fis1 molecules bound to one Mdv1 dimer. The two predicted beta-propeller domains that extend into the cytoplasm beyond the coiled-coil are responsible for binding and recruiting Dnm1.

An affinity purification performed by Griffin et al. identified an Mdv1 paralog in yeast called Caf4 (Griffin et al., 2005). Caf4 domain structure is similar to that of Mdv1. Like Mdv1, Caf4 has been shown to interact with Fis1 via its NTE domain, is predicted to dimerize via its central coiled-coiled domain, and interacts with Dnm1 through its predicted beta-propeller domain (Griffin et al., 2005; Koirala et al., 2010). Based on these similarities, it was anticipated that Caf4 would also play a major role in mitochondrial fission. Surprisingly, however, mitochondrial fission was nearly normal when Caf4 was absent, although loss of both Caf4 and Mdv1 caused more severe fission defects than loss of Mdv1 alone. These findings led to speculation that Caf4 was either not involved in mitochondrial fission, performed a minor regulatory role in fission or was required for fission under certain physiological conditions. Interestingly, homologs of Mdv1 and Caf4

have only been found in fungi, and the amino acid sequences and predicted structures of fission adaptors in mammals and plants are unrelated to Mdv1 and Caf4.

Fission complex assembly

The current working model for fission complex assembly comes from a combination of genetic, cellular, biochemical and structural studies. On the outer mitochondrial membrane, the Fis1-Mdv1 complex provides a landing platform for the pool of Dnm1 dimers in the cytoplasm (Bhar et al., 2006). Mdv1 and Dnm1 are both cytosolic when Fis1 is absent (Mozdy et al., 2000; Tieu et al., 2002), consistent with the idea that Fis1 acts as the membrane anchor. When Dnm1 adaptor is absent, Fis1 still localizes to the membrane, but Dnm1 remains in the cytoplasm (Cerveny and Jensen, 2003; Tieu et al., 2002). Mutations that disrupt the binding of the Mdv1 NTE domain to the Fis1 TPR domain inhibit Mdv1 recruitment, which not only reduces Mdv1 mitochondrial localization but also causes Dnm1 puncta to disperse into the cytoplasm (Karren et al., 2005). Yeast two hybrid (Tieu and Nunnari, 2000), co-immunoprecipitation (Bhar et al., 2006) and direct binding (Bui et al., 2012) studies indicate that the beta-propeller domains of the Mdv1 dimer recruit the Dnm1 GTPase to possible fission sites on the mitochondrial outer membrane. Consistent with this idea, mutations in the Mdv1 beta-propeller domain that reduce or block the Mdv1-Dnm1 interaction prevent Dnm1 membrane recruitment in vivo (Bui et al., 2012). Although the function of the Dnm1 Insert B domain remained a mystery for some time, recent work strongly suggests that the Insert B domain of Dnm1 interacts directly with the Mdv1 beta-propeller domain (Bui et al., 2012). Studies with fluorescently tagged Mdv1 and Dnm1

show that the two proteins colocalize in puncta on the mitochondrial membrane. In vitro studies suggest that these puncta may be co-assemblies of Mdv1 and Dnm1 spirals, and that Mdv1 stimulates both the assembly of Dnm1 into spirals and the GTP hydrolysis activity of Dnm1 that occurs upon self-assembly (Lackner and Nunnari, 2009). How Dnm1-Mdv1 coassembly and Dnm1 GTP hydrolysis catalyze mitochondrial fission remains unclear. However, new data have surfaced regarding the mechanism of mitochondrial constriction. Although it was originally suggested that Dnm1 assembly was sufficient to constrict the mitochondrial compartment prior to fission (Ingerman et al., 2005), a recent study showed that the endoplasmic reticulum (ER) encircles and constricts mitochondrial tubules prior to Dnm1 recruitment (Friedman et al., 2011). This finding suggests that it is ER-mitochondrial contact that marks sites of mitochondrial fission, and that Dnm1 is recruited to sites of prior constriction, which may facilitate Dnm1-GTP spiral assembly around the mitochondrial tubule.

Mitochondrial fission in mammals

Much of the mitochondrial fission machinery is conserved from yeast to human. Drp1 (Dynamin related protein) is the mammalian homolog of yeast Dnm1 and Fis1 is the homolog of yeast Fis1 (Chan, 2006). As in yeast, mammalian mitochondria are organized as a tubular network that spreads out from nucleus to the plasma membrane. In addition to long mitochondrial tubules, there are also shorter tubules and rods with multiple free ends. In fission defective cells, mitochondrial tubules are interconnected and in some cases form clumps that collapse near the nucleus. Some studies claim that mitochondria regulate apoptosis, due to the fact that mitochondrial fragmentation has

been observed preceding cytochrome c release after exposure to treatments that induce apoptosis (Desagher and Martinou, 2000; Frank et al., 2001). Apoptosis can be slowed or blocked by expressing a dominant negative form of Drp1 that prevents fission or knockdown Drp1 by RNAi (Frank et al., 2001; Lee et al., 2004). Researchers repeating these studies report that this response is not consistently reproducible and can vary depending on the cell type and apoptotic inducer used (Estaquier and Arnoult, 2007; Ishihara et al., 2009; Parone et al., 2006; Wakabayashi et al., 2009). Other studies suggest that fission defects have a significant effect on neuronal function. In mice, complete loss of Drp1 leads to embryonic lethality (Ishihara et al., 2009). Drp1 deficiency also induces abnormal synapse formation and the cells are sensitive to apoptosis. To date, there is one report on a patient born with a Drp1 mutation that died after 37 days (Waterham et al., 2007). The Drp1 mutation blocked fission and caused developmental abnormalities. The patient had small head circumference, hypotonia, optic atrophy and poor feeding. Over expressing this mutant allele in WT cells caused dominant-negative defects in fission, due to the fact that it disrupted Drp1 higher-order assembly (Waterham et al., 2007).

Mammalian fission proteins

Like Dnm1, Drp1 contains a GTPase domain, middle domain and a GED (GTPase effector domain) domain (Smirnova et al., 1998). Studies indicate that the function of Drp1 is similar to that of Dnm1 in yeast. Although Dnm1 forms stable mitochondrial puncta under normal growth conditions, Drp1 in cultured mammalian cells is mostly cytoplasmic (Smirnova et al., 1998). In response to a variety of cellular stresses, Drp1 is relocated from the cytoplasm to the mitochondrial outer membrane. Once on the

membrane, Drp1 oligomerizes into structures that wrap around the mitochondrial tubule (Frank et al., 2001; Labrousse et al., 1999). As shown for yeast, Drp1 assembles only at sites that are preconstricted by the ER (Friedman et al., 2011). In timelapse studies, some of the Drp1 assemblies are at sites that constrict further and complete fission (Frank et al., 2001). Inhibition of Drp1 by RNAi or expression of a dominant-negative Drp1 mutant protein produces elongated and interconnected mitochondrial networks (Lee et al., 2004; Smirnova et al., 2001).

hFis1 (human fission protein) is also conserved in mammalian cells (James et al., 2003). With an N-terminal TPR (tetratricopeptide repeat) and C-terminal transmembrane domain, hFis1, like yeast Fis1, is embedded in the mitochondrial outer membrane facing the cytoplasm. Initial studies suggested that over expression of hFis1 caused dominant-negative defects in mitochondrial fission (James et al., 2003; Yoon et al., 2003) and depletion of hFis1 by RNAi impaired fission leading to long mitochondrial tubule in HEK 293T (Gandre-Babbe and van der Bliek, 2008). However, later studies reported that mitochondrial morphology was not affected when hFis1 was knocked down in HeLa cells (Lee et al., 2004). Similar to Dnm1, The PH domain in Drp1 is replaced by an Insert B domain. As a result, Drp1 membrane recruitment is dependent on adaptor proteins. However, loss of hFis1 does not abolish Drp1 recruitment to mitochondria (Lee et al., 2004). Homologs of the fungal adaptors Mdv1 and Caf4 have not been identified in mammals, which is consistent with the finding that expression of hFi1 in yeast lacking yeast Fis1 does not rescue mitochondrial fission defects (Stojanovski et al., 2004). Although there was an early report that hFis1 and Drp1 directly interact (Gandre-Babbe

and van der Bliek, 2008; Yoon et al., 2003), there is currently no evidence that hFis1 and Drp1 interact in vivo or that an adaptor protein links the two proteins.

Mff (human Mitochondrial fission factor) consists of a C-terminal transmembrane domain and a predicted coiled-coil segment (Gandre-Babbe and van der Bliek, 2008). The remainder of the protein has no recognizable domains. Similar to hFis1, Mff is anchored to the mitochondrial outer membrane by its C-terminal domain with the rest of the protein facing the cytoplasm. Upon siRNA depletion of Mff, mitochondrial morphology is comparable to cells transfected with Drp1 siRNA (Gandre-Babbe and van der Bliek, 2008). Fluorescence imaging and in vivo and in vitro studies provide support that the N-terminal region of Mff interacts with Drp1 and recruits Drp1 to the cytoplasmic surface of mitochondria (Otera et al., 2010). A role for Mff in fission is also supported by the finding that depletion of Mff (but not hFis1) is able to block extensive mitochondrial fission and fragmentation when fusion is blocked by Opa1 RNAi (Otera et al., 2010).

MiD49 (mitochondrial dynamics protein of 49 kDa) and MiD51/MIEF (mitochondrial dynamics protein of 51kDa/mitochondrial elongation factor 1) are paralogs that are both anchored to the mitochondrial outer membrane proteins via an N-terminal transmembrane domain (Palmer et al., 2011). MiD49 has been shown to bind to Drp1 directly by yeast two-hybrid. Both MiD49 and MiD51 are able to interact with Drp1 and recruit Drp1 to the mitochondrial membrane independently. Over expression of either protein generates an elongated or collapsed mitochondrial network. However, the role of these fission adaptors is controversial. A study by Palmer et al. (date) indicated that MiD49/MiD51 participate in mitochondrial fission. This conclusion was based, in

part, on the observation that MiD49/MiD51 knockdown caused mitochondrial elongation and significantly reduced CCCP-induced mitochondrial fragmentation. On the other hand, Zhao et al. (2011) reported that knockdown of MiD51 alone leads to mitochondrial fragmentation, suggesting it is a negative regulator of fission or a positive regulator of mitochondrial fusion. Further studies led the authors to suggest that MiD51 interacts with Drp1 to inhibit fission. Studies are underway in a number of labs to repeat these findings and resolve this issue (Zhao et al., 2011).

Thesis overview

The role of the dynamin-related Dnm1/Drp1 GTPases in mitochondrial fission is now firmly established. However, there is still controversy about the functions of Fis1/hFis1 and adaptor proteins during Dnm1/Drp1 recruitment, fission complex assembly and mitochondrial membrane scission. In this dissertation, two studies are presented that explore the roles of adaptor proteins in the presence or absence of their adaptor counterpart(s). The first study examines the role of Caf4 in yeast fission in the presence or absence of Mdv1. The second study uses a novel fission null yeast strain to test the individual functions of yeast and mammalian Fis1 and adaptors in Dnm1/Drp1 recruitment and mitochondrial membrane scission. The results from these studies provide new evidence that some adaptors can work together or separately with their respective dynamin GTPase to assemble fission complexes and mediate membrane fission.

References

Abutbul-Ionita, I., Rujiviphat, J., Nir, I., McQuibban, G. A., and Danino, D. (2012). Membrane tethering and nucleotide-dependent conformational changes drive

mitochondrial genome maintenance (Mgm1) protein-mediated membrane fusion. J Biol Chem.

Alberts, B. (2002). Molecular biology of the cell, 4th edn (New York: Garland Science).

Andersson, S. G., Karlberg, O., Canback, B., and Kurland, C. G. (2003). On the origin of mitochondria: a genomics perspective. Philos Trans R Soc Lond B Biol Sci *358*, 165-177; discussion 177-169.

Anton, F., Fres, J. M., Schauss, A., Pinson, B., Praefcke, G. J., Langer, T., and Escobar-Henriques, M. (2011). Ugo1 and Mdm30 act sequentially during Fzo1-mediated mitochondrial outer membrane fusion. J Cell Sci *124*, 1126-1135.

Attardi, G., and Schatz, G. (1988). Biogenesis of mitochondria. Annu Rev Cell Biol *4*, 289-333.

Azpiroz, R., and Butow, R. A. (1993). Patterns of mitochondrial sorting in yeast zygotes. Mol Biol Cell *4*, 21-36.

Bhar, D., Karren, M. A., Babst, M., and Shaw, J. M. (2006). Dimeric Dnm1-G385D interacts with Mdv1 on mitochondria and can be stimulated to assemble into fission complexes containing Mdv1 and Fis1. J Biol Chem *281*, 17312-17320.

Bleazard, W., McCaffery, J. M., King, E. J., Bale, S., Mozdy, A., Tieu, Q., Nunnari, J., and Shaw, J. M. (1999). The dynamin-related GTPase Dnm1 regulates mitochondrial fission in yeast. Nat Cell Biol *1*, 298-304.

Bretscher, A. (2003). Polarized growth and organelle segregation in yeast: the tracks, motors, and receptors. J Cell Biol *160*, 811-816.

Bui, H. T., Karren, M. A., Bhar, D., and Shaw, J. M. (2012). A novel motif in the yeast mitochondrial dynamin Dnm1 is essential for adaptor binding and membrane recruitment. J Cell Biol *199*, 613-622.

Campello, S., Lacalle, R. A., Bettella, M., Manes, S., Scorrano, L., and Viola, A. (2006). Orchestration of lymphocyte chemotaxis by mitochondrial dynamics. J Exp Med *203*, 2879-2886.

Cerveny, K. L., and Jensen, R. E. (2003). The WD-repeats of Net2p interact with Dnm1p and Fis1p to regulate division of mitochondria. Mol Biol Cell *14*, 4126-4139.

Cerveny, K. L., McCaffery, J. M., and Jensen, R. E. (2001). Division of mitochondria requires a novel DMN1-interacting protein, Net2p. Mol Biol Cell *12*, 309-321.

Chan, D. C. (2006). Mitochondrial fusion and fission in mammals. Annu Rev Cell Dev Biol *22*, 79-99.

Chan, D. C. (2012). Fusion and fission: interlinked processes critical for mitochondrial health. Annu Rev Genet *46*, 265-287.

Chen, H., Chomyn, A., and Chan, D. C. (2005). Disruption of fusion results in mitochondrial heterogeneity and dysfunction. J Biol Chem *280*, 26185-26192.

Chen, H., Detmer, S. A., Ewald, A. J., Griffin, E. E., Fraser, S. E., and Chan, D. C. (2003). Mitofusins Mfn1 and Mfn2 coordinately regulate mitochondrial fusion and are essential for embryonic development. J Cell Biol *160*, 189-200.

Cohen, M. M., Amiott, E. A., Day, A. R., Leboucher, G. P., Pryce, E. N., Glickman, M. H., McCaffery, J. M., Shaw, J. M., and Weissman, A. M. (2011). Sequential requirements for the GTPase domain of the mitofusin Fzo1 and the ubiquitin ligase SCFMdm30 in mitochondrial outer membrane fusion. J Cell Sci *124*, 1403-1410.

Costa, V., Giacomello, M., Hudec, R., Lopreiato, R., Ermak, G., Lim, D., Malorni, W., Davies, K. J., Carafoli, E., and Scorrano, L. (2010). Mitochondrial fission and cristae disruption increase the response of cell models of Huntington's disease to apoptotic stimuli. EMBO Mol Med *2*, 490-503.

Desagher, S., and Martinou, J. C. (2000). Mitochondria as the central control point of apoptosis. Trends Cell Biol *10*, 369-377.

Detmer, S. A., and Chan, D. C. (2007). Functions and dysfunctions of mitochondrial dynamics. Nat Rev Mol Cell Biol *8*, 870-879.

Estaquier, J., and Arnoult, D. (2007). Inhibiting Drp1-mediated mitochondrial fission selectively prevents the release of cytochrome c during apoptosis. Cell Death Differ *14*, 1086-1094.

Faelber, K., Posor, Y., Gao, S., Held, M., Roske, Y., Schulze, D., Haucke, V., Noe, F., and Daumke, O. (2011). Crystal structure of nucleotide-free dynamin. Nature *477*, 556-560.

Fehrenbacher, K. L., Yang, H. C., Gay, A. C., Huckaba, T. M., and Pon, L. A. (2004). Live cell imaging of mitochondrial movement along actin cables in budding yeast. Curr Biol *14*, 1996-2004.

Ford, M. G., Jenni, S., and Nunnari, J. (2011). The crystal structure of dynamin. Nature *477*, 561-566.

Frank, S., Gaume, B., Bergmann-Leitner, E. S., Leitner, W. W., Robert, E. G., Catez, F., Smith, C. L., and Youle, R. J. (2001). The role of dynamin-related protein 1, a mediator of mitochondrial fission, in apoptosis. Dev Cell *1*, 515-525.

Fransson, S., Ruusala, A., and Aspenstrom, P. (2006). The atypical Rho GTPases Miro-1 and Miro-2 have essential roles in mitochondrial trafficking. Biochem Biophys Res Commun *344*, 500-510.

Frederick, R. L., Okamoto, K., and Shaw, J. M. (2008). Multiple pathways influence mitochondrial inheritance in budding yeast. Genetics *178*, 825-837.

Frederick, R. L., and Shaw, J. M. (2007). Moving mitochondria: establishing distribution of an essential organelle. Traffic *8*, 1668-1675.

Friedman, J. R., Lackner, L. L., West, M., DiBenedetto, J. R., Nunnari, J., and Voeltz, G. K. (2011). ER tubules mark sites of mitochondrial division. Science *334*, 358-362.

Gandre-Babbe, S., and van der Bliek, A. M. (2008). The novel tail-anchored membrane protein Mff controls mitochondrial and peroxisomal fission in mammalian cells. Mol Biol Cell *19*, 2402-2412.

Gomes, L. C., Di Benedetto, G., and Scorrano, L. (2011). During autophagy mitochondria elongate, are spared from degradation and sustain cell viability. Nat Cell Biol *13*, 589-598.

Gorsich, S. W., and Shaw, J. M. (2004). Importance of mitochondrial dynamics during meiosis and sporulation. Mol Biol Cell *15*, 4369-4381.

Gorska-Andrzejak, J., Stowers, R. S., Borycz, J., Kostyleva, R., Schwarz, T. L., and Meinertzhagen, I. A. (2003). Mitochondria are redistributed in Drosophila photoreceptors lacking milton, a kinesin-associated protein. J Comp Neurol *463*, 372-388.

Gray, M. W., Burger, G., and Lang, B. F. (1999). Mitochondrial evolution. Science *283*, 1476-1481.

Griffin, E. E., Graumann, J., and Chan, D. C. (2005). The WD40 protein Caf4p is a component of the mitochondrial fission machinery and recruits Dnm1p to mitochondria. J Cell Biol *170*, 237-248.

Henze, K., and Martin, W. (2003). Evolutionary biology: essence of mitochondria. Nature *426*, 127-128.

Herlan, M., Vogel, F., Bornhovd, C., Neupert, W., and Reichert, A. S. (2003). Processing of Mgm1 by the rhomboid-type protease Pcp1 is required for maintenance of

mitochondrial morphology and of mitochondrial DNA. J Biol Chem *278*, 27781-27788.

Hollenbeck, P. J., and Saxton, W. M. (2005). The axonal transport of mitochondria. J Cell Sci *118*, 5411-5419.

Hoppins, S., Lackner, L., and Nunnari, J. (2007). The machines that divide and fuse mitochondria. Annu Rev Biochem *76*, 751-780.

Ingerman, E., Perkins, E. M., Marino, M., Mears, J. A., McCaffery, J. M., Hinshaw, J. E., and Nunnari, J. (2005). Dnm1 forms spirals that are structurally tailored to fit mitochondria. J Cell Biol *170*, 1021-1027.

Ishihara, N., Eura, Y., and Mihara, K. (2004). Mitofusin 1 and 2 play distinct roles in mitochondrial fusion reactions via GTPase activity. J Cell Sci *117*, 6535-6546.

Ishihara, N., Nomura, M., Jofuku, A., Kato, H., Suzuki, S. O., Masuda, K., Otera, H., Nakanishi, Y., Nonaka, I., Goto, Y., *et al.* (2009). Mitochondrial fission factor Drp1 is essential for embryonic development and synapse formation in mice. Nat Cell Biol *11*, 958-966.

Itoh, T., Toh, E. A., and Matsui, Y. (2004). Mmr1p is a mitochondrial factor for Myo2p-dependent inheritance of mitochondria in the budding yeast. Embo J *23*, 2520-2530.

Itoh, T., Watabe, A., Toh, E. A., and Matsui, Y. (2002). Complex formation with Ypt11p, a rab-type small GTPase, is essential to facilitate the function of Myo2p, a class V myosin, in mitochondrial distribution in Saccharomyces cerevisiae. Mol Cell Biol *22*, 7744-7757.

James, D. I., Parone, P. A., Mattenberger, Y., and Martinou, J. C. (2003). hFis1, a novel component of the mammalian mitochondrial fission machinery. J Biol Chem *278*, 36373-36379.

Karren, M. A., Coonrod, E. M., Anderson, T. K., and Shaw, J. M. (2005). The role of Fis1p-Mdv1p interactions in mitochondrial fission complex assembly. J Cell Biol *171*, 291-301.

Kim, I., Rodriguez-Enriquez, S., and Lemasters, J. J. (2007). Selective degradation of mitochondria by mitophagy. Arch Biochem Biophys *462*, 245-253.

Koirala, S., Bui, H. T., Schubert, H. L., Eckert, D. M., Hill, C. P., Kay, M. S., and Shaw, J. M. (2010). Molecular architecture of a dynamin adaptor: implications for assembly of mitochondrial fission complexes. J Cell Biol *191*, 1127-1139.

Koshiba, T., Detmer, S. A., Kaiser, J. T., Chen, H., McCaffery, J. M., and Chan, D. C. (2004). Structural basis of mitochondrial tethering by mitofusin complexes. Science *305*, 858-862.

Labrousse, A. M., Zappaterra, M. D., Rube, D. A., and van der Bliek, A. M. (1999). C. elegans dynamin-related protein DRP-1 controls severing of the mitochondrial outer membrane. Mol Cell *4*, 815-826.

Lackner, L. L., and Nunnari, J. M. (2009). The molecular mechanism and cellular functions of mitochondrial division. Biochim Biophys Acta *1792*, 1138-1144.

Lee, Y. J., Jeong, S. Y., Karbowski, M., Smith, C. L., and Youle, R. J. (2004). Roles of the mammalian mitochondrial fission and fusion mediators Fis1, Drp1, and Opa1 in apoptosis. Mol Biol Cell *15*, 5001-5011.

Legesse-Miller, A., Massol, R. H., and Kirchhausen, T. (2003). Constriction and Dnm1p recruitment are distinct processes in mitochondrial fission. Mol Biol Cell *14*, 1953-1963.

Lewis, M. R., and Lewis, W. H. (1914). Mitochondria in tissue culture. Science *39*, 330-333.

Li, Z., Okamoto, K., Hayashi, Y., and Sheng, M. (2004). The importance of dendritic mitochondria in the morphogenesis and plasticity of spines and synapses. Cell *119*, 873-887.

Lyamzaev, K. G., Pletjushkina, O. Y., Saprunova, V. B., Bakeeva, L. E., Chernyak, B. V., and Skulachev, V. P. (2004). Selective elimination of mitochondria from living cells induced by inhibitors of bioenergetic functions. Biochem Soc Trans *32*, 1070-1071.

Manczak, M., Calkins, M. J., and Reddy, P. H. (2011). Impaired mitochondrial dynamics and abnormal interaction of amyloid beta with mitochondrial protein Drp1 in neurons from patients with Alzheimer's disease: implications for neuronal damage. Hum Mol Genet *20*, 2495-2509.

McBride, H. M., Neuspiel, M., and Wasiak, S. (2006). Mitochondria: more than just a powerhouse. Curr Biol *16*, R551-560.

McConnell, S. J., Stewart, L. C., Talin, A., and Yaffe, M. P. (1990). Temperature-sensitive yeast mutants defective in mitochondrial inheritance. J Cell Biol *111*, 967-976.

Mears, J. A., Lackner, L. L., Fang, S., Ingerman, E., Nunnari, J., and Hinshaw, J. E. (2010). Conformational changes in Dnm1 support a contractile mechanism for mitochondrial fission. Nat Struct Mol Biol *18*, 20-26.

Mears, J. A., Ray, P., and Hinshaw, J. E. (2007). A corkscrew model for dynamin constriction. Structure *15*, 1190-1202.

Miller, K. E., and Sheetz, M. P. (2004). Axonal mitochondrial transport and potential are correlated. J Cell Sci *117*, 2791-2804.

Mozdy, A. D., McCaffery, J. M., and Shaw, J. M. (2000). Dnm1p GTPase-mediated mitochondrial fission is a multi-step process requiring the novel integral membrane component Fis1p. J Cell Biol *151*, 367-380.

Nakamura, K., Nemani, V. M., Azarbal, F., Skibinski, G., Levy, J. M., Egami, K., Munishkina, L., Zhang, J., Gardner, B., Wakabayashi, J., *et al.* (2011). Direct membrane association drives mitochondrial fission by the Parkinson disease-associated protein alpha-synuclein. J Biol Chem *286*, 20710-20726.

Naylor, K., Ingerman, E., Okreglak, V., Marino, M., Hinshaw, J. E., and Nunnari, J. (2006). Mdv1 interacts with assembled dnm1 to promote mitochondrial division. J Biol Chem *281*, 2177-2183.

Nunnari, J., Marshall, W. F., Straight, A., Murray, A., Sedat, J. W., and Walter, P. (1997). Mitochondrial transmission during mating in Saccharomyces cerevisiae is determined by mitochondrial fusion and fission and the intramitochondrial segregation of mitochondrial DNA. Mol Biol Cell *8*, 1233-1242.

Okamoto, K., and Shaw, J. M. (2005). Mitochondrial morphology and dynamics in yeast and multicellular eukaryotes. Annu Rev Genet *39*, 503-536.

Otera, H., Wang, C., Cleland, M. M., Setoguchi, K., Yokota, S., Youle, R. J., and Mihara, K. (2010). Mff is an essential factor for mitochondrial recruitment of Drp1 during mitochondrial fission in mammalian cells. J Cell Biol *191*, 1141-1158.

Otsuga, D., Keegan, B. R., Brisch, E., Thatcher, J. W., Hermann, G. J., Bleazard, W., and Shaw, J. M. (1998). The dynamin-related GTPase, Dnm1p, controls mitochondrial morphology in yeast. J Cell Biol *143*, 333-349.

Palade, G. E. (1953). An electron microscope study of the mitochondrial structure. J Histochem Cytochem *1*, 188-211.

Palmer, C. S., Osellame, L. D., Laine, D., Koutsopoulos, O. S., Frazier, A. E., and Ryan, M. T. (2011). MiD49 and MiD51, new components of the mitochondrial fission machinery. EMBO Rep *12*, 565-573.

Parone, P. A., James, D. I., Da Cruz, S., Mattenberger, Y., Donze, O., Barja, F., and Martinou, J. C. (2006). Inhibiting the mitochondrial fission machinery does not prevent Bax/Bak-dependent apoptosis. Mol Cell Biol *26*, 7397-7408.

Pilling, A. D., Horiuchi, D., Lively, C. M., and Saxton, W. M. (2006). Kinesin-1 and Dynein are the primary motors for fast transport of mitochondria in Drosophila motor axons. Mol Biol Cell *17*, 2057-2068.

Praefcke, G. J., and McMahon, H. T. (2004). The dynamin superfamily: universal membrane tubulation and fission molecules? Nat Rev Mol Cell Biol *5*, 133-147.

Rambold, A. S., Kostelecky, B., Elia, N., and Lippincott-Schwartz, J. (2011). Tubular network formation protects mitochondria from autophagosomal degradation during nutrient starvation. Proc Natl Acad Sci U S A *108*, 10190-10195.

Rapaport, D., Brunner, M., Neupert, W., and Westermann, B. (1998). Fzo1p is a mitochondrial outer membrane protein essential for the biogenesis of functional mitochondria in Saccharomyces cerevisiae. J Biol Chem *273*, 20150-20155.

Russo, G. J., Louie, K., Wellington, A., Macleod, G. T., Hu, F., Panchumarthi, S., and Zinsmaier, K. E. (2009). Drosophila Miro is required for both anterograde and retrograde axonal mitochondrial transport. J Neurosci *29*, 5443-5455.

Sesaki, H., and Jensen, R. E. (1999). Division versus fusion: Dnm1p and Fzo1p antagonistically regulate mitochondrial shape. J Cell Biol *147*, 699-706.

Sesaki, H., and Jensen, R. E. (2001). UGO1 encodes an outer membrane protein required for mitochondrial fusion. J Cell Biol *152*, 1123-1134.

Sesaki, H., Southard, S. M., Yaffe, M. P., and Jensen, R. E. (2003). Mgm1p, a dynamin-related GTPase, is essential for fusion of the mitochondrial outer membrane. Mol Biol Cell *14*, 2342-2356.

Smirnova, E., Griparic, L., Shurland, D. L., and van der Bliek, A. M. (2001). Dynamin-related protein Drp1 is required for mitochondrial division in mammalian cells. Mol Biol Cell *12*, 2245-2256.

Smirnova, E., Shurland, D. L., Ryazantsev, S. N., and van der Bliek, A. M. (1998). A human dynamin-related protein controls the distribution of mitochondria. J Cell Biol *143*, 351-358.

Song, Z., Ghochani, M., McCaffery, J. M., Frey, T. G., and Chan, D. C. (2009). Mitofusins and OPA1 mediate sequential steps in mitochondrial membrane fusion. Mol Biol Cell *20*, 3525-3532.

Stojanovski, D., Koutsopoulos, O. S., Okamoto, K., and Ryan, M. T. (2004). Levels of human Fis1 at the mitochondrial outer membrane regulate mitochondrial morphology. J Cell Sci *117*, 1201-1210.

Suzuki, M., Neutzner, A., Tjandra, N., and Youle, R. J. (2005). Novel structure of the N terminus in yeast Fis1 correlates with a specialized function in mitochondrial fission. J Biol Chem *280*, 21444-21452.

Taguchi, N., Ishihara, N., Jofuku, A., Oka, T., and Mihara, K. (2007). Mitotic phosphorylation of dynamin-related GTPase Drp1 participates in mitochondrial fission. J Biol Chem *282*, 11521-11529.

Tieu, Q., and Nunnari, J. (2000). Mdv1p is a WD repeat protein that interacts with the dynamin-related GTPase, Dnm1p, to trigger mitochondrial division. J Cell Biol *151*, 353-366.

Tieu, Q., Okreglak, V., Naylor, K., and Nunnari, J. (2002). The WD repeat protein, Mdv1p, functions as a molecular adaptor by interacting with Dnm1p and Fis1p during mitochondrial fission. J Cell Biol *158*, 445-452.

Twig, G., Elorza, A., Molina, A. J., Mohamed, H., Wikstrom, J. D., Walzer, G., Stiles, L., Haigh, S. E., Katz, S., Las, G., *et al.* (2008). Fission and selective fusion govern mitochondrial segregation and elimination by autophagy. Embo J *27*, 433-446.

Verstreken, P., Ly, C. V., Venken, K. J., Koh, T. W., Zhou, Y., and Bellen, H. J. (2005). Synaptic mitochondria are critical for mobilization of reserve pool vesicles at Drosophila neuromuscular junctions. Neuron *47*, 365-378.

Wakabayashi, J., Zhang, Z., Wakabayashi, N., Tamura, Y., Fukaya, M., Kensler, T. W., Iijima, M., and Sesaki, H. (2009). The dynamin-related GTPase Drp1 is required for embryonic and brain development in mice. J Cell Biol *186*, 805-816.

Waterham, H. R., Koster, J., van Roermund, C. W., Mooyer, P. A., Wanders, R. J., and Leonard, J. V. (2007). A lethal defect of mitochondrial and peroxisomal fission. N Engl J Med *356*, 1736-1741.

Williamson, D. H., and Fennell, D. J. (1979). Visualization of yeast mitochondrial DNA with the fluorescent stain "DAPI". Methods Enzymol *56*, 728-733.

Yoon, Y., Krueger, E. W., Oswald, B. J., and McNiven, M. A. (2003). The mitochondrial protein hFis1 regulates mitochondrial fission in mammalian cells through an interaction with the dynamin-like protein DLP1. Mol Cell Biol *23*, 5409-5420.

Zhang, Y., and Chan, D. C. (2007). Structural basis for recruitment of mitochondrial fission complexes by Fis1. Proc Natl Acad Sci U S A *104*, 18526-18530.

Zhang, Y., Chan, N. C., Ngo, H. B., Gristick, H., and Chan, D. C. (2012). Crystal structure of mitochondrial fission complex reveals scaffolding function for mitochondrial division 1 (Mdv1) coiled coil. J Biol Chem *287*, 9855-9861.

Zhao, J., Liu, T., Jin, S., Wang, X., Qu, M., Uhlen, P., Tomilin, N., Shupliakov, O., Lendahl, U., and Nister, M. (2011). Human MIEF1 recruits Drp1 to mitochondrial outer membranes and promotes mitochondrial fusion rather than fission. Embo J *30*, 2762-2778.

Zheng, M., Beck, M., Muller, J., Chen, T., Wang, X., Wang, F., Wang, Q., Wang, Y., Baluska, F., Logan, D. C., *et al.* (2009). Actin turnover is required for myosin-dependent mitochondrial movements in Arabidopsis root hairs. PLoS One *4*, e5961.

Zick, M., Duvezin-Caubet, S., Schafer, A., Vogel, F., Neupert, W., and Reichert, A. S. (2009). Distinct roles of the two isoforms of the dynamin-like GTPase Mgm1 in mitochondrial fusion. FEBS Lett *583*, 2237-2243.

CHAPTER 2

THE MITOCHONDRIAL FISSION ADAPTORS Caf4 AND Mdv1 ARE NOT FUNCTIONALLY EQUIVALENT

Qian Guo, Sajjan Koirala, Edward M. Perkins,

J. Michael McCaffery and Janet M. Shaw

Introduction

An ancient genome wide duplication in the lineage including the budding yeast *Saccharomyces cerevisiae* played an important role in the evolution of this singled celled eukaryote (Kellis et al., 2004; Wolfe and Shields, 1997). After this event, duplicated genes (paralogs) experienced accelerated evolution, most often involving one member of the gene pair. Of the 5885 existing *S. cerevisiae* genes, there are 450 paralog pairs (Goffeau et al., 1996; Musso et al., 2007). For many of these, it remains unclear whether one of the genes has acquired a new function, maintains a redundant function, or has developed a specialized function within the same cellular process.

Mitochondrial fission is one cellular process that utilizes paralogous genes. Yeast mitochondrial membranes form tubular structures that undergo frequent fission and fusion events (Nunnari et al., 1997; Okamoto and Shaw, 2005). When fission is blocked, ongoing fusion creates a single, interconnected mitochondrial net (Bleazard et al., 1999; Otsuga et al., 1998; Sesaki and Jensen, 1999). A previous study demonstrated that defects in mitochondrial fission have a negative fitness cost in yeast, since these abnormal nets are inefficiently partitioned into newly formed daughter cells during meiotic division, and the resulting spores are inviable (Gorsich and Shaw, 2004). Successful mitochondrial fission requires an adaptor protein called Mdv1 (Cerveny et al., 2001; Tieu and Nunnari, 2000), which bridges the interaction between the cytoplasmic dynamin-related GTPase Dnm1 and the mitochondrial outer membrane-anchored protein Fis1 (Cerveny and Jensen, 2003; Mozdy et al., 2000; Tieu et al., 2002). On the membrane, Mdv1 promotes the assembly of Dnm1 into spirals that often surround the mitochondrial tubule (Ingerman et

al., 2005; Legesse-Miller et al., 2003). A subset of these structures are located at sites on mitochondria that ultimately divide (Legesse-Miller et al., 2003; Schauss et al., 2006).

An Mdv1 paralog called Caf4 was identified in a directed proteomics screen (Griffin et al., 2005). Like Mdv1, the Caf4 adaptor is composed of three domains, an N-terminal extension (NTE), a coiled-coil (CC) and C-terminal WD40 repeats predicted to form a β-propeller (Figure 2.1A). The NTE domains of Mdv1 or Caf4 form a clamp around the Fis1 TPR-like domain, which mediates adaptor localization to the mitochondrial surface (Zhang and Chan, 2007). The Mdv1 and Caf4 WD40/β-propeller domains interact with, and recruit, Dnm1 to the membrane (Cerveny and Jensen, 2003; Griffin et al., 2005; Tieu et al., 2002). Structural studies reveal that Mdv1 dimerizes via an antiparallel coiled-coil (Koirala et al., 2010; Zhang et al., 2012), and Caf4 is thought to dimerize by a similar mechanism. Caf4 and Mdv1 also interact in vivo (Griffin et al., 2005), though whether this occurs via coiled-coil formation between the two proteins is unclear.

Yeast cells lacking Mdv1 exhibit severe mitochondrial morphology defects, establishing an essential role for this adaptor in fission (Cerveny et al., 2001; Tieu and Nunnari, 2000). By contrast, loss of Caf4 function enhances mitochondrial fission defects when Mdv1 is absent, but does not cause obvious fission defects on its own (Griffin et al., 2005). Although Caf4 can function to recruit Dnm1 to mitochondria in vivo, it has not been shown to directly participate in membrane scission. Moreover, it is not clear whether there is functional divergence between the two adaptor proteins.

In this study, we directly test the function of Caf4 in mitochondrial fission. We show that Caf4 is a bona fide fission adaptor that assembles at sites of mitochondrial division.

Although Caf4 can function alone as an adaptor, complexes containing both Caf4 and Mdv1 exhibit no obvious defects in mitochondrial fission. Genomic swapping studies indicate that Caf4 cannot substitute for Mdv1 in vivo. Moreover, over expression of Caf4 (but not Mdv1) from a regulated promoter induces dominant negative fission defects. When combined with phylogenetic analysis, these findings establish that Caf4 mitochondrial fission activity has diverged from that of Mdv1.

Results

Caf4 is present at mitochondrial fission sites and is sufficient for fission

A genomewide analysis of yeast protein expression showed that the abundance of Caf4 is one sixth that of Mdv1 (Ghaemmaghami et al., 2003). This finding raised the possibility that lower expression of Caf4 relative to Mdv1 was responsible for the functional differences observed for the two fission adaptors. We tested this idea by examining the effect of increasing Caf4 expression on mitochondrial fission in vivo. As shown in Figure 2.1B, 100% of wildtype (WT, *CAF4 MDV1*) cells expressing Caf4 and Mdv1 had branched, tubular mitochondria, while cells lacking both adaptors had severe fission defects (*caf4*Δ *mdv1*Δ, 3% cells with WT morphology). Similar to previous reports (Griffin et al., 2005), an *mdv1*Δ strain expressing endogenous Caf4 exhibited significant fission defects (*CAF4 mdv1*Δ, 29% cells with WT morphology), and a *caf4*Δ strain expressing endogenous Mdv1 exhibited essentially no fission defects (*caf4*Δ *MDV1*, 95% cells with WT morphology). Importantly, when Caf4 expression was induced from the *MET25* promoter on a plasmid in the *caf4*Δ *mdv1*Δ strain, the population of cells with

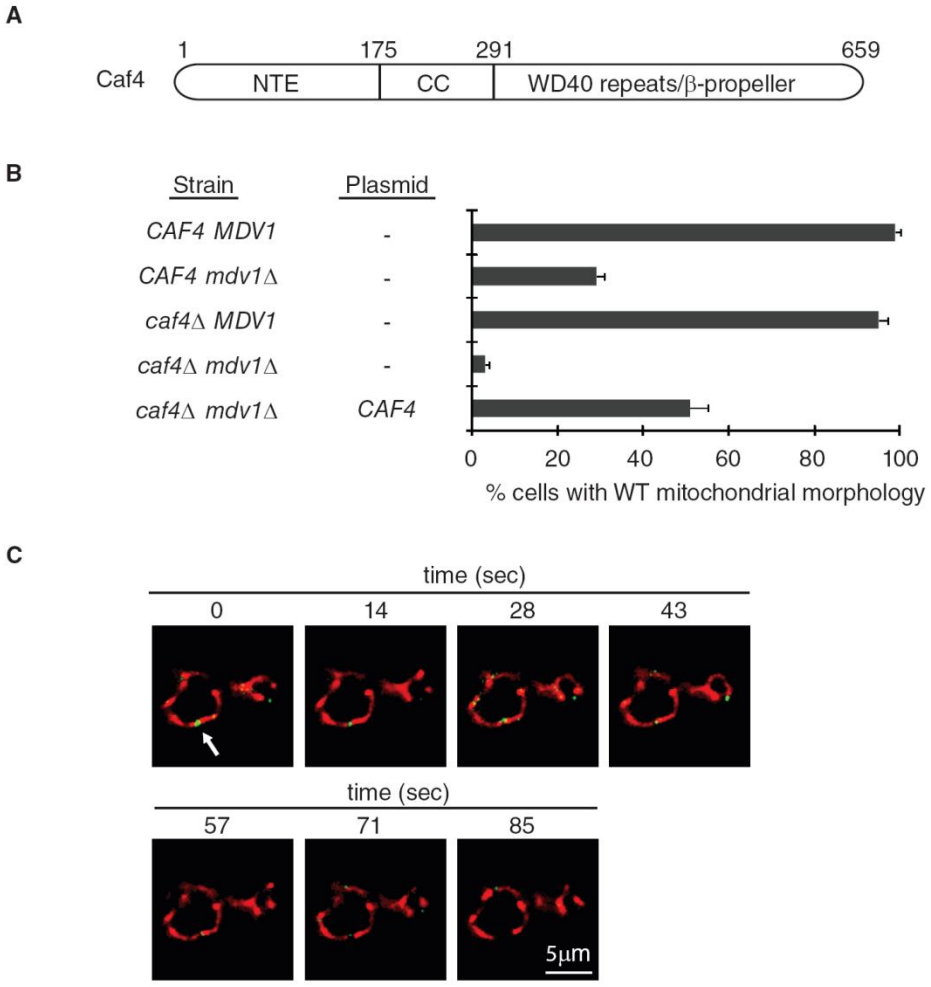

Figure 2.1. Caf4 functions independently as a mitochondrial fission adaptor. (**A**) Domain structure of the Caf4 fission adaptor, including the N-terminal extension (NTE), predicted coiled-coil (CC), and WD40 repeats predicted to form a β-propeller (WD40 repeats/ β-propeller). (**B**) Quantification of mitochondrial morphology in the indicated strains (n=100 cells). Bars and error bars are the mean and SD of three independent experiments. (**C**) Time-lapse imaging of a mitochondrial fission event mediated by GFP-Caf4 expressed in a *caf4Δ mdv1Δ* strain. Mitochondria are labeled with mt-RFP. Scale bar: 5 μm.

WT mitochondrial morphology increased to 51%. This increased rescue of fission defects was correlated with a 5.4-fold increase over native Caf4 expression (data not shown).

Time-lapse imaging studies confirmed that Caf4 in these cells was mediating mitochondrial fission when Mdv1 was absent. By epifluorescence microscopy, Dnm1-containing fission complexes appear as puncta that colocalize with mitochondrial tubules (Otsuga et al., 1998). Mdv1 or Caf4 also appear in these puncta after coassembly with Dnm1 (Cerveny et al., 2001; Griffin et al., 2005; Tieu and Nunnari, 2000). In *mdv1*Δ *caf4*Δ cells expressing GFP-Caf4 protein, green Caf4 puncta were observed on mt-RFP labeled mitochondrial tubules at sites where fission occurred (Figure 2.1C arrow, a representative example is shown). Together, these results indicate that Caf4 can function independently as a fission adaptor in yeast.

The Caf4 and Mdv1 adaptors are not functionally equivalent

Although Caf4 can carry out fission in the absence of Mdv1, the two adaptors may not be functionally equivalent. To test this possibility, Caf4 and Mdv1 were expressed from the *MET25* promoter in a *caf4*Δ *mdv1*Δ strain, and the abundance of each adaptor was increased by reducing the methionine concentration in the medium. WT mitochondrial morphology increased from 41% to 80% (Figure 2.2A) when Mdv1 steady state abundance was raised 4.2-fold by removing methionine from the medium (Figure 2.2B). By contrast, raising Caf4 steady-state abundance 1.3-fold (1.0 mM methionine, Figure 2.2B) initially increased WT mitochondrial morphology from 49% to 57% (Figure 2.2A). Further induction to 2.6-fold Caf4 over expression (0.0 mM methionine) reduced

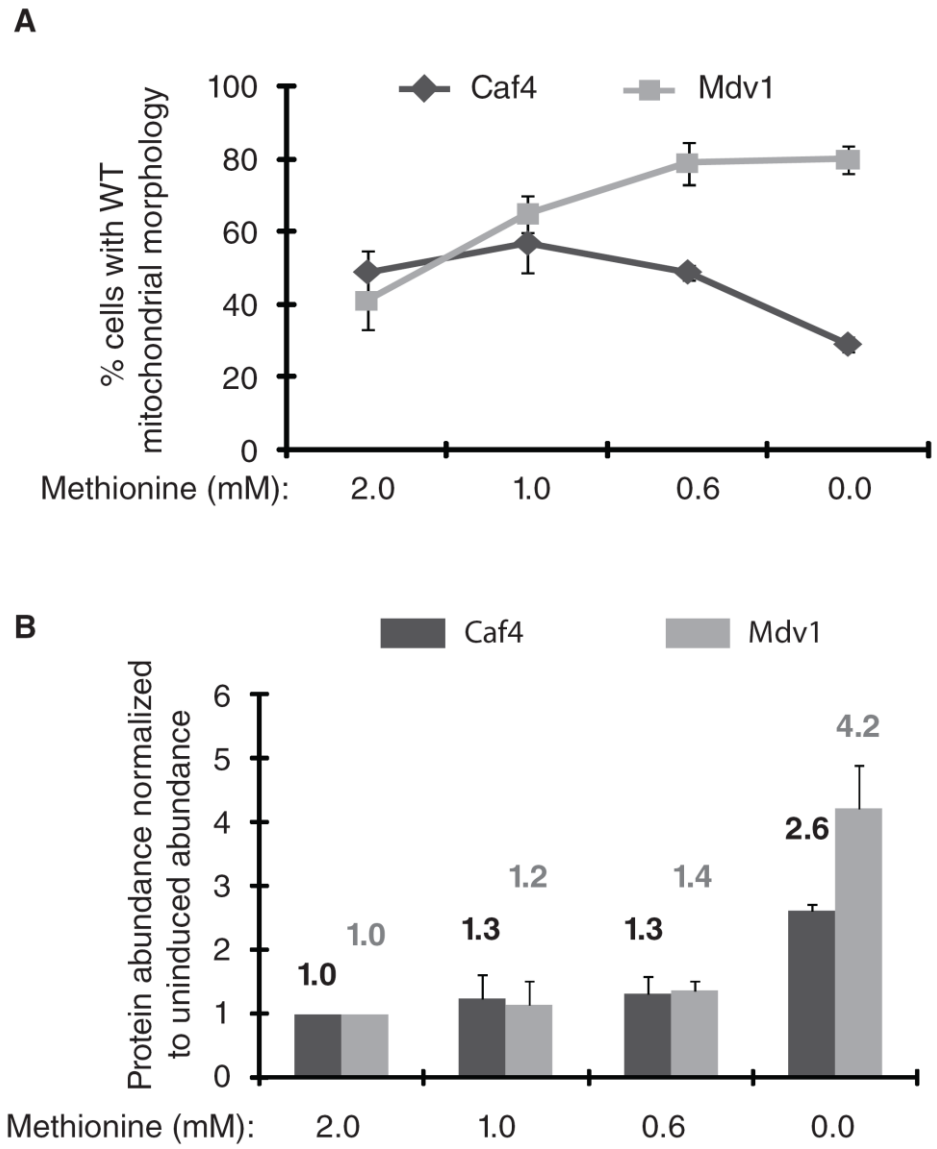

Figure 2.2. Caf4 and Mdv1 are not functionally equivalent. (**A**) Quantification of mitochondrial morphology in a *caf4Δ mdv1Δ* strain expressing Caf4 or Mdv1 from the repressible *MET25* promoter in media containing different methionine concentrations (n=100 cells). (**B**) Protein abundance of Caf4 or Mdv1 expressed from the repressible *MET25* promoter in difference methionine concentrations. The abundance of each protein was subsequently normalized to its abundance in 2.0 mM methionine. Bars and error bars are the mean and SD of three independent experiments.

the rescue to 29%, indicating that increasing Caf4 expression had a dominant negative effect on mitochondrial fission. Although we did not observe dominant-negative fission defects by increasing Mdv1 expression 4.2-fold (0.0 mM methionine) in these studies, we were able to induce dominant-negative defects by over expressing Mdv1 from the inducible *GAL1* promoter (~20-fold induction, data not shown) (Cerveny and Jensen, 2003). These different effects of Caf4 and Mdv1 over expression on mitochondrial fission support the idea that the fission adaptor functions of the two proteins are not equivalent.

We also tested whether expression of Caf4 from the native *MDV1* promoter and locus was sufficient to replace Mdv1 function. Mitochondrial morphology was WT in cells expressing only Mdv1 from its native locus (Figure 2.3A). When Caf4 alone was expressed from the *MDV1* promoter, Caf4 abundance increased 1.6-fold over the endogenous level (Figure 2.3B) but mitochondrial fission remained defective (Figure 2.3A, 20% WT morphology). (Note that this 1.6-fold increase is lower than the level of Caf4 expression shown to cause dominant negative fission defects in Figure 2.2). Thus, Caf4 expressed from the *MDV1* locus is not able to support WT levels of mitochondrial fission. By contrast, we observed a 0.6-fold decrease in expression of Mdv1 from the *CAF4* promoter with a corresponding decrease in WT mitochondrial morphology. We also noted a reproducible 1.3-fold increase in Caf4 expression from its native locus when the *MDV1* coding region was deleted. However, Mdv1 abundance did not change significantly when *CAF4* was absent. Thus, regulatory circuits that control expression from the *CAF4* gene may be able to sense and respond to changes in cellular Mdv1 abundance.

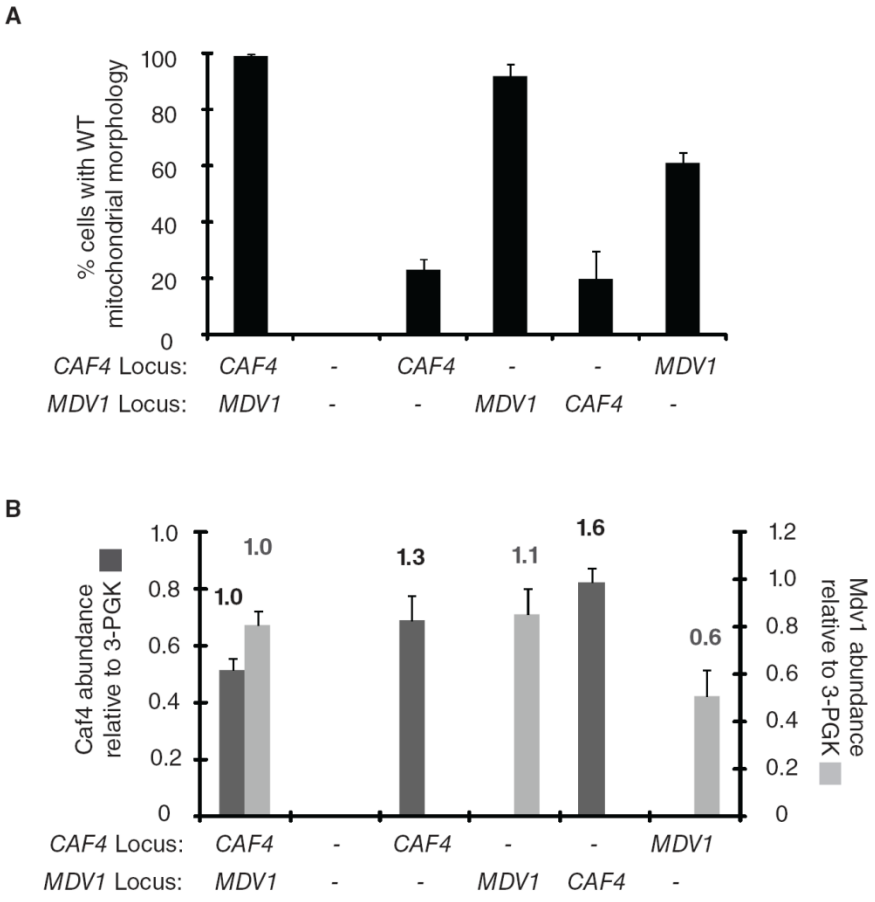

Figure 2.3. Caf4 causes dominant-negative fission defects when expressed from the *MDV1* promoter at the *MDV1* locus. (**A**) Quantification of mitochondrial morphology in the indicated strains (n=100 cells). (**B**) Steady-state abundance of Caf4 and Mdv1 in strains shown in (**A**). Owing to the use of different antibodies, the abundance of Caf4 and Mdv1 in the same and different strains should not be compared to one another. Bars and error bars are the mean and SD of three independent experiments.

Caf4 and Mdv1 can work together at a mitochondrial fission site

Mdv1 self-assembles via dimerization of an internal coiled-coil (Koirala et al., 2010; Zhang et al., 2012) and, based on structural predictions and two hybrid assays, Caf4 is predicted to behave in a similar manner. Caf4 and Mdv1 can also interact with one another (Griffin et al., 2005). However, it is not known whether Caf4 and Mdv1 canfunction together during mitochondrial fission. To address this question, we examined the extent and function of Caf4 and Mdv1 colocalization in vivo.

We began by quantifying the colocalization of GFP-Caf4 with RFP-Caf4 and GFP-Mdv1 with RFP-Mdv1 in cells lacking WT versions of the two proteins. Since fluorescent puncta in these experiments contain a single fission adaptor coassembled with Dnm1, these numbers represent the maximum colocalization we would expect to observe. Representative images of the categories scored are shown in Figure 2.4A (colocalized, a-c; not colocalized, d-f). Using this approach, 85% of Caf4 and 82% of Mdv1 signals colocalized in these studies, with the majority of puncta displaying the colocalization pattern shown in Figure 2.4A, a and b (72% and 81% respectively).

Next we quantified the colocalization of GFP-Caf4 and RFP-Mdv1 in mitochondrial puncta. We observed that 56% of RFP-Caf4 puncta colocalized with GFP-Mdv1 puncta (Figure 2.4B). Of these 56%, the majority (77%) displayed the colocalization pattern shown in Figure 2.4A, a and b. Similar results were obtained with GFP-Caf4 and RFP-Mdv1 (data not shown), indicating that placement of the fluorescent protein tags did not affect the experimental results.

Further analysis established that mitochondrial fission occurred at sites where Caf4 and Mdv1 colocalized. As shown in Figure 2.4C, time-lapse imaging studies of cells

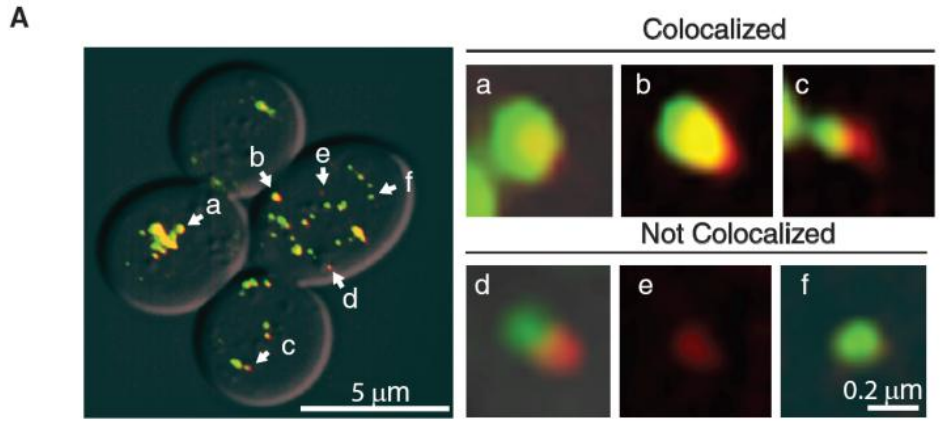

Figure 2.4. Mitochondrial puncta containing both Caf4 and Mdv1 are fission competent. (**A**) Large panel at the left shows a representative image of *caf4Δ mdv1Δ* cells expressing GFP-Caf4 and RFP-Mdv1. Scale bar: 5 μm. a-f marks puncta enlarged from the image in (A) at the left. Examples of partially or completely co-localized (**a-c**) versus isolated (**d-f)** puncta are shown. Scale bar: 0.2 μm. (**B**) Quantification of Caf4 and Mdv1 colocalization. GFP- or RFP-tagged Caf4 and Mdv1 were expressed in *caf4Δ mdv1Δ* cells in the pair-wise combinations indicated. The number of GFP puncta colocalized with RFP puncta was quantified and normalized to the total number of RFP puncta in each cell (n=10 cells). Bars and error bars are the mean and SD of three independent experiments. (**C**) Time lapse imaging of a mitochondrial fission event at a site where Caf4 and Mdv1 co-localize. Cerulean-tagged Caf4 (shown in cyan pseudo-color) and EYFP-Mdv1 were integrated at the *HO* and *MDV1* loci, respectively. Mitochondria were visualized using plasmid-borne mt-mCherry. The overlay contains true color images of all three channels. White areas indicate regions where signals from all three fluorescent proteins overlap. Scale Bar: 0.6 μm.

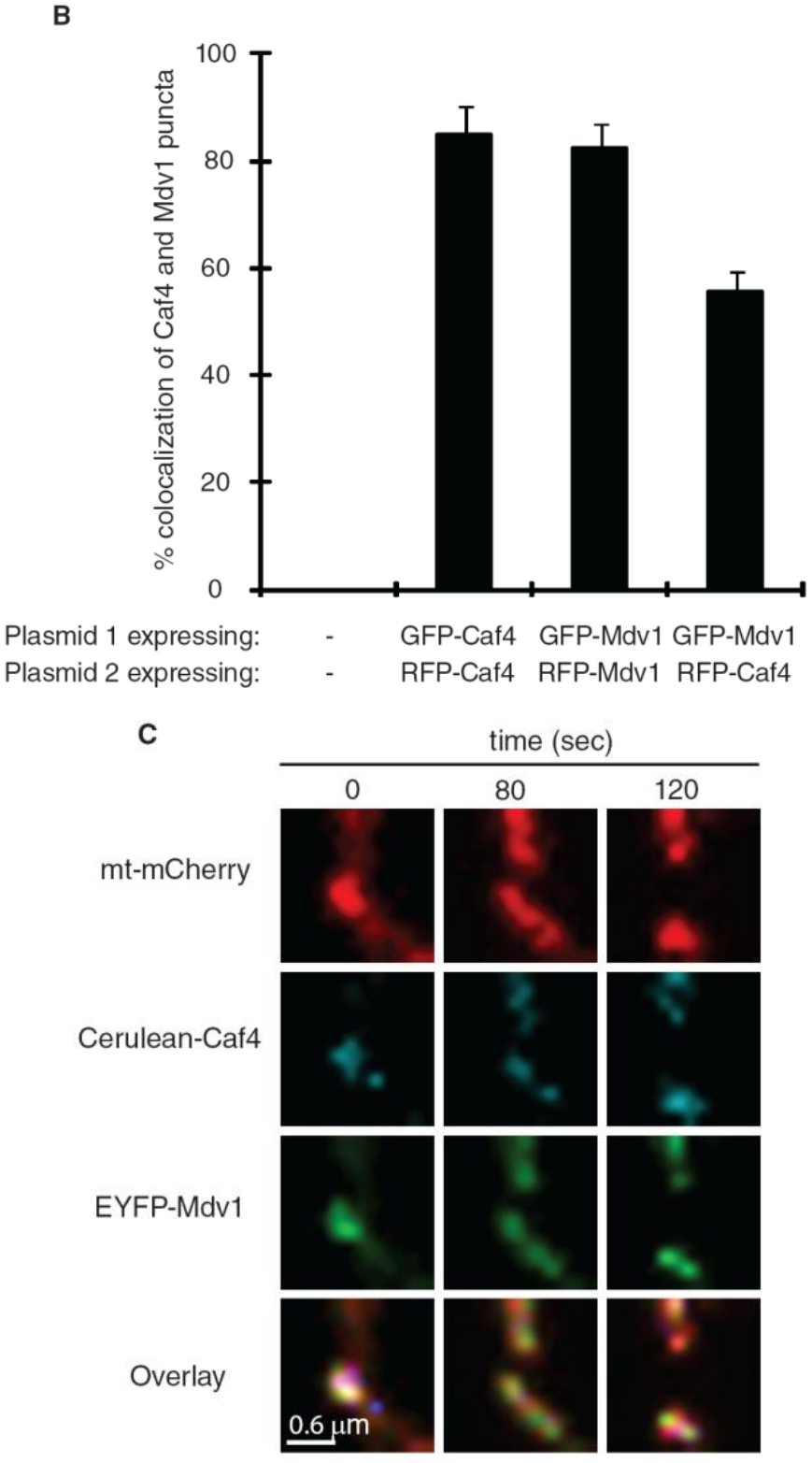

Figure 2.4. continued.

expressing Cerulean-Caf4 and EYFP-Mdv1 showed that puncta containing both adaptors (t = 0s, white signal in overlay) were able to mediate fission of an mCherry- labeled mitochondrial tubule. In the example shown, fission was complete after 80 seconds, at which point Caf4 and Mdv1 disassembled and dispersed along the surface of the separated tubules. These data provide a direct demonstration that Caf4 and Mdv1 can work together at the same mitochondrial fission site in vivo.

Evolution of the fungal fission adaptors

A major event in the evolutionary history of *Saccharomyces cerevisiae* was an ancestral whole genome duplication, which was followed by elimination of many redundant gene copies during the divergence of species in the genus *Saccharomyces* (Kellis et al., 2004; Wolfe and Shields, 1997). Our phylogenetic analysis indicates that *CAF4* and *MDV1* are among those redundant gene copies that have been retained during evolution. As shown in Figure 2.5, *Pichia pastoris*, *Lachancea thermotolerans* and *Aspergillus fumigatus* contain only a single gene that is homologous to *CAF4/MDV1*. Duplication of this ancestral gene gave rise to *CAF4* and *MDV1* in most *Saccharomyces* species, consistent with an origin resulting from whole genome duplication. The increased branch lengths in the Caf4 clade compared to the Mdv1 clade indicate that the Caf4 protein has undergone more amino substitutions than Mdv1 since the original duplication event. This observation suggests that Mdv1 is under tighter constraints to perform its essential function in mitochondrial fission, consistent with our functional analysis. One possible outcome of this accelerated rate of Caf4 protein evolution is that the *CAF4* gene will ultimately be lost from the *Saccharomyces* genome. However, it

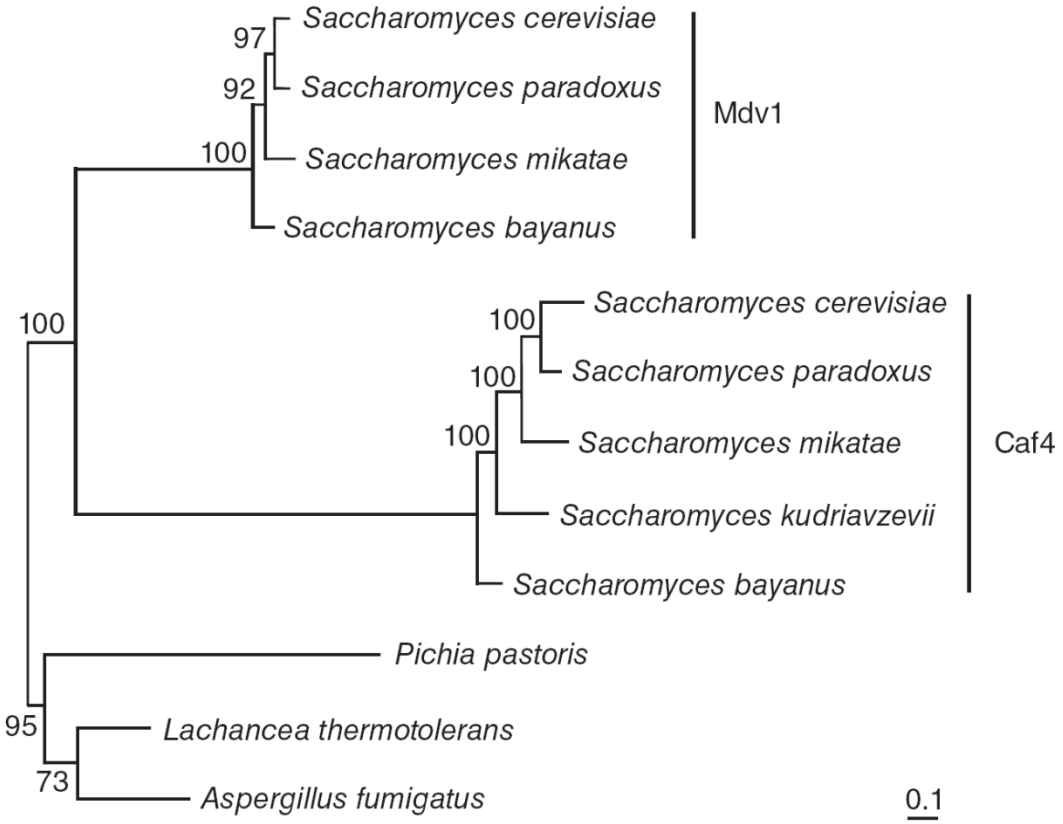

Figure 2.5. Phylogenetic relationship of Caf4 and Mdv1 in representative fungi. The amino acid sequences of paralogs from fully sequenced fungal genomes were aligned using ClustalW2 and a phylogenetic tree was constructed using the maximum-likelihood method. Bootstrap values above 50 are shown at the nodes of the branches. Branch lengths are proportional to the number of amino acid substitutions per site. The Caf4 and Mdv1 clades are marked by vertical lines. Scale bar: 0.1 substitution per site in the protein.

appears that *MDV1*, but not *CAF4*, was lost from *Saccharomyces kudriavzevii*. Thus, Caf4 can either substitute for Mdv1 function or a completely different protein has assumed the essential role in membrane fission in this species. An alternative outcome in species with both proteins is that Caf4 will acquire additional or novel function(s) (see discussion).

Disscusion

Prior to this study, the Caf4 adaptor was known to function early in fission to recruit Dnm1 to the outer mitochondrial membrane. However, whether Caf4 participated in mitochondrial membrane fission after Dnm1 recruitment was unclear. Our results provide a direct demonstration that, in the absence or presence of Mdv1, Caf4 localizes in complexes on mitochondria that carry out membrane division.

It has been suggested that Caf4 serves as regulator of mitochondrial fission. We think it is unlikely that Caf4 acts as a positive regulator, since its presence or absence has little effect on Mdv1-mediated fission in WT cells. Several observations also suggest that Caf4 does not act as a negative regulator. When Caf4 is expressed in the absence of Mdv1, fission occurs and the time course of fission is similar to WT. In addition, when Caf4 and Mdv1 are both present in mitochondrial puncta, fission appears to occur normally. However, Caf4 and Mdv1 are not functionally equivalent. When expressed at maximum levels from the *MET25* promoter, Caf4 (but not Mdv1) causes dominant-negative fission defects. Moreover, expression of the *CAF4* gene from the *MDV1* promoter in the genome is not sufficient to restore mitochondrial fission to levels observed in an *MDV1 caf4*Δ strain.

In many instances, one member of a duplicated gene pair is retained during evolution because it develops a specialized function (subfunctionalization) within a cellular process or because it acquires an entirely new function (neofunctionalization) (Kafri et al., 2009). There is evidence that Caf4 has acquired a specialized function in mitochondrial biology. Jakob and colleagues showed previously that Caf4 (but not Mdv1) plays a role in orienting a subset of mitochondrial Dnm1 puncta toward the yeast cell cortex (Schauss et al., 2006). This Dnm1 orientation is proposed to anchor mitochondria near the plasma membrane and distribute them at the cell periphery. Caf4 has also been shown to participate with Dnm1, Mdv1 and Fis1 in peroxisome division (Hofmann et al., 2009; Motley et al., 2008). Although it is possible that Caf4 has acquired specialized functions in peroxisome division, we do not observe changes in peroxisome morphology in *caf4*Δ cells relative to WT (data not shown). Moreover, cells lacking Caf4 grow as well as WT on carbon sources that require peroxisome function (i.e. oleate, data not shown). If Caf4 had acquired a new function in a critical cellular process, loss of Caf4 would be expected to affect yeast fitness. However, our extensive analyses of *caf4*Δ cells have not uncovered conditions that confer a fitness advantage or disadvantage relative to WT with respect to cell growth, sporulation, mtDNA maintenance, mitochondrial respiratory function, or drug sensitivity (data not shown). Future studies competing a *caf4*Δ mutant against wildtype strains under additional conditions may uncover a more subtle fitness cost.

Our phylogenetic analysis revealed a slightly accelerated rate of amino acid substitution for Caf4 relative to Mdv1. However, both adaptors have retained roles in mitochondrial fission, arguing against the idea that the *CAF4* gene is likely to be lost, like

many other paralogs originating from whole gene duplication. Instead, Caf4 and Mdv1 appear to work synergistically, with Mdv1 carrying out the majority of fission in proportion to its higher level of expression. Consistent with this model, we find that Caf4 and Mdv1 are cross-regulated, with Caf4 expression increasing when Mdv1 is absent. The fact that Caf4 has acquired the ability to orient Dnm1 at the cell cortex (Schauss et al., 2006) also supports the idea that the *CAF4* gene has been retained because it confers some type of selective advantage. It remains to be determined whether/how the Dnm1-orienting ability of Caf4 measurably contributes to overall fitness in yeast, and how species like *S. kudriavzevii* have compensated for the loss of Mdv1.

Materials and methods

Growth conditions, strains and plasmids

Yeast strains and plasmids used in this study are listed in supplementary material Table 2.1 and 2.2. Unless noted in the figure legend, standard rich or synthetic dropout media were used for growth, transformation and genetic manipulation of *S. cerevisiae* (Guthrie and Fink, 1991) and *E. coli* (Maniatis et al., 1982). Standard synthetic dextrose medium contains 0.6 mM methionine and cysteine.

The *CAF4* gene encodes two potential initiation codons that could result in methionine at positions 1 and 17 of the predicted protein. To determine whether this 16 amino acid difference at the N-terminus affected Caf4 function, we expressed proteins initiated from each methionine codon under control of the *MET25* promoter. Because we observed no difference in steady-state abundance or fission function of the two proteins (data not shown), the longer version was used for all constructs described in this study.

Table 2.1. Plasmids used in yeast adaptors study

Strain ID	Plasmid	Protein Expressed	Reference
B493	pRS415-*MET25*	None	ATCC 87322
B494	pRS416-*MET25*	None	ATCC 87324
B1642	pRS414-*GPD-mt-ffRFP*	*N. crassa* ATP9(1-69) + fast folding DsRed (RFP)	Karren et al., 2005
B2053	pRS416-*MET25-MDV1*	Mdv1	Karren et al., 2005
B2212	pRS416-*MET25-CAF4*	Caf4	This Study
B2290	pRS415-*MET25-GFP-CAF4*	GFP-Caf4	This Study
B2291	pRS416-*MET25-ffRFP-MDV1*	RFP-Mdv1	This Study
B2384	pRS415-*MET25-GFP-MDV1*	GFP-Mdv1	This Study
B2408	pRS416-*MET25-ffRFP-CAF4*	RFP-Caf4	This Study
B3002	p414-*GPD-mt-mCherry*	*N. crassa* ATP9(1-69) + mCherry	This Study

Table 2.2. Yeast strains used in yeast adaptors study

Strain ID	Mating type	Genotype	Reference
JSY5740	*MAT**a***	*ura3-52 leu2Δ1 his3Δ200 trp1Δ63*	Koirala et al., 2010
JSY8612	*MAT**a***	*ura3-52 leu2Δ1, his3Δ200, trp1Δ63, caf4::KanMx, mdv1::HIS3*	Koirala et al., 2010
JSY8614	*MAT**a***	*ura3-52 leu2Δ1 his3Δ200 trp1Δ63 caf4::KanMx*	This Study
JSY8616	*MAT**a***	*ura3-52 leu2Δ1 his3Δ200 trp1Δ63 mdv1::HIS3*	This Study
JSY9774	*MAT**a***	*ura3-52 leu2Δ1 his3Δ200 trp1Δ63 lys2Δ202 caf4::KanMX mdv1::MET-EYFP-MDV1 ho::MET25-Cerulean-CAF4*	This Study
JSY9886	*MAT**a***	*ura3-52 leu2Δ1 his3Δ200 trp1Δ63 lys2Δ202 caf4::KanMX mdv1::CAF4*	This Study
JSY9903	*MAT**a***	*ura3-52 leu2Δ1 his3Δ200 trp1Δ63 caf4::MDV1, mdv1::HIS3*	This Study

Plasmids pRS414-*GPD-mt-ffRFP* and pRS416-*MET25-MDV1* were described previously (Karren et al., 2005; Koirala et al., 2010). pRS414-*GPD-mt-mCherry* was generated by PCR amplification of the mCherry open reading frame that was cloned into the EcoRI and XhoI sites of pRS414-*GPD*-mt after digestion and removal of *ffRFP* by the same enzymes. pRS416-*MET25-CAF4* was generated by PCR amplification of the *CAF4* open reading frame that was cloned into the BamHI and SalI sites of pRS416-*MET25*. To construct pRS415-*MET25-GFP-CAF4*, the PCR amplified *CAF4* open reading frame was cloned into the BamHI and SalI sites of pRS416-*MET25-GFP*. To construct pRS415-*MET25-GFP-MDV1*, the PCR amplified *MDV1* open reading frame was cloned into the BamHI and SalI sites of pRS416-*MET15-GFP*. To construct pRS416-*MET25-ffRFP-MDV1*, the PCR amplified *ffRFP* coding region was cloned into the SpeI and BamHI sites of pRS416-*MET25-MDV1*. To construct pRS416-*MET25-RFP-CAF4*, PCR amplified *CAF4* was cloned into the BamHI and SalI sites of pRS-*MET25-RFP*.

Western blotting and protein quantification

Protein expression and abundance was analyzed in yeast whole cell extracts prepared by the alkaline extraction method (Kushnirov, 2000). 0.25 OD_{600} equivalents of extract was separated by SDS-PAGE and analyzed by Western blotting using the following primary antibodies: anti-yeast actin (1:5000, J. Cooper, Washington University Saint Louis), α-3-PGK (1: 5000, Invitrogen), anti-Mdv1 (1:1000, J. Nunnari, U. C. Davis) and anti-Caf4 (1:250, generated against bacterially expressed, 6His-Caf4 amino acids 175-659). Primary antibodies were detected using fluorescent secondary anti-goat, anti-

rabbit or anti-mouse IRDye 800 (LiCor). Fluorescent signals were quantified using an Odyssey scanner and Odyssey 3.0 analysis software (LiCor). In Figure 2.2B, anti-Caf4 or anti-Mdv1 signals were first normalized to anti-actin signals. The abundance of each protein was subsequently normalized to its abundance in 2.0 mM methionine. In Figure 2.3B, anti-Caf4 or anti-Mdv1 signals were normalized to anti-3-PGK. In all experiments, data are represented as the mean and SD of three independent experiments.

Quantification of mitochondrial morphology

Mitochondrial morphology was scored in WT and mutant cells expressing fast folding matrix-targeted red fluorescent protein (mt-ffRFP) as prescribed previous (Koirala et al., 2010). Strains were grown at 30°C in selective dextrose synthetic medium and scored in log phase (0.2-0.8 OD_{600}). Basal expression levels of Mdv1 and Caf4 proteins from the *MET25* promoter under these conditions result in an approximately five fold increase over endogenous Mdv1 or Caf4 protein levels with no adverse affects on mitochondrial morphology or fission (Karren et al., 2005)(data not shown). For the methionine titration experiments in Figure 2.2A, *caf4*Δ *mdv1*Δ (adaptor null JSY8612 cells) expressing the indicated Caf4 and Mdv1 proteins from the *MET25* promoter were grown in selective dextrose medium at 30°C overnight. Cultures were diluted to 0.2 OD_{600} in selective dextrose medium lacking cysteine and containing the indicated concentrations of methionine to suppress expression from the *MET25* promoter. Cultures were grown for 3 hours prior to scoring. Mitochondrial phenotypes were scored in 100 cells, and data are represented as the average and SD of three independent experiments.

Colocalization studies

Log phase *caf4*Δ *mdv1*Δ cells expressing GFP- or RFP-labeled Mdv1 and Caf4 were grown in standard selective dextrose medium, fixed in 4% formaldehyde (Fisher Scientific) for 5 minutes at room temperature and washed three times with phosphate buffered saline (PBS, 137mM NaCl, 2.7mM KCl, 4.3mM Na_2HPO_4, 1.47mM KH_2PO_4, pH 7.4). Cells were imaged on a Nikon fluorescence microscope using a 100X oil immersion objective, EGFP and DsRed filters and a Coolsnap HQ digital camera (Phototmetrics). Z-stacks (0.2 µm optical sections) were acquired and processed using the DeltaVisionRT system and accompanying DeltaVision software (Applied Precision, Issaquah, WA). Colocalization of GFP and RFP signals was determined in three dimensions using the Orthogonal View function of the DeltaVision software. The number of GFP puncta colocalized with RFP puncta was quantified and normalized to the total number of RFP puncta in each cell (n=10 cells). Bars and error bars represent the average and SD of three independent experiments.

Time-lapse imaging

For dual-color time-lapse imaging, log phase *caf4*Δ *mdv1*Δ cells expressing GFP-Caf4 and mitochondrial targeted RFP were grown in standard selective synthetic dextrose medium and applied to concanavalin A (2 mg/ml, Sigma) treated Lab-tek II Chamber wells (Thermo Scientific) maintained at 30°C. Z-stacks (0.2 µm optical sections) of fields of cells were acquired every seven seconds over a 20-minute time course using a 3-I Marianas Live Cell Imaging microscope workstation (Denver, CO), equipped with dual ultra-sensitive Cascade II 512B EMCCD cameras (Roper Scientific, RS) configured with

a Roper Dual-cam and Sutter DG-4 Illuminator (Sutter Instruments) for simultaneous two-channel TIRF/fluorescence acquisition with a 100X, 1.45 NA Plan-Apochromat objective (Zeiss). Data were deconvolved and analyzed using SlideBook 4.2 software (Intelligent Imaging Innovations, Inc). Substacks containing fission events were isolated from the entire stack to minimize signal background and assembled in Photoshop (CS3, Adobe). Brightness and contrast were adjusted using only linear operations applied to the entire image.

Three-color time-lapse imaging was carried out as described above with the following changes. Log phase *caf4*Δ *mdv1*Δ cells expressing integrated Cerulean-Caf4 and EYFP-Mdv1 from the *MET25* promoter (JSY9774) and plasmid-borne mt-mCherry were grown overnight at 30°C in selective synthetic dextrose medium. Cultures were diluted to 0.3 OD_{600} in medium lacking cysteine and containing 1.0 mM methionine 3 hours before imaging. Z-stacks (0.2 µm optical sections) of fields of cells were acquired every ten seconds over a 25-minute time course using a CerFP/EYFP/mCherry filter set (Semrock) and dual Cascade II 512B EMCCD cameras and Sutter DG-4 illuminator (Sutter Instruments) for imaging EYFP, mCherry, and Cerulean signals.

Phylogenetic Analysis

Blast (NCBI) was used to identify homologs of Caf4 and Mdv1. The genomic sequences of homologs were identified via the Saccharomyces Genome Database and GOLD (Genomes OnLine Database). Predicted protein sequences used to generate this tree were obtained from: YKR036C (*S. cerevisiae CAF4*), YJL112W (*S. cerevisiae MDV1*), PORF 13363 (*S. paradoxus CAF4*), PORF 11728 (*S. paradoxus MDV1*), PROF

13800 (*S. mikatae CAF4*), Contig 2819.8 (*S. mikatae MDV1*), PROF 15127 (*S. bayanus CAF4*), PROF 12617 (*S. bayanus MDV1*), Contig 1606.5 (*S. kudriavzevii CAF4*), GS115 (*P. pastoris ortholog*), KLTH0E15576p (*L. thermotolerans ortholog*), Af293 (*A. fumigatus ortholog*). Amino acid sequences were aligned using ClustalW2 (European Bioinformatics Institute) and indels were removed. PhyML (European Bioinformatics Institute) was used to calculate and assemble the phylogenetic tree.

Acknowledgement

We thank Jane Macfarlane for expertise in mutagenesis and plasmid construction, members of the Shaw laboratory for critical discussions, Nels Elde for guidance with phylogenetic tree construction and Markus Babst for use of his DeltaVision microscope. We also thank Beverly Wendland for use of her lab space while performing experiments in the Johns Hopkins Integrated Imaging Center. Sequencing and oligonucleotide synthesis services were provided by University of Utah Core Facilities.

References

Bleazard, W., McCaffery, J. M., King, E. J., Bale, S., Mozdy, A., Tieu, Q., Nunnari, J., and Shaw, J. M. (1999). The dynamin-related GTPase Dnm1 regulates mitochondrial fission in yeast. Nat Cell Biol *1*, 298-304.

Cerveny, K. L., and Jensen, R. E. (2003). The WD-repeats of Net2p interact with Dnm1p and Fis1p to regulate division of mitochondria. Mol Biol Cell *14*, 4126-4139.

Cerveny, K. L., McCaffery, J. M., and Jensen, R. E. (2001). Division of mitochondria requires a novel DMN1-interacting protein, Net2p. Mol Biol Cell *12*, 309-321.

Ghaemmaghami, S., Huh, W. K., Bower, K., Howson, R. W., Belle, A., Dephoure, N., O'Shea, E. K., and Weissman, J. S. (2003). Global analysis of protein expression in yeast. Nature *425*, 737-741.

Goffeau, A., Barrell, B. G., Bussey, H., Davis, R. W., Dujon, B., Feldmann, H., Galibert, F., Hoheisel, J. D., Jacq, C., Johnston, M., et al. (1996). Life with 6000 genes. Science *274*, 546, 563-547.

Gorsich, S. W., and Shaw, J. M. (2004). Importance of mitochondrial dynamics during meiosis and sporulation. Mol Biol Cell *15*, 4369-4381.

Griffin, E. E., Graumann, J., and Chan, D. C. (2005). The WD40 protein Caf4p is a component of the mitochondrial fission machinery and recruits Dnm1p to mitochondria. J Cell Biol *170*, 237-248.

Guthrie, C., and Fink, G. R. (1991). Guide to yeast genetics and molecular biology. Methods Enzymol *194*, 1-863.

Hofmann, L., Saunier, R., Cossard, R., Esposito, M., Rinaldi, T., and Delahodde, A. (2009). A nonproteolytic proteasome activity controls organelle fission in yeast. J Cell Sci *122*, 3673-3683.

Ingerman, E., Perkins, E. M., Marino, M., Mears, J. A., McCaffery, J. M., Hinshaw, J. E., and Nunnari, J. (2005). Dnm1 forms spirals that are structurally tailored to fit mitochondria. J Cell Biol *170*, 1021-1027.

Kafri, R., Springer, M., and Pilpel, Y. (2009). Genetic redundancy: new tricks for old genes. Cell *136*, 389-392.

Karren, M. A., Coonrod, E. M., Anderson, T. K., and Shaw, J. M. (2005). The role of Fis1p-Mdv1p interactions in mitochondrial fission complex assembly. J Cell Biol *171*, 291-301.

Kellis, M., Birren, B. W., and Lander, E. S. (2004). Proof and evolutionary analysis of ancient genome duplication in the yeast Saccharomyces cerevisiae. Nature *428*, 617-624.

Koirala, S., Bui, H. T., Schubert, H. L., Eckert, D. M., Hill, C. P., Kay, M. S., and Shaw, J. M. (2010). Molecular architecture of a dynamin adaptor: implications for assembly of mitochondrial fission complexes. J Cell Biol *191*, 1127-1139.

Kushnirov, V. V. (2000). Rapid and reliable protein extraction from yeast. Yeast *16*, 857-860.

Legesse-Miller, A., Massol, R. H., and Kirchhausen, T. (2003). Constriction and Dnm1p recruitment are distinct processes in mitochondrial fission. Mol Biol Cell *14*, 1953-1963.

Maniatis, T., Fritsch, E. F., and Sambrook, J. (1982). Molecular Cloning: A Laboratory Manual (Cold Spring Harbor, NY: Cold Spring Harbor Laboratory Press).

Motley, A. M., Ward, G. P., and Hettema, E. H. (2008). Dnm1p-dependent peroxisome fission requires Caf4p, Mdv1p and Fis1p. J Cell Sci *121*, 1633-1640.

Mozdy, A. D., McCaffery, J. M., and Shaw, J. M. (2000). Dnm1p GTPase-mediated mitochondrial fission is a multi-step process requiring the novel integral membrane component Fis1p. J Cell Biol *151*, 367-380.

Musso, G., Zhang, Z., and Emili, A. (2007). Retention of protein complex membership by ancient duplicated gene products in budding yeast. Trends Genet *23*, 266-269.

Nunnari, J., Marshall, W. F., Straight, A., Murray, A., Sedat, J. W., and Walter, P. (1997). Mitochondrial transmission during mating in Saccharomyces cerevisiae is determined by mitochondrial fusion and fission and the intramitochondrial segregation of mitochondrial DNA. Mol Biol Cell *8*, 1233-1242.

Okamoto, K., and Shaw, J. M. (2005). Mitochondrial morphology and dynamics in yeast and multicellular eukaryotes. Annu Rev Genet *39*, 503-536.

Otsuga, D., Keegan, B. R., Brisch, E., Thatcher, J. W., Hermann, G. J., Bleazard, W., and Shaw, J. M. (1998). The dynamin-related GTPase, Dnm1p, controls mitochondrial morphology in yeast. J Cell Biol *143*, 333-349.

Schauss, A. C., Bewersdorf, J., and Jakobs, S. (2006). Fis1p and Caf4p, but not Mdv1p, determine the polar localization of Dnm1p clusters on the mitochondrial surface. J Cell Sci *119*, 3098-3106.

Sesaki, H., and Jensen, R. E. (1999). Division versus fusion: Dnm1p and Fzo1p antagonistically regulate mitochondrial shape. J Cell Biol *147*, 699-706.

Tieu, Q., and Nunnari, J. (2000). Mdv1p is a WD repeat protein that interacts with the dynamin-related GTPase, Dnm1p, to trigger mitochondrial division. J Cell Biol *151*, 353-366.

Tieu, Q., Okreglak, V., Naylor, K., and Nunnari, J. (2002). The WD repeat protein, Mdv1p, functions as a molecular adaptor by interacting with Dnm1p and Fis1p during mitochondrial fission. J Cell Biol *158*, 445-452.

Wolfe, K. H., and Shields, D. C. (1997). Molecular evidence for an ancient duplication of the entire yeast genome. Nature *387*, 708-713.

Zhang, Y., and Chan, D. C. (2007). Structural basis for recruitment of mitochondrial fission complexes by Fis1. Proc Natl Acad Sci U S A *104*, 18526-18530.

Zhang, Y., Chan, N. C., Ngo, H. B., Gristick, H., and Chan, D. C. (2012). Crystal structure of mitochondrial fission complex reveals scaffolding function for mitochondrial division 1 (Mdv1) coiled coil. J Biol Chem *287*, 9855-9861.

CHAPTER 3

MULTIPLE ADAPTORS REGULATE MITOCHONDRIAL DYNAMIN GTPASE ASSEMBLY FOR MEMBRANE SCISSION

Sajjan Koirala, Qian Guo*, Raghav Kalia*, Debra M. Eckert,

Adam Frost and Janet M. Shaw

*These authors contributed equally to this study

Introduction

Dynamin-related proteins (DRPs) are self-assembling GTPases that regulate lipid remodeling events at different cellular membranes (Praefcke and McMahon, 2004). Two of these DRPs, Dnm1 (yeast) and Drp1 (human), play conserved roles in mitochondrial fission, which is important for biological processes including mitochondrial inheritance during cell division (Gorsich and Shaw, 2004; Taguchi et al., 2007), clearance of defective mitochondria via mitophagy (Gomes et al., 2011; Parone et al., 2008; Rambold et al., 2011; Twig et al., 2008) and mammalian development (Ishihara et al., 2009; Wakabayashi et al., 2009).

In vivo, both the Dnm1 and Drp1 GTPases assemble from the cytoplasm into structures that encircle mitochondria at sites of future fission (Bleazard et al., 1999; Labrousse et al., 1999; Otsuga et al., 1998; Sesaki and Jensen, 1999). In vitro, addition of GTP to Dnm1-lipid tubules is sufficient to constrict synthetic liposomes (Ingerman et al., 2005; Mears et al., 2011). However, a recent study revealed that mitochondrial constriction in yeast and mammals occurs at sites where endoplasmic reticulum (ER) tubules circumscribe mitochondria (Friedman et al., 2011). This ER-mediated mitochondrial constriction occurs prior to Dnm1 or Drp1 recruitment, suggesting that DRPs act after the initial constriction event to complete membrane fission. Neither Dnm1 nor Drp1 has ever been shown to independently catalyze membrane scission in vivo or in vitro.

A variety of adaptor proteins localized to the outer mitochondrial membrane (OMM) play important, but poorly understood, roles in Dnm1/Drp1 recruitment and function. The membrane recruitment step is best understood in yeast, where Dnm1 binds

to the fungal-specific adaptor Mdv1 (Cerveny et al., 2001; Tieu and Nunnari, 2000), which is in turn bound to the tail-anchored Fis1 protein (Mozdy et al., 2000). Fluorescence microscopy studies show that Mdv1 colocalizes with Dnm1 at sites of mitochondrial fission (Naylor et al., 2006). In vitro, Mdv1 interacts with the GTP-bound form of Dnm1 and stimulates Dnm1 self-assembly (Lackner and Nunnari, 2009).

Fis1 is conserved in humans (hFis1), but does not appear to recruit Drp1 to mitochondria. Instead, Drp1 recruitment is mediated by Mff, another tail-anchored protein (Gandre-Babbe and van der Bliek, 2008; Otera et al., 2010). Two additional human proteins, the orthologs MiD49 and MiD51, are N-terminally anchored in the OMM and also play a role in Drp1 recruitment (Palmer et al., 2011; Zhao et al., 2011). Neither Mff or MiDs are related by sequence or predicted secondary structure to Mdv1. The Mff and MiD49/51 proteins form rings surrounding mitochondria, suggesting that they coassemble with Drp1 (Palmer et al., 2011); however, their specific roles in Drp1 assembly and membrane scission are not well understood. Thus, major unanswered questions remain regarding whether or not adaptor proteins participate in lipid remodeling and membrane scission and whether they act independently or in concert in vivo.

Here we use a yeast strain devoid of fission proteins to identify the minimal combination of DRPs and adaptors sufficient for mitochondrial fission. We provide new evidence that Fis1 is dispensable for mitochondrial membrane scission. We also demonstrate that Mdv1, Mff, or MiDs paired individually with their respective DRPs are interchangeable, in that each is sufficient to catalyze fission. Importantly, co-assembly of a MiD protein with Drp1 dramatically decreases the diameter of the Drp1 structures

formed. This result provides a direct demonstration that an adaptor protein can alter the architecture of a DRP assembly in a manner that could facilitate their membrane constriction and severing ability.

Results

Requirements of individual yeast proteins for mitochondrial fission

In WT yeast, opposing fission and fusion events maintain branched mitochondrial tubules positioned at the cell cortex. When fission is disrupted, fusion continues unopposed and cells contain mitochondrial nets or a single, interconnected mitochondrion, which often collapses to one side of the cell (Bleazard et al., 1999; Otsuga et al., 1998). To determine the minimal protein requirements for fission, we generated a yeast 'tester' strain lacking Dnm1, the Mdv1 adaptor and Fis1. This strain also lacked a paralog of the Mdv1 adaptor, Caf4, which was previously shown to be dispensable for fission in vivo (Griffin et al., 2005). This tester strain exhibited severe mitochondrial fission defects but was viable, grew as well as WT on a variety of media, and did not show increased mitochondrial DNA loss (unpublished data). To identify the minimal set of proteins sufficient for fission, we expressed combinations of wildtype (WT) and mitochondrial membrane-tethered Dnm1 and Mdv1 in the tester strain. Immunoblotting of whole cell extracts confirmed that all proteins were stably expressed at levels similar to the wildtype proteins in vivo (unpublished results). Mitochondrial morphology was then quantified to assess the ability of different protein combinations to restore WT mitochondrial fission and morphology.

Expression of cytoplasmic Dnm1, or Dnm1 tethered to the outer mitochondrial membrane by its N- or C-terminus was unable to rescue mitochondrial fission defects in the tester strain (unpublished data). Pair wise combinations of cytoplasmic Dnm1 expressed with WT Fis1 or Mdv1 alone also failed to rescue mitochondrial morphology in this strain (unpublished results). By contrast, normal mitochondrial morphology was restored in 80% of the cells by expressing cytoplasmic Dnm1 together with WT Mdv1 and Fis1 (Figure 3.1B). To determine whether Fis1 was necessary for post Dnm1 recruitment steps in fission, we expressed cytoplasmic Dnm1 with full-length and truncated forms of Mdv1 tethered to the outer mitochondrial membrane by the Tom20 membrane anchor (T20, Figure 3.1A). Mdv1 contains three domains, an N-terminal extension (NTE) that binds Fis1 (Tieu et al., 2002), a middle domain that dimerizes Mdv1 via an antiparallel coiled-coil (CC) (Koirala et al., 2010), and a predicted β-propeller domain that interacts with Dnm1 (Cerveny and Jensen, 2003; Tieu et al., 2002) (Figure 3.1A). Surprisingly, although WT mitochondrial morphology was restored in strains expressing Dnm1 plus all three tethered forms of Mdv1, the full-length construct was not the most efficient. The lack of a Fis1 binding partner for the NTE domain in the full-length Mdv1 construct may affect the conformation of the protein and be responsible for this effect. Consistent with this idea, the most efficient rescue occurred upon expression of the tethered Mdv1 coiled-coil plus β-propeller domain (lacking the NTE domain) (Figure 3.1B). The mitochondrial morphology rescue observed in these studies suggests that soluble Dnm1 and tethered forms of Mdv1 are sufficient to catalyze fission in the absence of Fis1.

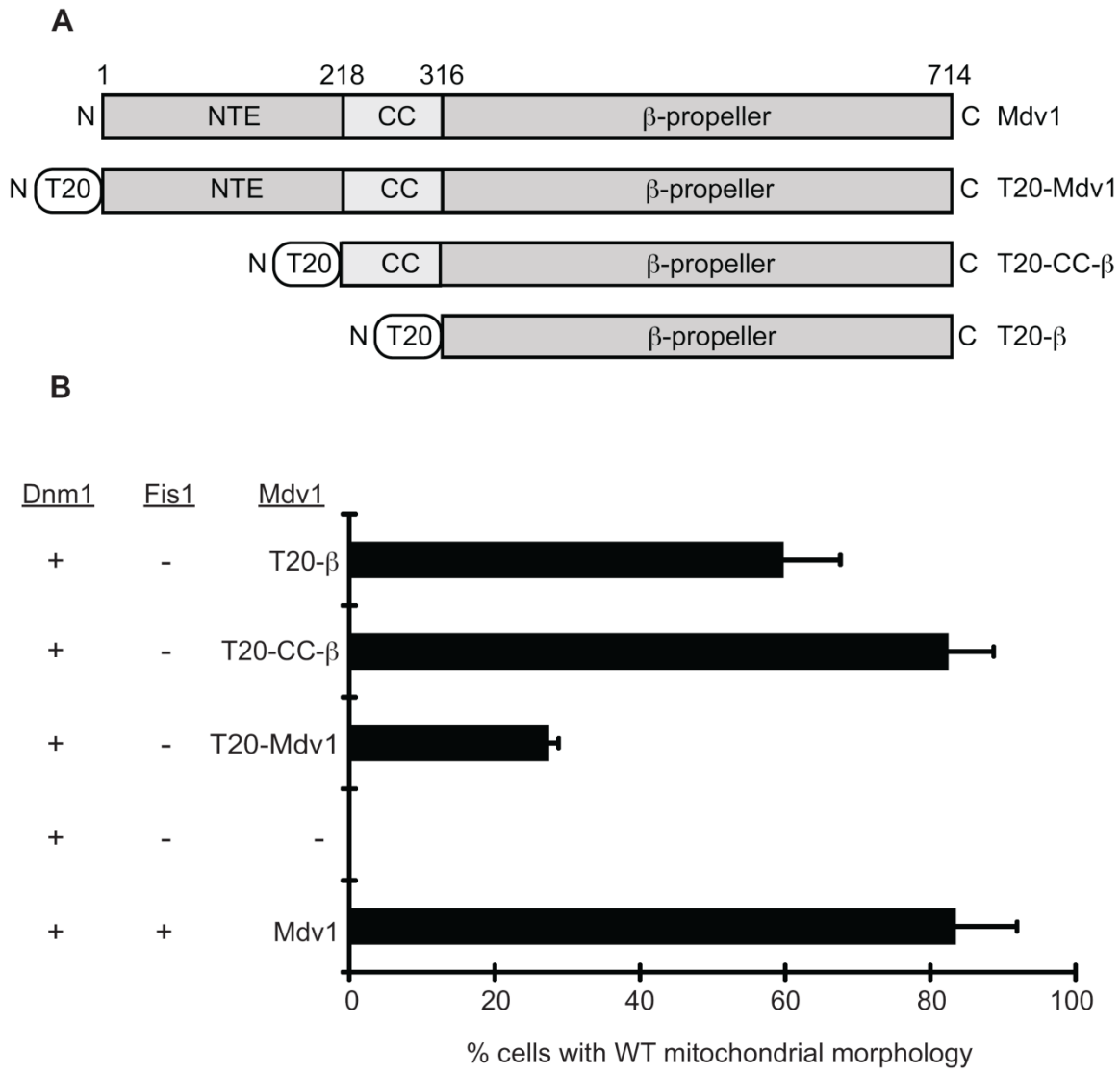

Figure 3.1. Fis1 is dispensable for mitochondrial fission. (A) Domain structure of WT Mdv1 and Mdv1 constructs fused to the N-terminal transmembrane anchor of yeast TOM20 (T20). NTE (N-terminal extension), CC (coiled coil), and predicted β-propeller domains are shown. (B) Quantification of mitochondrial morphology in cells expressing the indicated fission proteins. All values are mean ± SEM, n ≥ 300. A representative image of WT tubular mitochondria is shown in Figure 3.4C.

Fis1 is not essential for Dnm1 assembly into fission complexes or membrane scission

When cells lack Mdv1 and Fis1, GFP-Dnm1 cannot be recruited to mitochondria and instead remains in the cytoplasm (unpublished results). When WT Mdv1 and Fis1 are present, GFP-Dnm1 assembles into punctate fission complexes distributed evenly along mitochondrial tubules (Figure 3.2A and B, bottom row). Consistent with their ability to rescue fission defects, all three forms of tethered Mdv1 were able to recruit GFP-Dnm1 to mitochondria in the absence of Fis1 (Figure 3.2A and B). The formation and distribution of GFP-Dnm1 complexes were similar to that observed in WT cells (Figure 3.2B), despite the fact that fission complexes formed by two of the tethered Mdv1 proteins (T20-Mdv1, T20β) were less functional than Mdv1 T20-CC-β (Figure 3.1B). In vivo, yeast mitochondrial fission and fusion are coordinated, each process occurring approximately once every two minutes (Nunnari et al., 1997). Although the molecular basis of this coordination is unknown, the balance is critical for robust mitochondrial function (Twig and Shirihai, 2011). Quantification of fission and fusion events in time lapse imaging studies confirmed that these processes were balanced in our WT yeast strain (Figure 3.3A). We next determined whether the balance of fission and fusion was altered when fission occurred without Fis1 in the tester strain (Figure 3.3B). When cells expressed only cytoplasmic Dnm1, unopposed fusion formed interconnected mitochondria with few or no free tips. As a consequence, once the system achieved steady state, neither fission nor fusion was observed. By contrast, when cells expressed cytoplasmic Dnm1 and tethered forms of Mdv1, fission and fusion events were once

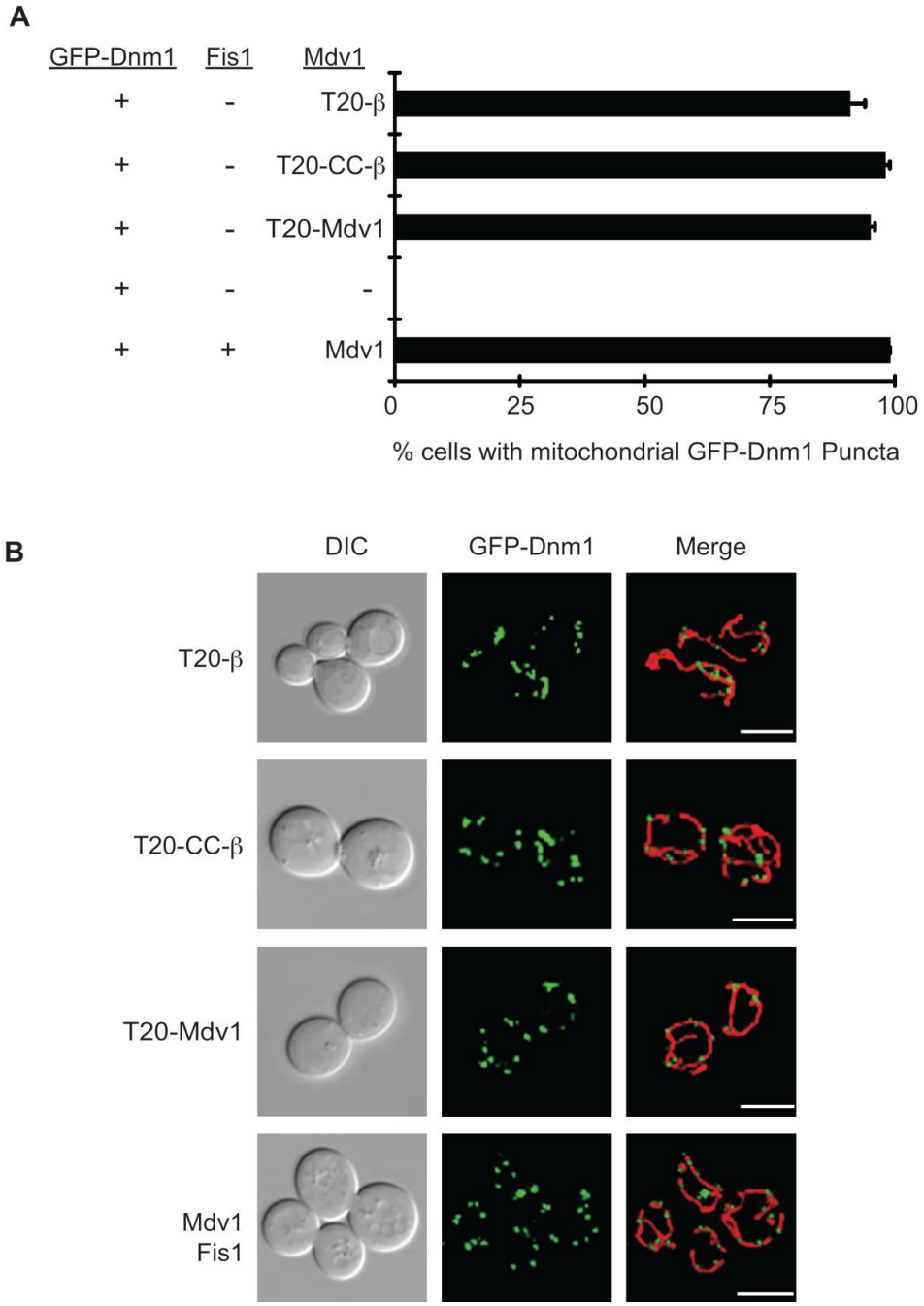

Figure 3.2. Dnm1 fission complexes assemble on mitochondria in the absence of Fis1. (A) Punctate GFP-Dnm1 fission complexes on mitochondria were quantified in strains expressing the indicated fission proteins. All values are mean ± SEM, n ≥ 300. (B) Representative images of GFP-Dnm1 puncta on mitochondria quantified in (A). Differential interference contrast (DIC), GFP-Dnm1, and merged mito-RFP (mitochondrial-matrix targeted dsRed) images are shown. Scale bar, 5 µm.

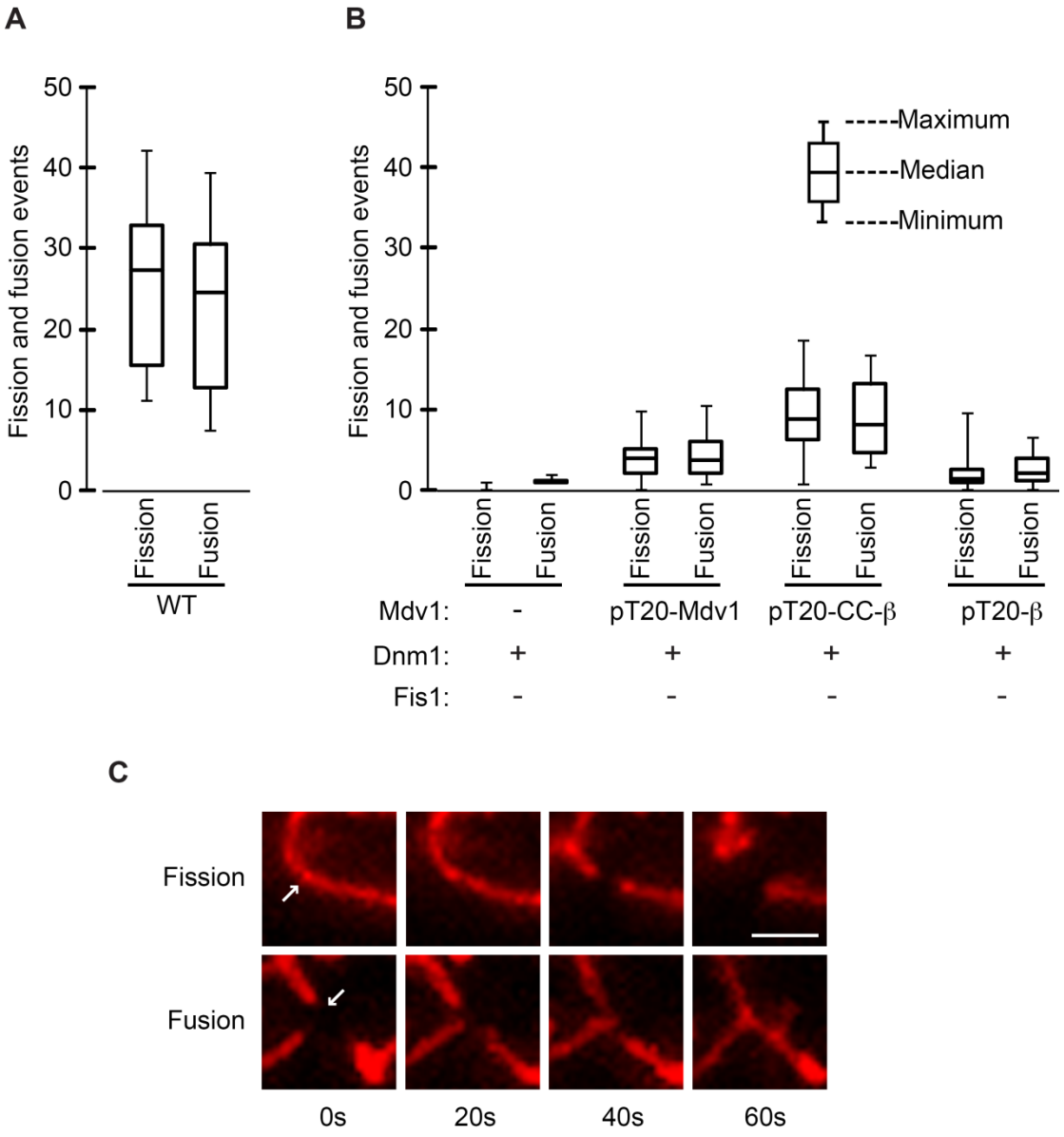

Figure 3.3. Mitochondrial fission and fusion events in cells lacking Fis1. Box-and-whisker plot showing the distribution of fission ($n \geq 10$ cells) and fusion ($n \geq 10$ cells) events in (A) WT and (B) strains expressing the indicated fission proteins. Total fission or fusion events per cell for a 20-minute interval are indicated. (C) Representative mito-RFP labeled mitochondria are shown undergoing fission (top, arrow) and fusion (bottom, arrow) in cells expressing Dnm1 and tethered Mdv1 (T20-β).

again balanced. Representative images of fission and fusion events in these cells are shown in Figure 3.3C. Together, our results demonstrate that after Mdv1 and Dnm1 are recruited to the mitochondrial surface, Fis1 is not required for assembly of functional fission complexes and the subsequent membrane scission event. Moreover, a balance between fission and fusion is achieved in these strains.

Mff or MiDs are sufficient to recruit human Drp1 to mitochondria and catalyze fission

The hFis1, Mff and MiD49/51 adaptors are all expressed in mammalian cells. As a consequence, it has been difficult to definitively determine whether these adaptors work individually or in concert to influence fission complex assembly or mitochondrial division after Drp1 membrane recruitment. To address this issue, we individually expressed OMM tethered forms of each adaptor protein with soluble Drp1 (variant 3, NP_005681.2) in the yeast testerstrain. To maintain their appropriate membrane topologies, the cytoplasmic domains of hFis1 and Mff were targeted using the yeast C-terminal Fis1 anchor (yTM) and the MiD proteins were targeted using the yeast N-terminal Tom20 anchor (T20) (Figure 3.4A).

In the absence of Drp1, expression of any of the three tethered forms shown in Figure 3.4A individually or in combination did not rescue fission defects (unpublished results). In addition, mitochondrial fission was not rescued by expression of Drp1 alone (unpublished results) or Drp1 with tethered hFis1 (Figure 3.4B). The latter result is consistent with a previous report that hFis1 is not essential for Drp1 recruitment in mammalian cells (Otera et al., 2010). By contrast, expression of soluble Drp1 with

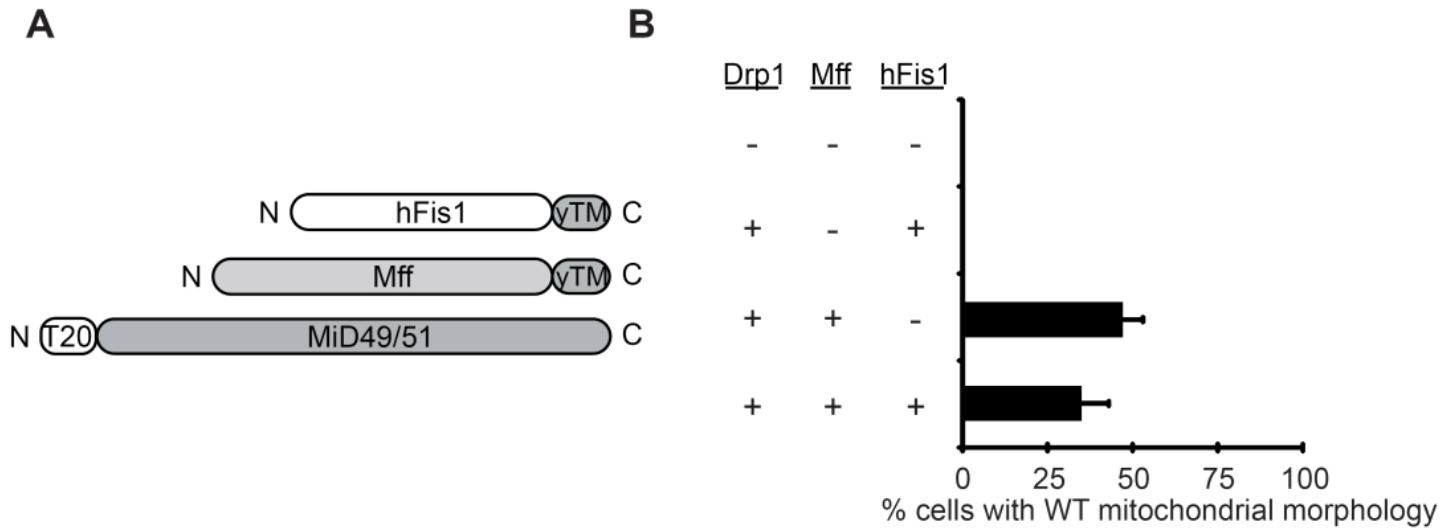

Figure 3.4. Mammalian Drp1 and mitochondrial-tethered adaptor proteins rescue mitochondrial fission defects in yeast. (A) Domain structures of human Fis1 (hFis1) and Mff fused to the C-terminal outer membrane anchor of yeast Fis1 (yTM). Human MiD49 or MiD51 were targeted to the mitochondrial outer membrane via fusion to the N-terminal transmembrane anchor of yeast Tom20 (T20). (B) Quantification of mitochondrial morphology in cells expressing Mff plus the indicated fission proteins and mito-OMGFP. All values are mean ± SEM, n ≥ 300. (C) The graph shows quantification of mitochondrial morphologies observed in cells during induction of Drp1 and MiD51 from the *MET25* promoter. The merged DIC and mito-OMGFP images to the right of the graph are representative of the mitochondrial morphology categories scored. Scale bar, 5 µm. (D) Time-lapse images of GFP-Drp1 at fission sites in cells expressing Mff (top), MiD49 (middle) or MiD51 (bottom). Boxed regions mark fission sites imaged at 30 second intervals in each row. Scale bar, 2 µm.

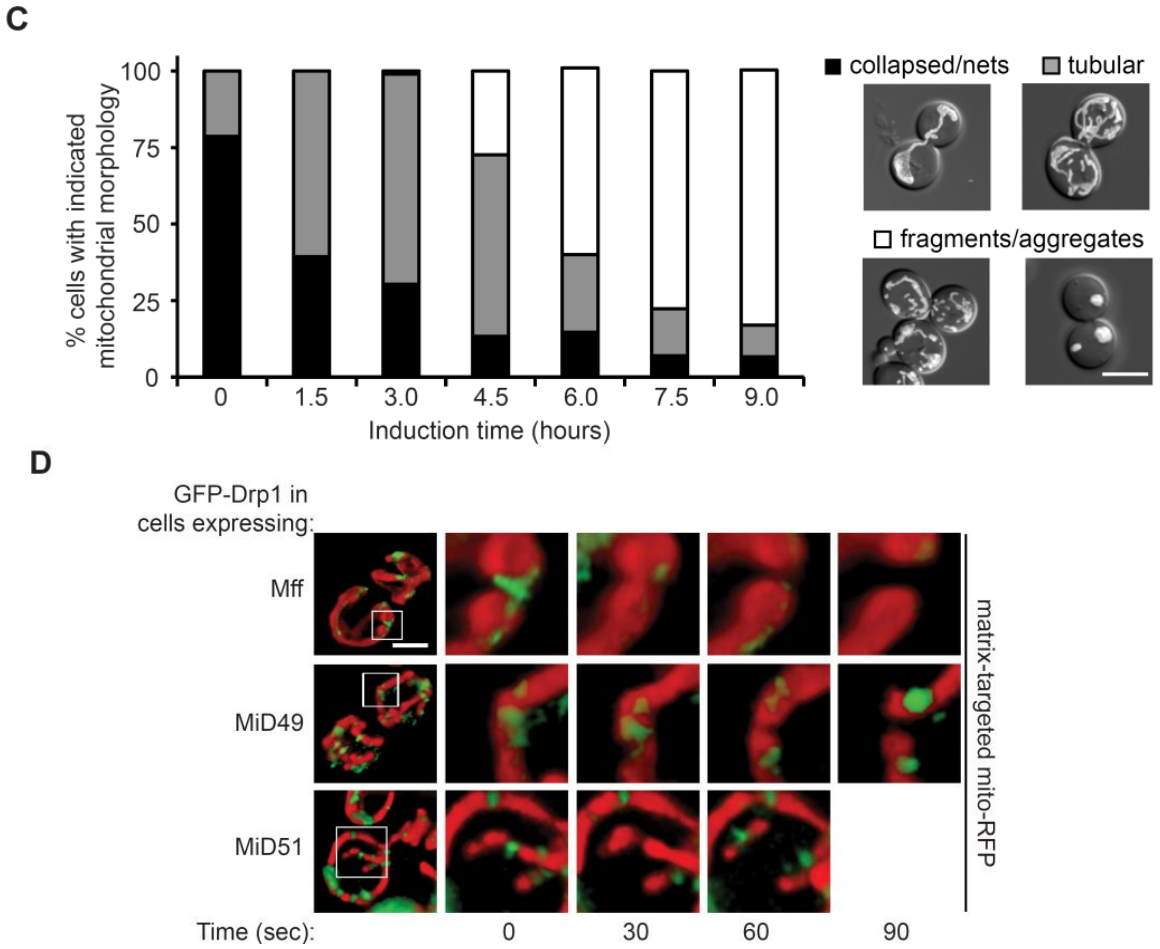

Figure 3.4. continued.

tethered Mff was sufficient to partially rescue mitochondrial fission and WT mitochondrial morphology in vivo (Figure 3.4B). Expressing tethered hFis1 in addition to Mff had little effect on this rescue. Thus, hFis1 does not appear to impact fissionmediated by Drp1 and tethered Mff in this system.

We also examined mitochondrial fission rescue in a tester strain expressing Drp1 and MiD51 from the repressible *MET25* promoter. Prior to induction (Figure 3.4C, 0 hour.),approximately 79% of the cells in the population contained collapsed mitochondria and interconnected nets characteristic of a fission defect (Figure 3.4C, black). The remaining 21% contained WT tubular mitochondria (Figure 3.4C, grey) due to the fact that the *MET25* promoter is inefficiently repressed under these conditions and produces low levels of both Drp1 and MiD51 proteins. WT mitochondrial morphology increased to 61% and 69% after 1.5 or 3.0 hours of MiD51 induction, respectively, suggesting that cytoplasmic Drp1 and tethered MiD51 are sufficient to catalyze fission in the yeast tester strain. Upon further induction (4.5-9 hours), the percentage of cells containing tubular mitochondrial morphology was reduced and the percentage of the population containing fragmented and aggregated mitochondrial membranes steadily increased from 27% to 83% (Figure 3.4C, white). This aggregated mitochondrial phenotype was also observed when MiD49 and MiD51 were over expressed in mammalian cells (Palmer et al., 2011). Similar results were obtained when the experiment was performed with MiD49 in place of MiD51 (unpublished results).

Time-lapse imaging studies confirmed that the mitochondrial morphology changes observed upon expression of Drp1 with either Mff, MiD49 or MiD51 was due to mitochondrial fission. In our tester strain expressing functional GFP-Drp1 and Mff,

MiD49 or MiD51, green Drp1 puncta were observed on RFP-labeled mitochondrial tubules at sites where fission occurred (Figure 3.4D). Together, these results establish that Drp1 is able to function with multiple adaptors to catalyze mitochondrial membrane fission.

The effect of Mff and MiD adaptors on GTP hydrolysis by Drp1

To determine whether mammalian adaptor proteins altered the kinetic properties of Drp1, we purified untagged versions of all three proteins (Drp1, Mff and MiD49). Analytical ultracentrifugation studies are consistent with Drp1 and Mff forming dimers, while MiD49 behaves as a monomer in solution (Figure 3.5). As is characteristic of self-assembling GTPases in the dynamin family, Drp1 pelleted in low, but not high, ionic strength buffer in a standard sedimentation assay (Figure 3.6C). GTP-hydrolysis by Drp1 also increased up to 15 fold in low ionic strength buffer, indicating that self-assembly stimulated GTP hydrolysis (Figure 3.6A). Under assembly-stimulated conditions (low ionic strength, Figure 3.6B and D), the catalyticactivity of Drp1 (kcat = 6.5/min) was similar to that reported for the yeast mitochondrial dynamin dynamin Dnm1 (Lackner and Nunnari, 2009). However, the Drp1 catalytic activity shown here is 7.6 times greater than that reported previously for a CBP-Drp1 fusion protein (CBP, calmodulin-binding peptide) (Chang et al., 2010). It is possible that the N-terminal CBP tag on Drp1 or the bacterialof Mff (E) or MiD49 (F) purified from yeast were included at 0.5 μM. Similar results were obtained with Mff purified from yeast (shown here) and bacteria

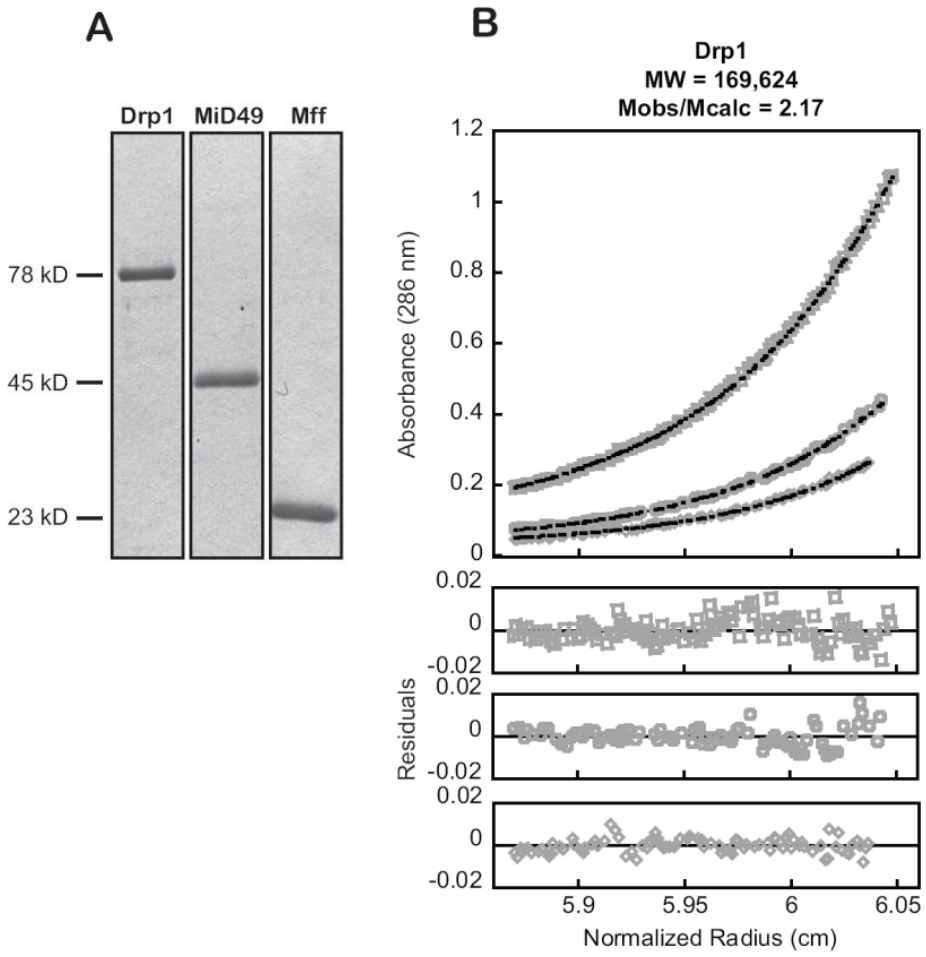

Figure 3.5. Purification and analytical equilibrium sedimentation analysis of Drp1, MiD49 and Mff. (A) SDS-PAGE of the indicated purified proteins stained with Coomassie Brilliant Blue. Analytical equilibrium sedimentation analysis of (B) Drp1 (14.8 μM, 7.4 μM, 3.7 μM). (C) MiD49 (9.4 μM, 4.7 μM, 2.3 μM), and (D) Mff (130.0 μM, 65.1 μM, 32.6 μM). In (B-D), corresponding fits (MW_{obs}/M_{calc}) are indicated above each graph and residuals for the nonlinear least squared fits are shown below. See also Supplemental Experimental Procedures.

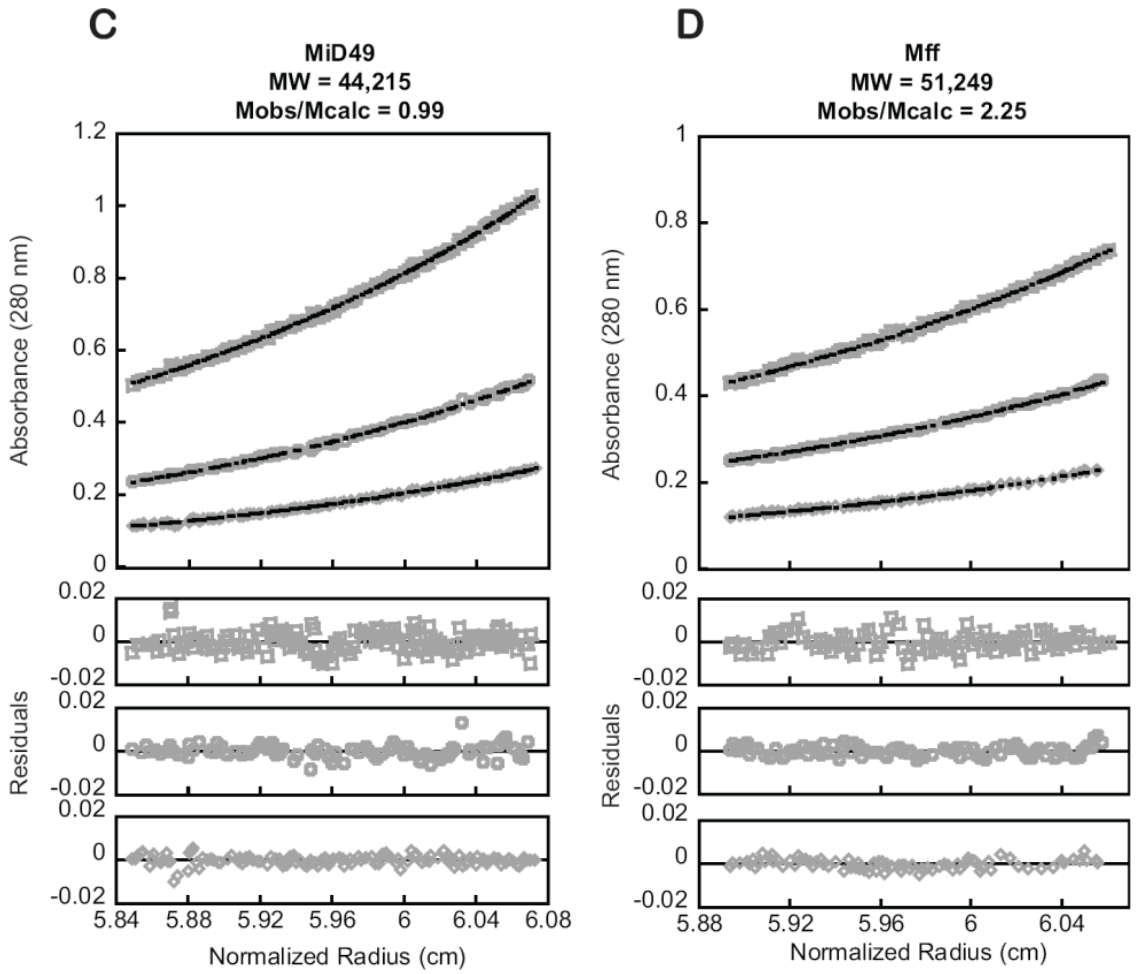

Figure 3.5. continued.

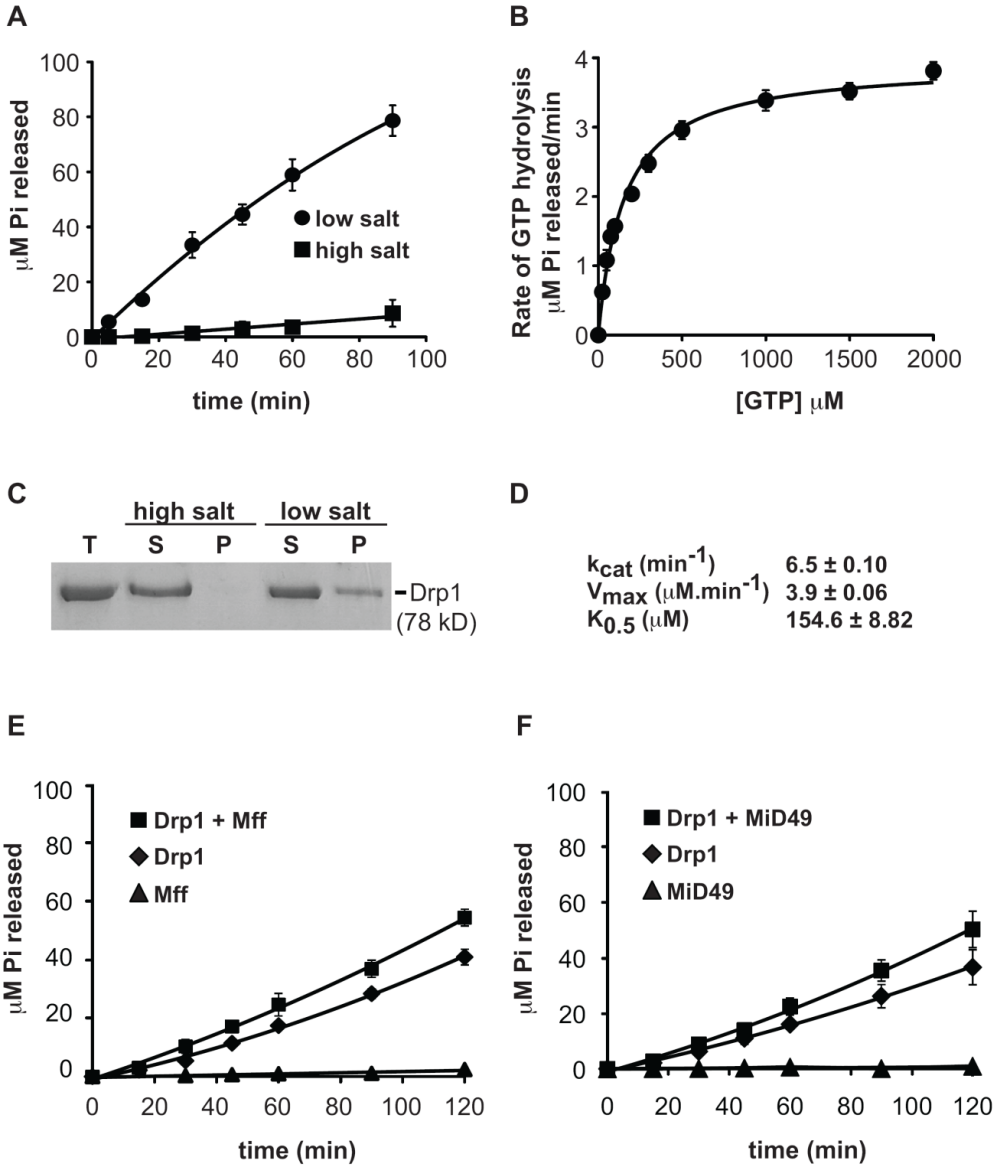

Figure 3.6. Effects of Mff and MiD49 on Drp1 GTPase activity. (A) Time course of GTP hydrolysis by Drp1 (0.6 μM) measured in 100 μM GTP, 37°C at high (500 mM KCl) and low (50 mM KCl) ionic strength. (B) Steady state kinetics of Drp1 (0.6 μM) GTP hydrolysis measured at low ionic strength (50 mM KCl), 37°C. (C) A Coomasie blue stained gel showing velocity sedimentation of Drp1 at high and low ionic strength. T, total; S, supernatant; P, pellet. (D) Drp1 kinetic parameters determined as described in (B) and the methods. k_{cat}, turnover number; V_{max}, maximal rate of hydrolysis; $K_{0.5}$, substrate concentration where velocity is one-half maximal. (E and F) GTP hydrolysis by Drp1 (0.1 μM) measured in 200 μM GTP, 50 mM KCl, 37°C in the presence and absence of the indicated adaptor proteins. Cytoplasmic domains of Mff (E) or MiD49 (F) purified from yeast were included at 0.5 μM. Similar results were obtained with Mff purified from yeast (shown here) and bacteria (unpublished data).

(unpublished data).expression system used to purify the CBP-Drp1 fusion protein contributed to the lower activity observed in the Chang et al. study. Importantly, the addition of Mff or MiD49 only modestly increased the assembly-driven GTP hydrolysis activity of Drp1 (Figure 3.6E and F). Thus, these adaptors do not act as classical effectors to enhance GTP hydrolysis by Drp1.

MiD49 Coassembles With Drp1 and Reduces Polymer Diameter

We used negative staining transmission electron microscopy (TEM) to analyze the structures formed by Drp1 in vitro. At low temperature, apo-Drp1 (without nucleotide) did not assemble into well-ordered structures (Figure 3.7A). When the non hydrolyzable analog GMP-PCP was added, Drp1 assembled into rings with an average external diameter of 33.5 ± 4.1 nm (Figure 3.7B and G). Raising the temperature to 25°C in the presence of GMP-PCP, produced Drp1 spirals (34.4 ± 6.4 nm) that often excluded DOPS containing lipids present in the reaction (Figure 3.7C and asterisk). Less frequently, Drp1 was able to deform DOPS lipids in the presence of GMP-PCP at 25°C, forming tubes with ordered striations along their length (Figure 3.7D). Interestingly, the diameter of these Drp1 tubes was significantly smaller (64.7 ± 7.2 nm) than that reported previously for Dnm1 assembled on lipids (109-121 nm, (Ingerman et al., 2005; Mears et al., 2011)). Constriction of these structures occurred upon exposure to GTP (Figure 3.7E and G), generating polymers with an average diameter of 30.7 ± 4.9 nm (Figure 3.7F and G).

We also analyzed the interaction of Drp1 with MiD49. In the presence of GMP-PCP, Drp1 self-assembles and pellets in a sedimentation assay (Figure 3.8A). Although

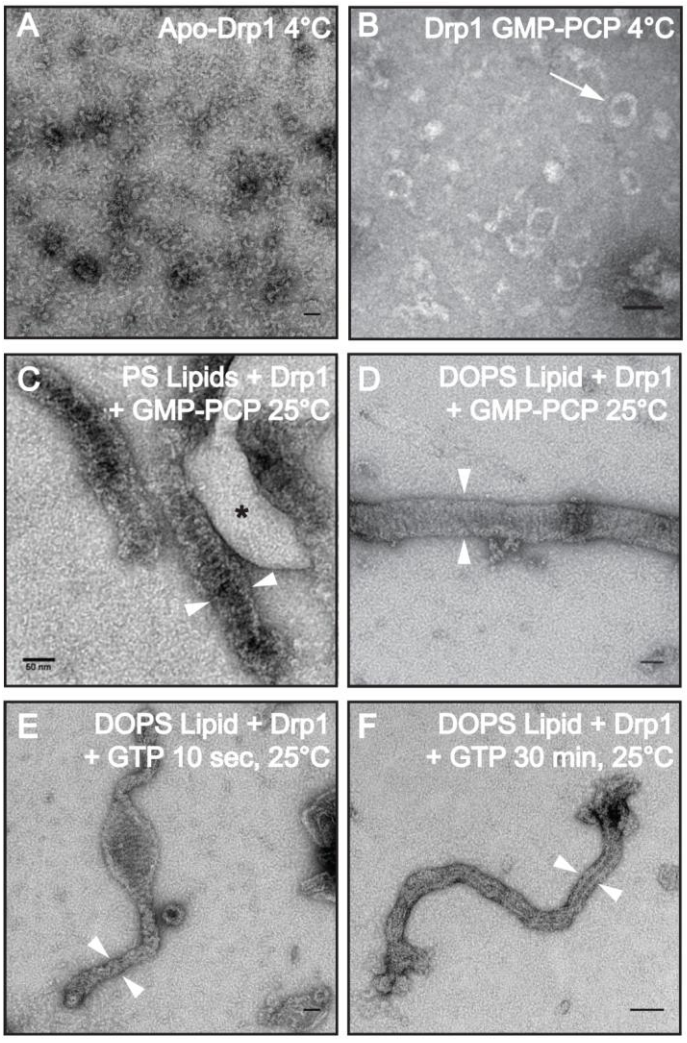

G

Structure	External diameter (nm)
Drp1 rings	33.5 +/- 4.1
Drp1 ring stacks	34.4 +/- 6.4
DOPS + Drp1 + GMP-PCP	64.7 +/- 7.2
DOPS + Drp1 + GTP	30.7 +/- 4.9

Figure 3.7. Drp1 self-assembly induces lipid tubulation and constriction in vitro. (A-C) Transmission electron micrographs of negatively-stained Drp1 assemblies. (A) Drp1 protomers do not assemble in the absence of nucleotide at 4°C. (B) Drp1 assembles into limited rings in the presence of GMP-PCP at low temperature (white arrow). (C) At 25°C, Drp1 forms spirals or stacks of rings in the presence of GMP-PCP that exclude PS-containing lipids (asterisk). (D) Drp1 assembles around DOPS liposomes in the presence of GMP-PCP at 25°C. Drp1-decorated lipid tubes assembled in the presence of GMP-PCP were imaged after treatment with (E) 1mM GTP for 10 seconds or (F) 30 minutes. (G) Average external diameters of Drp1 structures in B-F (white arrowheads). For all measurements, n = 50. Bars are 50 nm

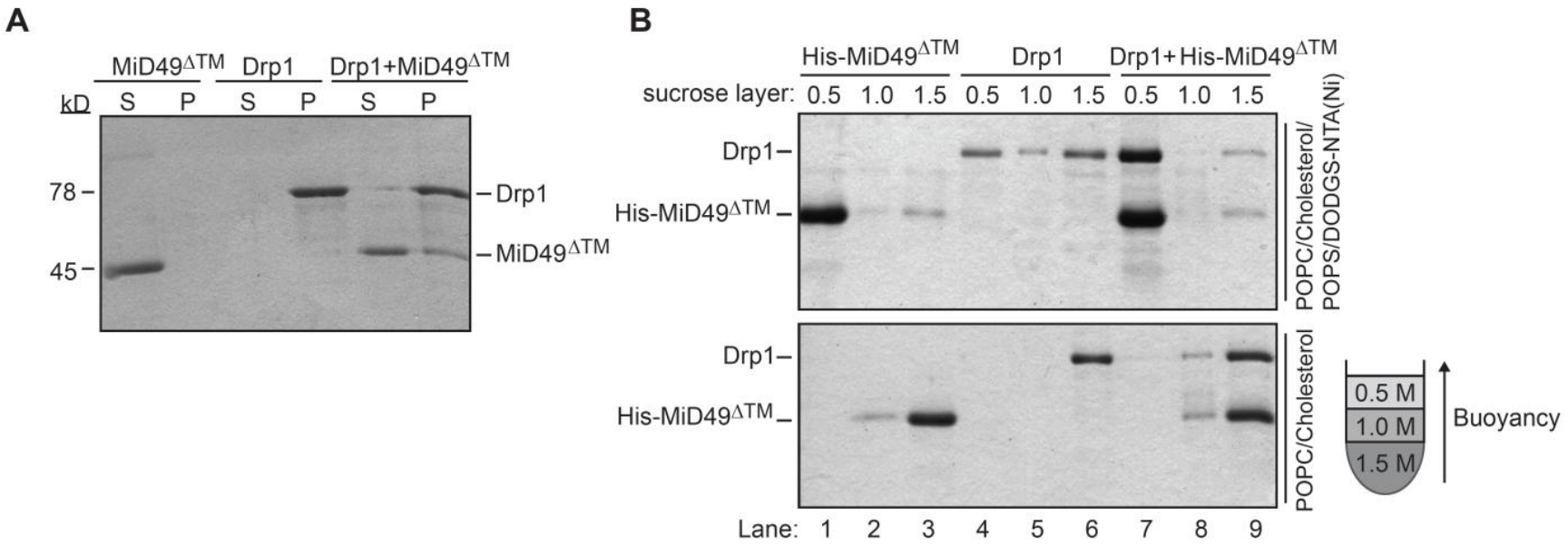

Figure 3.8. MiD49 copolymerizes with Drp1 and decreases polymer diameter. (A) MiD49$^{\Delta TM}$ (lacking the transmembrane domain) cosediments with Drp1. (B) DO DGS-NTA(Ni)-containing liposomes (top panel) decorated with His-tagged MiD49$^{\Delta TM}$ promote flotation of Drp1 in a sucrose step gradient. Charge-neutral liposomes (POPC/Cholesterol, bottom panel) bind His-tagged MiD49$^{\Delta TM}$ poorly and do not promote Drp1 flotation. As depicted in the cartoon gradient at the right, protein-bound liposomes float to the top of the 0.5 M sucrose layer. (C) Top, in the presence of MiD49$^{\Delta TM}$, Drp1 forms ordered polymers (arrows) with a diameter of 14.9 ± 1.5 nm. Bottom, periodicity (~5 nm) measured along the length of the Drp1:MiD49 polymers. (D) Effect of Drp1:MiD49 (molar:molar) ratios on polymer assembly. Decreasing MiD49 concentration reduces formation of narrow (14.9 nm) polymers (white arrowheads) and increases the diameter of larger (34.4 nm) polymers (black arrowheads).

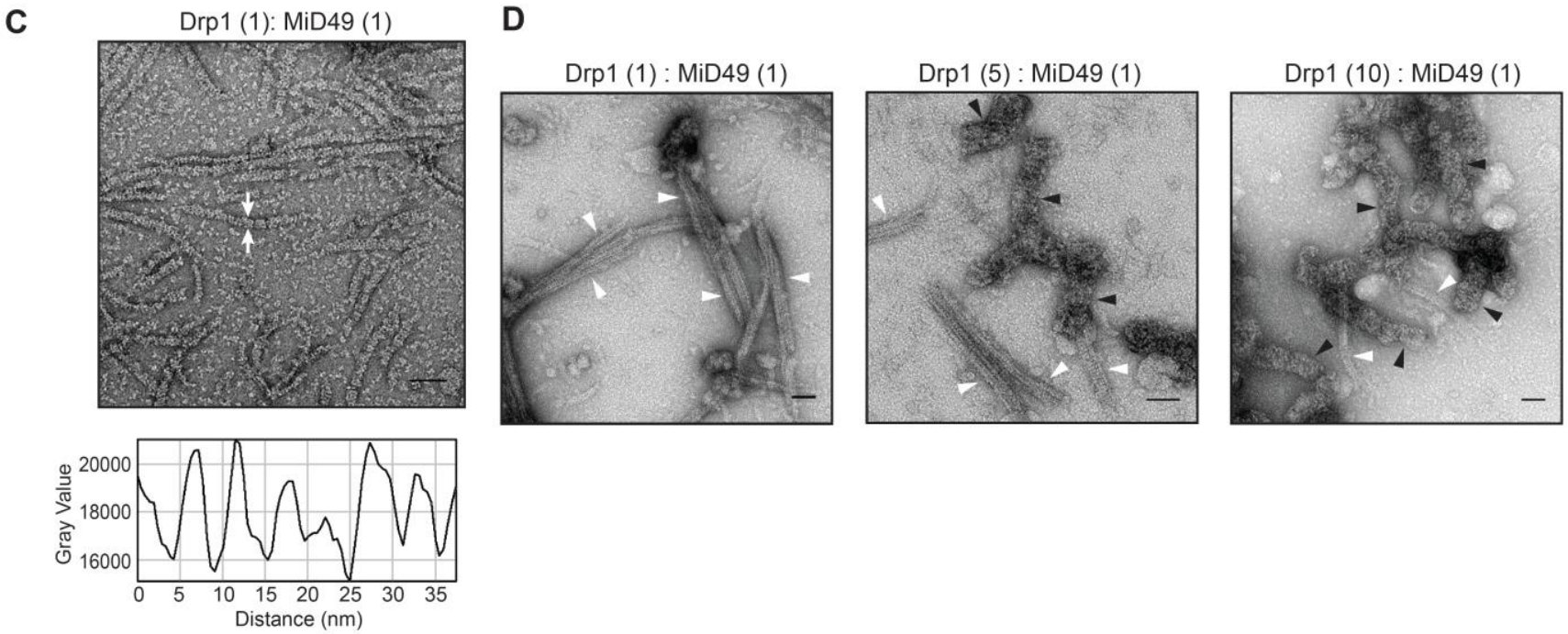

Figure 3.8. continued.

the cytoplasmic domain of MiD49 alone (MiD49$^{\Delta TM}$) remains in the supernatant fraction, the adaptor sediments in the presence of Drp1, consistent with the idea that the two proteins bind to each other and may coassemble (Figure 3.8A). These findings were confirmed using a flotation assay (in the presence of GMP-PCP). His-tagged MiD49$^{\Delta TM}$ alone (His-MiD49$^{\Delta TM}$) was able to bind and float with liposomes containing nickel-modified lipids after centrifugation in a sucrose step gradient (Figure 3.8B, top, lane 1). This fractionation pattern was dependent upon the presence of nickel (Ni-NTA) lipids and did not occur when membranes lacking the Ni-NTA moiety were substituted in the experiment (Figure 3.8B, bottom, lane 1). Although Drp1 has a weak affinity for the Ni-NTA liposomes on its own (Figure 3.8B, top, lane 4), the fraction of Drp1 bound to these liposomes visibly increased in the presence of the MiD49 adaptor (Figure 3.8B, top, lane 7). In control experiments, MiD49 and Drp1 (alone or in combination) did not float with electrostatically-neutral lipids (Figure 3.8B, bottom, lanes 6 and 9).

Negative stain TEM revealed a dramatic effect of MiD49 on Drp1 polymer formation. At 25°C in the presence of GMP-PCP, Drp1 plus MiD49 formed extended, uniform polymers with distinct striations (Figure 3.8C, top). These polymers had an average external diameter of 14.9 ± 1.5 nm, which is less than half the diameter of ring stacks formed by Drp1 alone (34.4 ± 6.4 nm, Figure 3.7G). Measurement of pixel intensity along the length of these structures revealed a highly regular ~5 nm periodicity (Figure 3.8C, bottom). In control studies, MiD49 did not reproducibly assemble into visible structures in the presence or absence of GTP or GTP analogs (unpublished results).

To further investigate the nature of these narrower polymers, we examined assembly in the presence of different Drp1:MiD49 (molar:molar) ratios. Incubation of Drp1 and MiD49 at a 1:1 ratio in the presence of GMP-PCP produced mainly polymers with the smaller average diameter (Figure 3.8D, white arrowheads, 14.9 ± 1.5 nm). These polymers often associated laterally into bundles. When a ratio of Drp1:MiD49 of 5:1 or 10:1 was examined, fewer narrow polymers were observed (Figure 3.8D, white arrowheads), with a concomitant increase in polymers of larger diameter (black arrowheads). Both the appearance and the diameter of the latter spirals were similar to those formed by Drp1 alone (Figure 3.7C). These data are consistent with the idea that coassembly of MiD49 with Drp1 is stoichiometric, and suggests that MiD49 copolymerizes with Drp1 rather than simply nucleating assembly of a Drp1 homopolymer.

Discussion

The adaptor proteins studied here were originally shown to mediate the recruitment of the Dnm1 or Drp1 GTPases to mitochondria, however, their post-recruitment roles in mitochondrial fission were not clear. In this study, we demonstrate that individual adaptor-GTPase pairs act after recruitment to catalyze membrane division in vivo. In the case of Drp1, coassembly with one of these adaptors increases the order, and dramatically decreases the diameter of the polymers formed.

The identification of Fis1 and Dnm1/Drp1 in yeast and mammals initially suggested that the basic molecular machinery for mitochondrial fission was conserved during evolution. While the role of yeast Fis1 in Mdv1-Dnm1 recruitment to

mitochondria has never been questioned, data supporting a function for mammalian Fis1 in Drp1 recruitment were contradictory. This issue was recently resolved by the demonstration that it is human Mff, rather than Fis1, that acts as the mitochondrial receptor for Drp1 (Otera et al., 2010). Soon after MiD49 and MiD51 were also reported to mediate Drp1 mitochondrial recruitment (Palmer et al., 2011; Zhao et al., 2011). We show here that yeast Fis1 is dispensable for fission when the Mdv1 adaptor is membrane-tethered, allowing Dnm1 recruitment to mitochondria. Moreover, expression of human Fis1 and Drp1 in yeast was not sufficient to rescue mitochondrial fission defects. Thus, Fis1 has not been conserved throughout evolution because of an essential role in Dnm1/Drp1-mediated membrane scission. What, then, is the conserved function of Fis1? Although mitochondrial fission proteins have also been implicated in peroxisome division and mitophagy in yeast and mammals (Koch et al., 2003; Kuravi et al., 2006; Li and Gould, 2003), Fis1 appears to be dispensable for peroxisome fission in human cells (Otera et al., 2010) and for mitophagy in yeast (Mendl et al., 2011; Okamoto et al., 2009). In addition, it was recently suggested that mammalian Fis1 directly interacts with MiD51 (also called MIEF1) to negatively regulate fission (Zhao et al., 2011). Further studies are clearly necessary to determine whether Fis1 has a conserved function(s) in organelle division.

Our findings show unambiguously that a single type of adaptor protein is sufficient for mitochondrial membrane scission by human Drp1. Why, then, do mammalian cells simultaneously express Mff, MiD49 and MiD51? Studies to date have not identified significant differences in the mitochondrial fission events mediated by these different adaptors (Otera et al., 2010; Palmer et al., 2011; Zhao et al., 2011).

However, the assays used in these studies (morphological quantification and fixed time-point analysis) would fail to detect significant temporal, spatial or mechanistic differences in Drp1 recruitment, assembly and/or membrane scission that are specific to each adaptor. In addition, the physiological circumstances (i.e., apoptosis, mitophagy) in which each adaptor is activated might differ. Documented posttranslational modifications of Drp1 including phosphorylation (Cereghetti et al., 2008; Chang and Blackstone, 2007; Cribbs and Strack, 2007; Han et al., 2008; Kim et al., 2011; Taguchi et al., 2007), sumoylation (Braschi et al., 2009; Figueroa-Romero et al., 2009; Wasiak et al., 2007; Zunino et al., 2009), nitrosylation (Cho et al., 2009) and ubiquitination (Horn et al., 2011; Karbowski et al., 2007; Nakamura et al., 2006; Wang et al., 2011; Yonashiro et al., 2006) could also influence the identity of the adaptor used for fission (as could posttranslational modifications of the adaptors themselves) . Finally, it is possible that multiple adaptors work together with Drp1 at a single division site. Such cooperation has been documented for the paralogous adaptors Mdv1 and Caf4 in yeast (Guo et al., Submitted) and it seems likely that the MiD49 and MiD51 paralogs will also have the capacity to function with Drp1 at the same fission site in mammals.

Distances of ≤ 1 nm between opposing lipid bilayers are thought to be necessary for initiation of inner leaflet hemifusion and subsequent membrane scission (Bashkirov et al., 2008; Hernandez et al., 2012). Taking into account the diameter of a lipid bilayer (~ 5 nm) (Leforestier et al., 2012; Wang et al., 2006), and the fact that mitochondria have a double membrane, the average external diameter we measured for Drp1-lipid tubules (30.7 nm, Figure 3.7G) would not produce a lumenal distance small enough to initiate fission of both the inner and outer mitochondrial membranes. This problem could be

overcome by coassembling MiD49 with Drp1, as the ~15 nm average external diameter of the Drp1:MiD49 copolymer is sufficiently narrow to drive fission. Like the copolymers formed by coincubation of dynamin-1 with endophilin (Sundborger et al., 2011) or amphiphysin (Takei et al., 1999), the MiD49:Drp1 copolymers shown here also change the structural properties of a dynamin GTPase polymer. In the case of N-BAR proteins and dynamin-1, the hybrid coat has a different diameter and different pitch. A detailed understanding of how MiD49 alters structural features of the Drp1 polymer, and the functional consequences of the hybrid assembly for the fission process requires further study.

Our findings clarify the individual functions of mitochondrial adaptors and challenge the notion that these proteins act solely to recruit and stimulate assembly of the DRPs Dnm1 and Drp1 on the correct cellular membrane. Instead, coassembly of adaptors with DRPs may work generally to change the physical properties of the resulting polymers in a manner that promotes or regulates membrane scission. For example, coassembly could prevent promiscuous fission by altering contacts between adjacent turns of the DRP helix, thereby inhibiting mechanochemical conformational changes that lead to constriction and fission. Such an inhibited state may be regulatory, delaying constriction until a signaling event or another factor is recruited. Alternatively, as shown here, the copolymer may have different geometric properties and be able to form a more compact state that promotes membrane constriction and fission. Regardless of the mechanism, we suggest that the ability to modulate polymer geometry will be a common function of mitochondrial dynamin adaptors.

Experimental procedures

Yeast strains and growth conditions

Yeast strains and plasmids used in this study are listed in Tables 3.1 and 3.2. Standard yeast and bacterial techniques were used for construction and growth of strains (Green and Sambrook, 2012; Guthrie and Fink, 2002).

Plasmid construction

Plasmids used in this study are listed in Table 3.2. Plasmids B1642, B1808 and B2053 were described previously (Karren et al., 2005). To construct B1607 and B1816,DNA sequences encoding full length *FIS1* and human *DRP1* isoform 3 were PCR amplified and cloned into BamHI and SalI sites of the *pRS415MET25* and *pRS416MET25* vectors (Stratagene). To create B2729, DNA sequences encoding *TOM20 (1-51aa)* (Ramage et al., 1993)were PCR amplified and cloned into the XbaI and BamHI sites of B1808 (in-frame with the existing FL *MDV1* coding region). B2730 and B2731 were constructed by replacing BamHI-*MDV1*-SalI in B2729 with the indicated *MDV1* coding sequences. For B3090, a three-way ligation reaction was performed with the *pRS415MET25* vector (Stratagene) and PCR amplified fragments ofmonomeric GFP^{A207K} and yeast $Fis1^{131\text{-}155aa}$ to generate *pRS415MET25-BamHI-mOMGFP-BsiWI-*$Fis1^{131\text{-}155aa}$*-SalI-pRS415* vector. For B3162, the StarGate® cloning system (IBA Solutions for Life Sciences) was used to introduce *-PreScission Protease Cleavage Site-BamHI-hDRP1 isoform 3-* into the EcoRI and SalI sites of the *pYSG-IBA167* vector. For B3259, B3262 and B3294, the indicated coding sequences were exchanged for *hDRP1* using existing

Table 3.1: Yeast strains used in yeast and mammalian study

ID	Genotype
JSY5740	*MAT*a, *leu2Δ1, his3Δ200, trp1Δ63, ura3-52, lys2Δ202*
JSY9548	*MAT*a, *leu2Δ1, his3Δ200, trp1Δ63, ura3-52, lys2Δ202, dnm1::GFP-DNM1, caf4::KanMX*
JSY9612	*MAT*a, *can1, ade2, trp1, ura3, his3, leu2, pep4::HIS3, prb1::LEU2, bar1::HISG, lys2::GAL1/10-GAL4*
JSY9801	*MATα, leu2Δ1, his3Δ200, trp1Δ63, ura3-52, lys2Δ202, fis1::HIS3, caf4::KanMX, mdv1:: MET25-TOM20(1-51aa)-MDV1(1-714aa)*
JSY9802	*MATα, leu2Δ1, his3Δ200, trp1Δ63, ura3-52, lys2Δ202, fis1::HIS3, caf4::KanMX, mdv1:: MET25-TOM20(1-51aa)-MDV1(218-714aa)*
JSY9803	*MATα, leu2Δ1, his3Δ200, trp1Δ63, ura3-52, lys2Δ202, fis1::HIS3, caf4::KanMX, mdv1:: MET25-TOM20(1-51aa)-MDV1(317-714aa)*
JSY9804	*MATa, leu2Δ1, his3Δ200, trp1Δ63, ura3-52, lys2Δ202, fis1::HIS3, caf4::KanMX, dnm1::GFP-DNM1, mdv1:: MET25-TOM20(1-51aa)-MDV1(1-714aa)*
JSY9805	*MATa, leu2Δ1, his3Δ200, trp1Δ63, ura3-52, lys2Δ202, fis1::HIS3, caf4::KanMX, dnm1::GFP-DNM1, mdv1:: MET25-TOM20(1-51aa)-MDV1(218-714aa)*
JSY9806	*MATa, leu2Δ1, his3Δ200, trp1Δ63, ura3-52, lys2Δ202, fis1::HIS3, caf4::KanMX, dnm1::GFP-DNM1, mdv1:: MET25-TOM20(1-51aa)-MDV1(317-714aa)*
JSY9807	*MATα, leu2Δ1, his3Δ200, trp1Δ63, ura3-52, lys2Δ202, caf4::KanMX, mdv1:: MET25-MDV1*
JSY10005	*MATα, leu2Δ1, his3Δ200, trp1Δ63, ura3-52, lys2Δ202, dnm1::HIS3, fis1::HIS3, caf4::KanMX, mdv1:: MET25-hfis1(1-119aa)-yfis1(122-155aa)*

Table 3.1 continued

ID	Genotype
JSY10006	*MATα, leu2Δ1, his3Δ200, trp1Δ63, ura3-52, lys2Δ202, dnm1::HIS3, fis1::HIS3, caf4::KanMX, mdv1:: MET25-hmff(1-198aa)-yfis1(127-155aa)*
JSY10007	*MATα, leu2Δ1, his3Δ200, trp1Δ63, ura3-52, lys2Δ202, dnm1::HIS3, fis1::HIS3, caf4::KanMX, mdv1:: MET25-TOM20(1-51aa)-hMiD49(48-454aa)*
JSY10009	*MATα, leu2Δ1, his3Δ200, trp1Δ63, ura3-52, lys2Δ202, dnm1::HIS3, fis1::HIS3, caf4::KanMX, mdv1:: MET25-TOM20(1-51aa)-hMiD51(47-463aa)*

Table 3.2: Plasmids used in yeast and mammalian study

ID	Plasmid	Protein expressed
B1642	*p414GPD-mito-ffRFP*	*N. crassa* ATP9$^{1\text{-}69aa}$ +ff DsRed
B1816	*pRS416MET25-hDRP1*	hDrp1 (isoform 3)
B1808	*pRS415MET25-MDV1*	Mdv1
B2053	*pRS416MET25-MDV1*	Mdv1
B2729	*pRS415MET25-T20-mdv1^{FL}*	T20$^{(1\text{-}51aa)}$-Mdv1$^{1\text{-}714aa}$
B2731	*pRS415MET25-T20-mdv1^{CCWD}*	T20$^{(1\text{-}51aa)}$-Mdv1$^{218\text{-}714aa}$
B2732	*pRS415MET25-T20-mdv1^{WD}*	T20$^{(1\text{-}51aa)}$-Mdv1$^{317\text{-}714aa}$
B3090	*pRS415MET25-mOMGFP-yFis1*	mOMGFP-yFis1-TM$^{131\text{-}155aa}$
B3162	*pYSG-IBA167-hDrp1*	Flag-Strep-PP-hDrp1 (isoform 3)
B3259	*pYSG-IBA167-hMiD49*	Flag-Strep-PP-hMiD49$^{48\text{-}454aa}$
B3262	*pYSG-IBA167-hMff*	Flag-Strep-PP-hMff $^{1\text{-}198aa}$
B3265	*pRS416CUP1-mGFP-hDrp1*	mGFP-hDrp1 (isoform 3)
B3294	*pYSG-IBA167-10xHis-hMiD49*	Flag-Strep-PP-10xHis-hMiD49 $^{(48\text{-}454aa)}$
B3357	*pMAL-c2x-hMff*	MBP-10xHIS-PP-hMff $^{(1\text{-}198aa)}$

Abbreviations: h, human; y, yeast; PP, PreScission Protease Cleavage Site; T20, TOM20; mOMGFP, monomeric mitochondrial outer membrane GFP; aa, amino acids; TM, trans-membrane domain; FL, full length; CCWD, coiled coil + WD repeat; WD, WD repeat

BamHI and *SalI* sites. For B3265, a two-step cloning protocol was used. First, the PCR amplified *CUP1* promoter sequence was introduced into the *SacII* and *SalI* sites of the *pRS416* vector (Strategene) to create *pRS416CUP1*. This cloning step also introduced *EagI* and *BamHI* sites upstream of the *SalI* site. Second, a three-way ligation reaction was performed with *pRS416CUP1* and PCR amplified fragments encoding monomeric GFP^{A207K} and human Drp1 using *EagI*, *BamHI* and *SalI* sites. B3265 contains the following order of genes and restriction sites: *pRS416 vector-SacII-CUP1-EagI-mGFP-BamHI-DRP1-SalI- pRS416 vector*. B3357 was created by cloning PCR amplified sequences encoding residues 1-198aa of human Mff into the *EcoRI* and *HinDIII* sites of pMAL-c2x vector (New England Biolabs).

Fluorescence microscopy

Mitochondrial morphologies were quantified as described previously (Amiott et al., 2009; Koirala et al., 2010) in the indicated strains expressing mitochondrial-matrix targeted fast-folding RFP (mito-ffRFP also referred to as mito-RFP) or mitochondrial outer membrane-targeted GFP (mito-OMGFP, Figure 4). Unless noted in the text, Mdv1, Mff and MiD49/51 proteins were expressed from the *MET25* promoter and integrated at the *MDV1* locus. Dnm1 and GFP-Dnm1 were expressed from the native promoter and locus. Drp1 (variant 3) and GFP-Drp1 were expressed from the *MET25* and *CUP1* promoters, respectively, on pRS416.

Overnight cultures were grown at 30°C in the appropriate selective synthetic dextrose (SD) medium containing 100 µg/mL methionine were diluted to 0.2 OD_{600} in medium containing 10 µg/mL methionine and grown for 3-5 hours. Western blotting and

imaging confirmed that DRP and adaptor proteins were stably expressed from the *MET25* and *CUP1* promoters under these conditions. For 4C, cells were grown as described above but continually diluted into SD medium lacking methionine (to maintain an OD_{600} between 0.2 and 1.0) and scored at the indicated times. Mitochondrial phenotypes and formation of GFP-Dnm1 puncta were scored in 100 cells, and data are represented as the average and S.E.M. of at least three independent experiments. Images were acquired and processed as described (Koirala et al., 2010).

Time-lapse imaging

For single-color time-lapse imaging (Figure 3.3), cells expressing mito-RFP were grown in selective synthetic dextrose medium and applied to concanavalin A (2 mg/ml, Sigma) treated Lab-tek II Chamber wells (Thermo Scientific) maintained at 30°C. Z-stacks (0.2 μm optical sections) of fields of cells were acquired every seven seconds over a 20-minute time course using a 3-I Marianas Live Cell Imaging microscope workstation (Denver, CO), equipped with dual ultra-sensitive Cascade II 512B EMCCD cameras (Roper Scientific, RS) configured with a Roper Dual-cam and Sutter DG-4 Illuminator (Sutter Instruments) with a 100X, 1.45 NA Plan-Apochromat objective (Zeiss). Data were deconvolved and analyzed using SlideBook 4.2 software (Intelligent Imaging Innovations, Inc). Substacks containing fission events were isolated from the entire stack to minimize signal background and assembled in Photoshop (CS3, Adobe). Brightness and contrast were adjusted using only linear operations applied to the entire image. For quantification, only cells that underwent one or more fission or fusion event during the

time-course were selected for analysis. The results were expressed as the number of fission or fusion events per cell per 20-minute interval.

For two-color time-lapse imaging (Figure 4D), cells expressing GFP-Drp1, mito-RFP and the indicated mammalian adaptor (MiD49, MiD51 or Mff) were grown in selective synthetic dextrose medium and applied to a Microfluidic chamber Y04c (Cellasic Corp.). Injection of cells and medium was controlled by an ONIX Microfluidic Perfusion System and ONIX FG Version 2.6 software (Cellasic Corp.). Z-stacks of cells (0.3 μm optical sections) were imaged every 30 seconds over an 30-minute time-course using an Observer Z1 microscope (Zeiss) equipped with HE GFP (set 38) and mRFP (set 63) shift free filter sets, an Axiocam MRm Rev.3 camera and a 100X, 1.4 NA Plan-Apochromat objective (Zeiss). GFP and DsRed channels were acquired sequentially using AxioVision 4.8 software (Zeiss), and data were deconvolved and analyzed using AxioVision 4.6 software (Zeiss). Substacks containing fission events were isolated and assembled as described above.

Protein production

Human Drp1 (isoform 3; NP_005681.2), MiD49 (accession number Q96C03) and Mff (accession number Q9GZY8) constructs, each containing an N-terminal PreScission protease cleavage site and a FLAG®-One-STrEP tag (IBA), were expressed in JSY9612. Overnight cultures were diluted into selective SD medium containing 1 mM $CuSO_4$ to induce expression (final OD_{600} of 0.2) and grown in a Belco fermentor at 30°C for 24 hours. After harvesting, cell pellets were snap frozen in liquid nitrogen as small droplets and pulverized in a Freezer Mill (3 minutes x 15 cycles). All subsequent purification

steps were performed at 4°C. Cell powders were dissolved in either high ionic strength lysis buffer (for hDrp1 – 100 mM Tris-Cl-pH-8.0, 500 mM NaCl, 1 mM DTT, 1 mM EDTA) or low ionic strength buffer (for MiD49 or Mff - 100 mM Tris-Cl-pH-8.0, 150 mM NaCl, 1 mM DTT, 1 mM EDTA) containing Protease Inhibitor Cocktail III (Calbiochem). The lysates were clarified by centrifugation at 30,000 x g for 1 hour, filtered (0.45 µm), loaded onto 5 mL StrepTrap HP column (GE Healthcare), washed with 1 liter lysis buffer and cleaved in the column with PreScission protease (GE Healthcare) for 16 hours. Drp1 was dialyzed against 20 mM HEPES pH 7.4, 150 mM KCl, 2 mM $MgCl_2$, 1 mM DTT, 0.5 mM EDTA, snap frozen in liquid nitrogen and stored at -80^{o}C. Mff and MiD49 were further purified by size exclusion chromatography (Sepharose 200, GE Healthcare), dialyzed against 20 mM HEPES pH 7.4, 150 mM KCl, 2 mM $MgCl_2$, 1 mM DTT, 0.5 mM EDTA and stored at 4^{o}C. Equilibrium sedimentation analysis performed on purified protein indicated that Drp1 variant 3 is a dimer in high ionic strength buffer (MW_{obs}/MW_{cal} = 2.17), the cytoplasmic domain of Mff is a dimer ((MW_{obs}/MW_{cal} = 2.25) and the cytoplasmic domain of MiD49 is a monomer (MW_{obs}/MW_{cal} = 0.99).

Analytical equilibrium sedimentation

The purified Drp1, MiD49 and Mff proteins were each centrifuged at a minimum of three concentrations (see Figure 3.5 legend) and two speeds (Drp1, 8,000 and 10,000 rpm; MiD49, 8,000, 10,000 and 12,000 rpm; and Mff, 10,000 and 12,000 rpm) at 4°C until equilibrium was established. Data were globally fit to an ideal single species model with a floating molecular weight using nonlinear least squares analysis as implemented in

HETEROANALYSIS (Cole, 2004). Representative data are shown for 10,000 rpm, with the MW fit and oligomeric state indicated. Buffers used for the analysis were Drp1 (20 mM Hepes 7.4, 500 mM KCl, 2 mM $MgCl_2$, 1 mM EDTA, 1 mM DTT), MiD49 (100 mM Tris-Cl 8.0, 150 mM NaCl, 1 mM EDTA, 1 mM TCEP), and Mff (50 mM Sodium Phosphate 7.4, 150 NaCl). Bottom panels show the residual differences between the data and the fit. Buffer densities and protein partial specific volumes were calculated with SEDNTERP (version 1.09) (Laue et al., 1992). For Drp1, 11% of the sample was lost during centrifugation (either to self-assembly or aggregation).

GTPase assay

Inorganic phosphate release was measured using the malachite green phosphate assay (POMG-25H; BioAssay Systems) as described by the manufacturer and in Leonard et al. (Leonard et al., 2005). For the time course analysis, Drp1 (0.6 µM) was assayed at 37°C in high (500 mM KCl) or low (50 mM KCl) ionic strength buffer containing 20 mM HEPES pH 7.4, 2 mM $MgCl_2$, 1 mM DTT, 100 µM GTP. Reactions were halted at the indicated times by diluting 20 µL in 25 mM EDTA (final concentration) in a microtiter plate. Although 25mM EDTA was sufficient to halt the reaction, we found that higher EDTA concentrations lowered the signal generated by the malachite reagent during the development step. Samples were incubated at room temperature with 20 µL Malachite Reagent (BioAssay Systems) and 60 µL water for 30 minutes and the absorbance at 600 nm was measured using a Modulus^{TM} Microplate Reader (Turner BioSystems). For the steady state kinetic analyis, GTP assays were performed at 37°C in reactions containing 0.6 µM Drp1, 20 mM HEPES pH 7.4, 50 mM KCl, 2 mM $MgCl_2$, 1

mM DTT containing variable GTP concentrations (0, 25, 50, 75, 100, 200, 300, 500, 1000, 1500 and 2000 µM). Fixed volumes were removed every 5 minutes for 70 minutes, quenched by EDTA and developed as described above. K_{cat} and $k_{0.5}$ were calculated in GraphPad Prism using nonlinear regression curve fitting. For time course analyses with adaptor proteins, GTPase assays were performed in reactions containing Drp1 (0.1 µM) plus or minus Mff (0.5 µM) or MiD49 (0.5 µM) at 37°C in 50 µM KCl, 20 mM HEPES pH 7.4, 2 mM $MgCl_2$, 1 mM DTT and 200 µM GTP. In all experiments, data shown are the average and S.E.M. values obtained from triplicate samples analyzed at the same time. Each experiment was repeated three times.

Velocity sedimentation and flotation assays

For the velocity sedimentation assay (Figure 3.6C), 1.25 µM Drp1 was incubated either in low ionic strength buffer (20 mM HEPES – pH 7.4, 50 mM KCl, 2 mM $MgCl_2$, 1 mM DTT) or high ionic strength buffer (20 mM HEPES – pH 7.4, 500 mM KCl, 2 mM $MgCl_2$, 1 mM DTT) for 1 hour at 37^{o}C. The reactions were spun down at 40,000 rpm (TLA 100 rotor) in a Beckman Optima MAX Ultracentrifuge for 1 hour at 25^{o}C. Supernatants were removed and pellet fractions were resuspended in an equal volume of buffer. Twenty-five µL of total, supernatant and pellet fractions were separated on 10% SDS-PAGE gels and stained with Coomassie Brilliant Blue (CBB) dye. For the velocity sedimentation in Figure 3.8A, 1.25 µM MiD49$^{\Delta TM}$, 1.25 µM Drp1 or 1.25 µM of both proteins were dialyzed at 25°C into 20 mM HEPES – pH 7.4, 25 mM KCl, 2 mM $MgCl_2$, 1 mM DTT, 200 µM GMP-PCP for 6 hours. Samples were pelleted and processed for SDS-PAGE as described above.

Liposome Preparation

(POPC) 1-palmitoyl-2-oleoyl-*sn*-glycero-3-phosphocholine, (POPS) 1-palmitoyl-2-oleoyl-*sn*-glycero-3-phospho-L-serine, Cholesterol, (Rhodamine-PE) 1,2-dipalmitoyl-*sn*-glycero-3-phosphoethanolamine-N-(lissamine rhodamine B sulfonyl) (ammonium salt), (Ni^{2+}-NTA-DOGS) 1,2-dioleoyl-*sn*-glycero-3-[(N-(5-amino-1-carboxypentyl)iminodiacetic acid)succinyl] (nickel salt) and (DOPS) 1,2-dioleoyl-*sn*-glycero-3-phospho-L-serine were purchased from Avanti Polar Lipids in chloroform. 4 types of mixtures were prepared: 1) POPC, POPS, Cholesterol, Rhodamine-PE were mixed in a molar ratio 44.4:37:18:5:0.007 (37%PS liposomes), 2) POPC, POPS, Cholesterol and Ni2+-NTA-DOGS were mixed in a molar ratio 44.4:31:18.5:6 (Nickel liposomes), 3) 100% DOPS (DOPS liposomes) and 4) POPC:Cholesterol were mixed in a molar ratio 80:20 (neutral liposomes).

Chloroform was evaporated by gentle vortexing under a steady stream of Nitrogen gas to make a thin lipid film around the walls of glass vials. These films were dried under vacuum for 1 hour at room temperature. Dried lipid films were then resolubilized in absolute hexane. The hexane was also evaporated under streaming nitrogen while vortexing, followed by a second round of dessication for 3-4 hours at room temperature. Lipid films were suspended in aqueous buffer (20mM HEPES pH 7.5, 100mM KCl) by vortexing at room temperature. Aliquots from the liposome preparation were stored at -80°C.

Flotation assays

Liposomes and proteins were mixed in a molar ratio 1000:1 (lipid:protein) in Beckman polycarbonate centrifuge tubes. After a 1-hour incubation at 4°C, the mixtures were homogenized with 300μL 2M sucrose in 20 mM Hepes 7.5, 100 mM KCl, 1 mM GMP-PCP (~1.5M final sucrose concentration). Two additional layers of 1M (150μL) and 0.5M (300μL) sucrose in the same buffer were carefully overlaid (in that order) on top of the homogenized mixture. The mixtures were spun using a TLS-55 rotor in a Beckman centrifuge for 1 hour at 54000 rpm (4°C). After the spin, the liposomes migrated to interfaces between individual sucrose layers and could be seen as turbid bands. The interfaces between individual sucrose layers were collected by pipetting and analyzed by 10% SDS-PAGE and CBB staining.

In vitro membrane binding and tubulation reactions

For DRP1 tubulation reactions, DOPS liposomes were mixed with protein (1:1, mass:mass). After 1 hour, GMP-PCP was added and the sample was incubated for 4 hours at room temperature. The effects of GTP hydrolysis were analyzed in two ways. First, after adsorption of the lipid and protein mixtures to EM grids, the sample was washed in 1mM GTP before immediately blotting and staining. Second, a stock of 10mM GTP was added to lipid-protein mixtures to a final concentration of 1mM GTP for 30 minutes before applying to EM grids for staining.

For DRP1-MID49 co-polymerization, proteins were mixed 1:1 mass:mass, with or without liposomes and dialyzed overnight against 20mM HEPES, 25mM KCl, 200mM GMP-PCP, 20mM $MgCl_2$ and 1mM DTT.

Electron microscopy

For negative stain EM, carbon coated copper grids were glow discharged for 15 seconds. 5μL of the sample was added to the surface, blotted and stained with 1% Uranyl Acetate. Images were acquired using an FEI Tecnai T12 electron microscope equipped with a LaB6 filament and operated at 120kV. Magnifications of 21000X-42000X were recorded on a Gatan CCD.

Acknowledgements

We thank Jane Macfarlane for expertise in mutagenesis and plasmid construction, Sarah Saffran for assistance with the initial GTPase assays, Mike Ryan and Alex van der Bliek for providing MiD and Mff plasmids and antibodies, Michael McCaffery for use of the John Hopkins University Integrated Imaging Facility and Beverly Wendland for the use of her lab space while working at the JHU facility. We are grateful to Michael Kay, Tim Formosa and members of the Shaw and Frost laboratories for stimulating discussions. This work was supported by NIH grants GM53466 and GM84970 to J.M.S. D.M.E. and the University of Utah Protein Interaction Core Facility are supported by NIH grant GM82545.

References

Amiott, E. A., Cohen, M. M., Saint-Georges, Y., Weissman, A. M., and Shaw, J. M. (2009). A mutation associated with CMT2A neuropathy causes defects in Fzo1 GTP hydrolysis, ubiquitylation, and protein turnover. Mol Biol Cell *20*, 5026-5035.

Bashkirov, P. V., Akimov, S. A., Evseev, A. I., Schmid, S. L., Zimmerberg, J., and Frolov, V. A. (2008). GTPase cycle of dynamin is coupled to membrane squeeze and release, leading to spontaneous fission. Cell *135*, 1276-1286.

Bleazard, W., McCaffery, J. M., King, E. J., Bale, S., Mozdy, A., Tieu, Q., Nunnari, J., and Shaw, J. M. (1999). The dynamin-related GTPase Dnm1 regulates mitochondrial fission in yeast. Nat Cell Biol *1*, 298-304.

Braschi, E., Zunino, R., and McBride, H. M. (2009). MAPL is a new mitochondrial SUMO E3 ligase that regulates mitochondrial fission. EMBO Rep *10*, 748-754.

Cereghetti, G. M., Stangherlin, A., Martins de Brito, O., Chang, C. R., Blackstone, C., Bernardi, P., and Scorrano, L. (2008). Dephosphorylation by calcineurin regulates translocation of Drp1 to mitochondria. Proc Natl Acad Sci U S A *105*, 15803-15808.

Cerveny, K. L., and Jensen, R. E. (2003). The WD-repeats of Net2p interact with Dnm1p and Fis1p to regulate division of mitochondria. Mol Biol Cell *14*, 4126-4139.

Cerveny, K. L., McCaffery, J. M., and Jensen, R. E. (2001). Division of mitochondria requires a novel DMN1-interacting protein, Net2p. Mol Biol Cell *12*, 309-321.

Chang, C. R., and Blackstone, C. (2007). Cyclic AMP-dependent protein kinase phosphorylation of Drp1 regulates its GTPase activity and mitochondrial morphology. J Biol Chem *282*, 21583-21587.

Chang, C. R., Manlandro, C. M., Arnoult, D., Stadler, J., Posey, A. E., Hill, R. B., and Blackstone, C. (2010). A lethal de novo mutation in the middle domain of the dynamin-related GTPase Drp1 impairs higher order assembly and mitochondrial division. J Biol Chem *285*, 32494-32503.

Cho, D. H., Nakamura, T., Fang, J., Cieplak, P., Godzik, A., Gu, Z., and Lipton, S. A. (2009). S-nitrosylation of Drp1 mediates beta-amyloid-related mitochondrial fission and neuronal injury. Science *324*, 102-105.

Cole, J. L. (2004). Analysis of heterogeneous interactions. Methods Enzymol *384*, 212-232.

Cribbs, J. T., and Strack, S. (2007). Reversible phosphorylation of Drp1 by cyclic AMP-dependent protein kinase and calcineurin regulates mitochondrial fission and cell death. EMBO Rep *8*, 939-944.

Figueroa-Romero, C., Iniguez-Lluhi, J. A., Stadler, J., Chang, C. R., Arnoult, D., Keller, P. J., Hong, Y., Blackstone, C., and Feldman, E. L. (2009). SUMOylation of the mitochondrial fission protein Drp1 occurs at multiple nonconsensus sites within the B domain and is linked to its activity cycle. Faseb J *23*, 3917-3927.

Friedman, J. R., Lackner, L. L., West, M., DiBenedetto, J. R., Nunnari, J., and Voeltz, G. K. (2011). ER tubules mark sites of mitochondrial division. Science *334*, 358-362.

Gandre-Babbe, S., and van der Bliek, A. M. (2008). The novel tail-anchored membrane protein Mff controls mitochondrial and peroxisomal fission in mammalian cells. Mol Biol Cell *19*, 2402-2412.

Gomes, L. C., Di Benedetto, G., and Scorrano, L. (2011). During autophagy mitochondria elongate, are spared from degradation and sustain cell viability. Nat Cell Biol *13*, 589-598.

Gorsich, S. W., and Shaw, J. M. (2004). Importance of mitochondrial dynamics during meiosis and sporulation. Mol Biol Cell *15*, 4369-4381.

Green, M. R., and Sambrook, J. (2012). Molecular Cloning: A Laboratory Manual, Forth edn: Cold Spring Harbor Laboratory Press).

Griffin, E. E., Graumann, J., and Chan, D. C. (2005). The WD40 protein Caf4p is a component of the mitochondrial fission machinery and recruits Dnm1p to mitochondria. J Cell Biol *170*, 237-248.

Guo, Q., Koirala, S., Perkins, E. M., McCaffery, J. M., and Shaw, J. M. (Submitted). The mitochondrial fission adaptors Caf4 and Mdv1 are not functionally equivalent.

Guthrie, C., and Fink, G. (2002). Guide to Yeast Genetics and Molecular Biology, Vol 194).

Han, X. J., Lu, Y. F., Li, S. A., Kaitsuka, T., Sato, Y., Tomizawa, K., Nairn, A. C., Takei, K., Matsui, H., and Matsushita, M. (2008). CaM kinase I alpha-induced phosphorylation of Drp1 regulates mitochondrial morphology. J Cell Biol *182*, 573-585.

Hernandez, J. M., Stein, A., Behrmann, E., Riedel, D., Cypionka, A., Farsi, Z., Walla, P. J., Raunser, S., and Jahn, R. (2012). Membrane fusion intermediates via directional and full assembly of the SNARE complex. Science *336*, 1581-1584.

Horn, S. R., Thomenius, M. J., Johnson, E. S., Freel, C. D., Wu, J. Q., Coloff, J. L., Yang, C. S., Tang, W., An, J., Ilkayeva, O. R., *et al.* (2011). Regulation of mitochondrial morphology by APC/CCdh1-mediated control of Drp1 stability. Mol Biol Cell *22*, 1207-1216.

Ingerman, E., Perkins, E. M., Marino, M., Mears, J. A., McCaffery, J. M., Hinshaw, J. E., and Nunnari, J. (2005). Dnm1 forms spirals that are structurally tailored to fit mitochondria. J Cell Biol *170*, 1021-1027.

Ishihara, N., Nomura, M., Jofuku, A., Kato, H., Suzuki, S. O., Masuda, K., Otera, H., Nakanishi, Y., Nonaka, I., Goto, Y., *et al.* (2009). Mitochondrial fission factor Drp1 is essential for embryonic development and synapse formation in mice. Nat Cell Biol *11*, 958-966.

Karbowski, M., Neutzner, A., and Youle, R. J. (2007). The mitochondrial E3 ubiquitin ligase MARCH5 is required for Drp1 dependent mitochondrial division. J Cell Biol *178*, 71-84.

Karren, M. A., Coonrod, E. M., Anderson, T. K., and Shaw, J. M. (2005). The role of Fis1p-Mdv1p interactions in mitochondrial fission complex assembly. J Cell Biol *171*, 291-301.

Kim, H., Scimia, M. C., Wilkinson, D., Trelles, R. D., Wood, M. R., Bowtell, D., Dillin, A., Mercola, M., and Ronai, Z. A. (2011). Fine-tuning of Drp1/Fis1 availability by AKAP121/Siah2 regulates mitochondrial adaptation to hypoxia. Mol Cell *44*, 532-544.

Koch, A., Thiemann, M., Grabenbauer, M., Yoon, Y., McNiven, M. A., and Schrader, M. (2003). Dynamin-like protein 1 is involved in peroxisomal fission. J Biol Chem *278*, 8597-8605.

Koirala, S., Bui, H. T., Schubert, H. L., Eckert, D. M., Hill, C. P., Kay, M. S., and Shaw, J. M. (2010). Molecular architecture of a dynamin adaptor: implications for assembly of mitochondrial fission complexes. J Cell Biol *191*, 1127-1139.

Kuravi, K., Nagotu, S., Krikken, A. M., Sjollema, K., Deckers, M., Erdmann, R., Veenhuis, M., and van der Klei, I. J. (2006). Dynamin-related proteins Vps1p and Dnm1p control peroxisome abundance in Saccharomyces cerevisiae. J Cell Sci *119*, 3994-4001.

Labrousse, A. M., Zappaterra, M. D., Rube, D. A., and van der Bliek, A. M. (1999). C. elegans dynamin-related protein DRP-1 controls severing of the mitochondrial outer membrane. Mol Cell *4*, 815-826.

Lackner, L. L., and Nunnari, J. M. (2009). The molecular mechanism and cellular functions of mitochondrial division. Biochim Biophys Acta *1792*, 1138-1144.

Laue, T., Shah, B., Ridgeway, T., and Pelletier, S. (1992). Computer-aided interpretatio of analytical sedimentation data for proteins (Cambridge, England, UK: Royal Society of Chemistry).

Leforestier, A., Lemercier, N., and Livolant, F. (2012). Contribution of cryoelectron microscopy of vitreous sections to the understanding of biological membrane structure. Proc Natl Acad Sci U S A *109*, 8959-8964.

Leonard, M., Song, B. D., Ramachandran, R., and Schmid, S. L. (2005). Robust colorimetric assays for dynamin's basal and stimulated GTPase activities. Methods Enzymol *404*, 490-503.

Li, X., and Gould, S. J. (2003). The dynamin-like GTPase DLP1 is essential for peroxisome division and is recruited to peroxisomes in part by PEX11. J Biol Chem *278*, 17012-17020.

Mears, J. A., Lackner, L. L., Fang, S., Ingerman, E., Nunnari, J., and Hinshaw, J. E. (2011). Conformational changes in Dnm1 support a contractile mechanism for mitochondrial fission. Nat Struct Mol Biol *18*, 20-26.

Mendl, N., Occhipinti, A., Muller, M., Wild, P., Dikic, I., and Reichert, A. S. (2011). Mitophagy in yeast is independent of mitochondrial fission and requires the stress response gene WHI2. J Cell Sci *124*, 1339-1350.

Mozdy, A. D., McCaffery, J. M., and Shaw, J. M. (2000). Dnm1p GTPase-mediated mitochondrial fission is a multi-step process requiring the novel integral membrane component Fis1p. J Cell Biol *151*, 367-380.

Nakamura, N., Kimura, Y., Tokuda, M., Honda, S., and Hirose, S. (2006). MARCH-V is a novel mitofusin 2- and Drp1-binding protein able to change mitochondrial morphology. EMBO Rep *7*, 1019-1022.

Naylor, K., Ingerman, E., Okreglak, V., Marino, M., Hinshaw, J. E., and Nunnari, J. (2006). Mdv1 interacts with assembled dnm1 to promote mitochondrial division. J Biol Chem *281*, 2177-2183.

Nunnari, J., Marshall, W. F., Straight, A., Murray, A., Sedat, J. W., and Walter, P. (1997). Mitochondrial transmission during mating in Saccharomyces cerevisiae is determined by mitochondrial fusion and fission and the intramitochondrial segregation of mitochondrial DNA. Mol Biol Cell *8*, 1233-1242.

Okamoto, K., Kondo-Okamoto, N., and Ohsumi, Y. (2009). Mitochondria-anchored receptor Atg32 mediates degradation of mitochondria via selective autophagy. Dev Cell *17*, 87-97.

Otera, H., Wang, C., Cleland, M. M., Setoguchi, K., Yokota, S., Youle, R. J., and Mihara, K. (2010). Mff is an essential factor for mitochondrial recruitment of Drp1 during mitochondrial fission in mammalian cells. J Cell Biol *191*, 1141-1158.

Otsuga, D., Keegan, B. R., Brisch, E., Thatcher, J. W., Hermann, G. J., Bleazard, W., and Shaw, J. M. (1998). The dynamin-related GTPase, Dnm1p, controls mitochondrial morphology in yeast. J Cell Biol *143*, 333-349.

Palmer, C. S., Osellame, L. D., Laine, D., Koutsopoulos, O. S., Frazier, A. E., and Ryan, M. T. (2011). MiD49 and MiD51, new components of the mitochondrial fission machinery. EMBO Rep *12*, 565-573.

Parone, P. A., Da Cruz, S., Tondera, D., Mattenberger, Y., James, D. I., Maechler, P., Barja, F., and Martinou, J. C. (2008). Preventing mitochondrial fission impairs mitochondrial function and leads to loss of mitochondrial DNA. PLoS One *3*, e3257.

Praefcke, G. J., and McMahon, H. T. (2004). The dynamin superfamily: universal membrane tubulation and fission molecules? Nat Rev Mol Cell Biol *5*, 133-147.

Ramage, L., Junne, T., Hahne, K., Lithgow, T., and Schatz, G. (1993). Functional cooperation of mitochondrial protein import receptors in yeast. Embo J *12*, 4115-4123.

Rambold, A. S., Kostelecky, B., Elia, N., and Lippincott-Schwartz, J. (2011). Tubular network formation protects mitochondria from autophagosomal degradation during nutrient starvation. Proc Natl Acad Sci U S A *108*, 10190-10195.

Sesaki, H., and Jensen, R. E. (1999). Division versus fusion: Dnm1p and Fzo1p antagonistically regulate mitochondrial shape. J Cell Biol *147*, 699-706.

Sundborger, A., Soderblom, C., Vorontsova, O., Evergren, E., Hinshaw, J. E., and Shupliakov, O. (2011). An endophilin-dynamin complex promotes budding of clathrin-coated vesicles during synaptic vesicle recycling. J Cell Sci *124*, 133-143.

Taguchi, N., Ishihara, N., Jofuku, A., Oka, T., and Mihara, K. (2007). Mitotic phosphorylation of dynamin-related GTPase Drp1 participates in mitochondrial fission. J Biol Chem *282*, 11521-11529.

Takei, K., Slepnev, V. I., Haucke, V., and De Camilli, P. (1999). Functional partnership between amphiphysin and dynamin in clathrin-mediated endocytosis. Nat Cell Biol *1*, 33-39.

Tieu, Q., and Nunnari, J. (2000). Mdv1p is a WD repeat protein that interacts with the dynamin-related GTPase, Dnm1p, to trigger mitochondrial division. J Cell Biol *151*, 353-366.

Tieu, Q., Okreglak, V., Naylor, K., and Nunnari, J. (2002). The WD repeat protein, Mdv1p, functions as a molecular adaptor by interacting with Dnm1p and Fis1p during mitochondrial fission. J Cell Biol *158*, 445-452.

Twig, G., Elorza, A., Molina, A. J., Mohamed, H., Wikstrom, J. D., Walzer, G., Stiles, L., Haigh, S. E., Katz, S., Las, G., *et al.* (2008). Fission and selective fusion govern mitochondrial segregation and elimination by autophagy. Embo J *27*, 433-446.

Twig, G., and Shirihai, O. S. (2011). The interplay between mitochondrial dynamics and mitophagy. Antioxid Redox Signal *14*, 1939-1951.

Wakabayashi, J., Zhang, Z., Wakabayashi, N., Tamura, Y., Fukaya, M., Kensler, T. W., Iijima, M., and Sesaki, H. (2009). The dynamin-related GTPase Drp1 is required for embryonic and brain development in mice. J Cell Biol *186*, 805-816.

Wang, H., Song, P., Du, L., Tian, W., Yue, W., Liu, M., Li, D., Wang, B., Zhu, Y., Cao, C., *et al.* (2011). Parkin ubiquitinates Drp1 for proteasome-dependent degradation: implication of dysregulated mitochondrial dynamics in Parkinson disease. J Biol Chem *286*, 11649-11658.

Wang, L., Bose, P. S., and Sigworth, F. J. (2006). Using cryo-EM to measure the dipole potential of a lipid membrane. Proc Natl Acad Sci U S A *103*, 18528-18533.

Wasiak, S., Zunino, R., and McBride, H. M. (2007). Bax/Bak promote sumoylation of DRP1 and its stable association with mitochondria during apoptotic cell death. J Cell Biol *177*, 439-450.

Yonashiro, R., Ishido, S., Kyo, S., Fukuda, T., Goto, E., Matsuki, Y., Ohmura-Hoshino, M., Sada, K., Hotta, H., Yamamura, H., *et al.* (2006). A novel mitochondrial ubiquitin ligase plays a critical role in mitochondrial dynamics. Embo J *25*, 3618-3626.

Zhao, J., Liu, T., Jin, S., Wang, X., Qu, M., Uhlen, P., Tomilin, N., Shupliakov, O., Lendahl, U., and Nister, M. (2011). Human MIEF1 recruits Drp1 to mitochondrial outer membranes and promotes mitochondrial fusion rather than fission. Embo J *30*, 2762-2778.

Zunino, R., Braschi, E., Xu, L., and McBride, H. M. (2009). Translocation of SenP5 from the nucleoli to the mitochondria modulates DRP1-dependent fission during mitosis. J Biol Chem *284*, 17783-17795.

CHAPTER 4

DISCUSSION

Overview

This dissertation includes two studies that are focused on the roles of Fis1 and mitochondrial fission adaptors in yeast and in mammals. Chapter 2 explores the function of Caf4 in mitochondrial fission and the relationship of Caf4 and Mdv1 during evolution. The results demonstrate for the first time that Caf4 is a bona fide fission adaptor protein that is able to independently mediate fission events. However, the Caf4 and Mdv1 adaptors are not functionally equivalent. Caf4 is prone to induce dominate-negative defects when over expressed, while Mdv1 is able to continue to rescue fission defects at the same level of over-expression. Moreover, expressing Caf4 or Mdv1 from each other's endogenous promoters does not rescue fission defects to the same extent. These studies also show that Caf4 is able to form co-complexes with Mdv1 to carry out fission. Phylogenic analysis reveals that Caf4 and Mdv1 are a result of a gene duplication event in *Saccharomyces cerevisiae*. Unlike Mdv1, Caf4 had undergone numerous genomic alterations during evolution. Despite this, Caf4 has retained the ability to function as a fission adaptor.

The study in Chapter 3 advances the field in several ways. First, this study provides the first demonstration that yeast Fis1 is not required for mitochondrial fission after Dnm1 recruitment to the membrane. Second, the minimal mammalian fission machinery is identified. By expressing the mammalian fission adaptors, Mff and MiD49/51, together with Drp1 in yeast, we showed that mitochondrial fission is reconstituted in a yeast fission null strain. Each of the mammalian adaptors is equally capable of recruiting Drp1 and mediating fission. Third, this study partially clarifies a controversy in the field by demonstrating that MiD49/51 mediates fission. Lastly,

biochemical studies suggest that the Mff and MiD49 mammalian adaptors do not stimulate the GTPase activity of Drp1. However, MiD49 is able to co-assemble with Drp1 and change the structural properties of Drp1 assembly.

Exploring the functions of Caf4

Caf4 is a bona fide fission adaptor in yeast mitochondrial fission

Time-lapse imaging and microscopy studies in Chapter 2 provide direct evidence that Caf4 alone is capable of mediating fission (Figure 2.1C), in addition to its ability to recruit Dnm1 to the mitochondrial surface (Griffin et al., 2005). This finding explains the observation of other groups that fission is not completely blocked when Mdv1 is absent. Yeast two-hybrid studies suggest that Caf4 interacts with Mdv1 via its CC domain (Griffin et al., 2005). Studies in Chapter 2 established that Caf4 and Mdv1 are able to colocalize in punctate complexes on mitochondria that perform fission (Figure 2.4A and 4C). We do not yet know whether this colocalization is the result of Caf4-Mdv1 dimerization or is simply due to coassembly of separate Caf4 and Mdv1 dimers with Dnm1 into fission complexes. Further biochemical and structural studies are required to resolve this issue. The time-lapse studies also reveal that the Caf4 and Mdv1 adaptors are initially in puncta but spread away from the initial site along the tubule as fission proceeds. It may be that the adaptors are forced to move away from the punctate fission complex to allow Dnm1 access to the membrane for lipid remodeling and scission. Alternatively, this spreading may simply represent disassembly of Caf4 and Mdv1 from the complex after fission reaches a particular stage or is complete. In either case, it is not yet known whether Caf4 and Mdv1 disassemble prior to, during or after membrane

scission. Answering this question will require a system that fully reconstitutes mitochondrial fission in vitro.

Domains of Caf4 and Mdv1 are not interchangeable

When Caf4 is the only adaptor protein in fission complexes, it does not rescue fission defects as well as Mdv1 alone. Each domain of Caf4 and Mdv1 has specific functions in forming fission complexes (Cerveny et al., 2001; Griffin et al., 2005; Mozdy et al., 2000; Tieu and Nunnari, 2000). As noted previously, the NTE and beta-propeller domains of Caf4 and Mdv1 bridge the interaction between Fis1 and Dnm1. The CC domain of Mdv1 is required for Mdv1 dimerization, which in turn stabilizes the Fis1-Mdv1 scaffold and positions the beta-propeller domains for Dnm1 dimer binding (Koirala et al., 2010).

It is not clear which Caf4 domain(s) contributes to the difference in fission activity relative to Mdv1. To test this, I expressed a series of chimeric proteins that systematically exchanged domains of Mdv1 and Caf4 in adaptor null cells (*caf4*Δ *mdv1*Δ). As shown in Figure 4.1, Mdv1 chimeras containing one Caf4 domain were able to rescue mitochondrial morphology as well as (but not better than) WT Mdv1 in adaptor null cells. By contrast, none of the Caf4 chimeras rescued fission defects as well as WT Caf4. Thus, there is not a single domain of Mdv1 that improves Caf4 function, and there is not a single domain of Caf4 that makes Mdv1 function worse.

The results of these chimera studies are difficult to interpret for several reasons. First, the amino acid sequences of Caf4 and Mdv1 are only 38% identical (or 57% similar) (Griffin et al., 2005). These amino acid changes may alter critical interactions in the

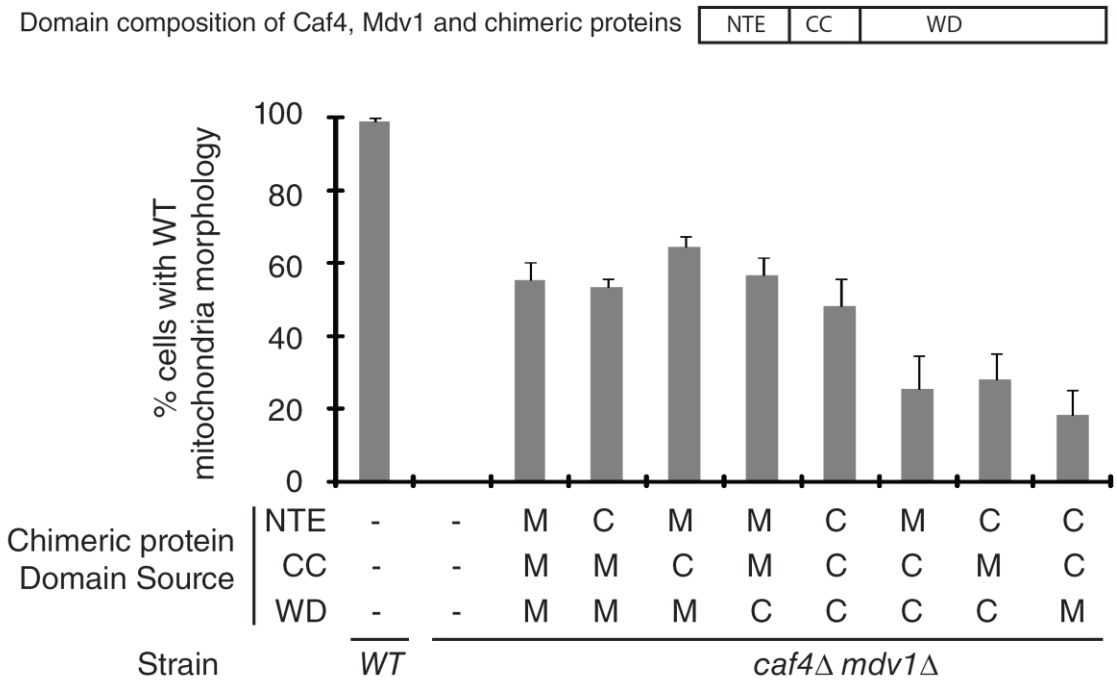

Figure 4.1. Mitochondrial fission function of Caf4/Mdv1 domain chimeras. The amino acid boundaries of the domains in Caf4 and Mdv1 are shown at the top and were determined using a combination of structural information (Zhang and Chan, 2007), the MultiCoil CC prediction program (Wolf et al., 1997) and sequence alignments of the Caf4 and Mdv1 amino acid sequences (Larkin et al., 2007). Bottom, the ability of the indicated chimeric proteins expressed from the *MET25* promoter to rescue mitochondrial morphology defects in the *caf4*Δ *mdv1*Δ strain was quantified (n=100). Bars and error bars are the mean and s.d. of three independent experiments.

protein dimer or interactions with the Fis1 and Dnm1 binding partners. Second, the boundaries chosen for the domain swaps were determined by sequence comparison before structural information was available. Thus, the boundaries chosen for the domain swaps may be incompatible with optimal protein folding and binding partner interactions and may impair function.

Additional functions of Caf4 in yeast

Within the yeast genome, Caf4/Mdv1 is not the only duplicated gene pair. Out of ~6000 genes, there are 450 genes that have paralogs arising from gene duplication (Goffeau et al., 1996; Kellis et al., 2004; Musso et al., 2007). These paralogs are mostly metabolic enzymes, ribosomal proteins, membrane transporters and stress response proteins. Studies from groups focusing on duplicated gene pairs suggest that one gene of a duplicated pair usually undergoes multiple mutations whereas the sequence of the other stays stable (Musso et al., 2007). This is also true of the Caf4/Mdv1 paralogs. Caf4 contains more genetic variation than Mdv1 (Figure 2.5). In many duplicated gene pairs, the functions of the two paralogs are partially overlapping and compensate for each other's absence (Musso et al., 2007). This is consistent with what I observed for Caf4 and Mdv1 (Chapter 2). In addition, the duplicated gene that contains more sequence alterations may sometimes acquire a new function or a specialized function in the same pathway. For example, it has been reported that Caf4, but not Mdv1, is able to orient fission complexes toward the cell cortex (Schauss et al., 2006). During the course of my thesis work, I performed a number of different assays to explore additional specialized functions of Caf4. The results of these studies are presented below. Although I identified

no major differences in Caf4 and Mdv1 function, minor differences suggest that there may be meaningful divergence of Caf4 and Mdv1 function that could be revealed under specialized circumstances.

The requirement for Caf4 under stress

Yeast has the ability to adjust to its environment. Changing growth medium carbon source or including chemicals in the medium can stimulate yeast to utilize necessary or essential pathway(s) for survival. Cells lacking proteins critical for the function in these pathways can slow division or cause growth arrest. To test whether Caf4 is required during different environmental stress conditions, I used serial dilution assays to compare the growth of *WT*, *caf4 null*, *mdv1 null* and *double null* strains in medium supplied with different carbon sources. As shown in Figure 4.2, the growth of strains in all carbon sources tested was very similar. Baudin-baillieu et al. reported that paralogous genes can behave differently even though the absence of either gene does not affect cell growth rate (Baudin-Baillieu et al., 1997). In the same study, they demonstrated that the functionality of the paralog is proportional to the expression level. To test whether this was the case with fission adaptors, protein abundance was quantified in strains expressing genomic HA-tagged Caf4 or Mdv1 in different media for cells grown into log or stationary phase. In log phase cultures, Caf4-HA steady-state abundance varied in each type of medium but was consistently lower than that of Mdv1-HA (Figure 4.3A and 3B). Steady state abundance of the protein in stationary phase cultures exhibited the same trend. I next applied chemicals to stress mitochondrial function (Figure 4.3C-3F). Most of

Figure 4.2. Growth of strains lacking *CAF4, MDV1* or both under different conditions. Ten fold dilutions of the indicated strains were spotted on synthetic solid medium containing the indicated carbon sources or synthetic dextrose medium containing the indicated chemicals or vehicle (DMSO used to solubilize FCCP and CCCP and ethanol used to solubilize antimycin A, oligomycin and rapamycin). Strains were grown for three days at 30°C.

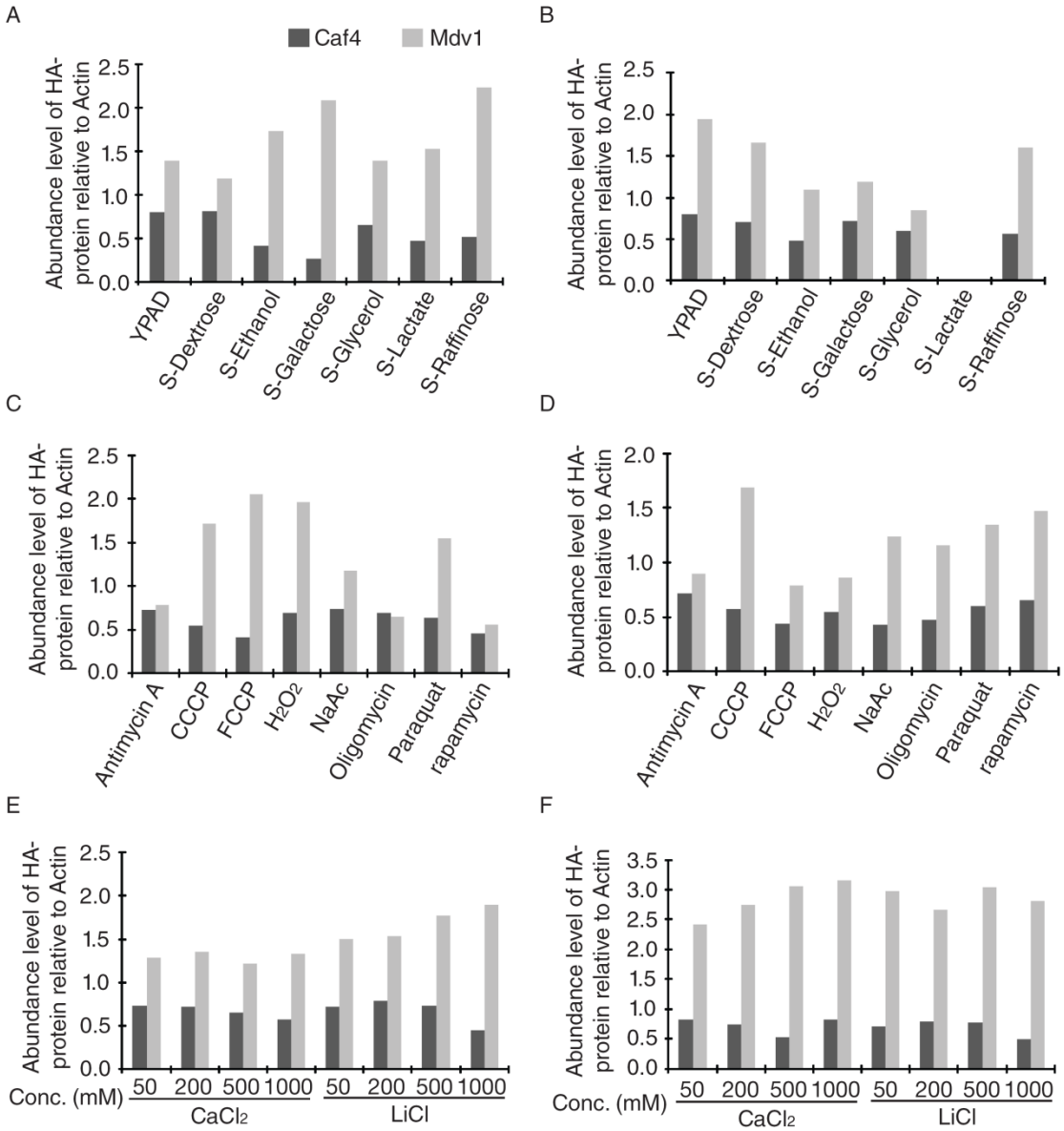

Figure 4.3. HA tagged Caf4 and Mdv1 abundance levels in the indicated conditions. CAF4 or MDV1 is tagged with HA in WT cells. The abundance levels are normalized to Actin. (A and B) HA tagged Caf4 and Mdv1 abundance level in media containing 2% of indicated carbon sources, or 3% of glycerol or ethanol. (C and D) HA tagged Caf4 and Mdv1 abundance level in SD media with indicated chemicals, Antibycin A (10µM), CCCP(10µM), FCCP(10µM), H_2O_2 (3mM), Na actetate (3%), Oligomycin (10µM), Paraquat (500mM), or Rapamycin (200ng/ml). (E and F) HA tagged Caf4 and Mdv1 levels with indicated $CaCl_2$ or LiCl. (A, C, E) HA tagged Caf4 and Mdv1 levels at log phase. (B, D, F) HA tagged Caf4 and Mdv1 levels at stationary phase.

the chemicals disturbed the mitochondrial respiratory chain, while others interfered with mTor or mitochondrial inner membrane potential. Although we observed changes in Mdv1-HA steady-state abundance under some of these conditions, the abundance of Caf4-HA remained relatively similar (Figure 4.3B-D). Despite these changes in protein abundance, the growth of cells lacking *CAF4*, *MDV1* or both was not affected by addition of these chemicals. Mitochondrial morphology in mdv1null, caf4 null or caf null mdv1 null strain was also not affected in the presence of these chemicals (data not shown). These combined results suggest that the presence or absence of Caf4 does not affect cell growth under the conditions tested. In addition, I was not able to identify conditions that increased the steady-state level of Caf4 in a way that could be correlated with increased or decreased cell fitness.

It has also been shown that the mitochondrial fission machinery localizes to and divides peroxisomes in yeast and mammalian cells (Hofmann et al., 2009; Motley et al., 2008). To determine whether loss of *CAF4* had an effect on peroxisome fission, peroxisome function was stimulated in *WT*, *caf4 null*, *mdv1 null* and *double null* strains by growing in oleate containing medium. As expected for this poor carbon source, all the strains grew slowly but no dramatic difference in growth rate was observed between strains (Figure 4.4). Moreover, fluorescent-labeling studies showed that mitochondrial and peroxisomal morphology in all three null strains was similar to WT during the time course.

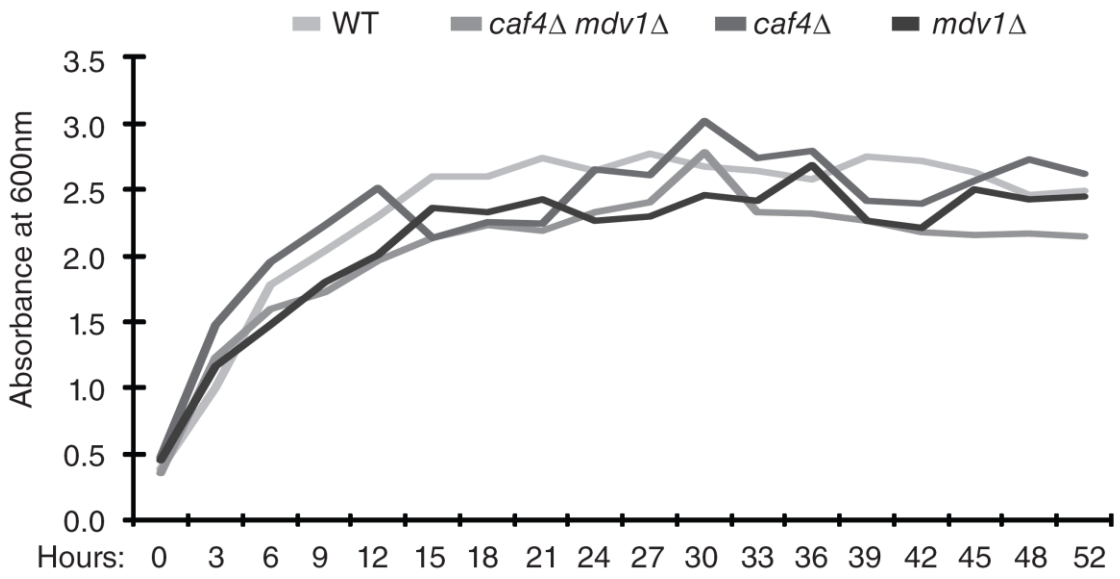

Figure 4.4. Growth curve of indicated strains grow comparable to *WT* in oleate containing medium. Strains were back diluted to 0.5 OD/ml from SD overnight culture to synthetic dextrose containg 0.1% oleic acid. Cell density of each strain was measured at indicated timepoints.

The effect of Caf4 loss on yeast fitness

A study by Gorsich et al. revealed that mitochondrial fission is important during yeast sporulation, since fission mutants failed to distribute mitochondria evenly into all four spores (Gorsich and Shaw, 2004). Spores that failed to inherit a mitochondrial compartment were unable to germinate. This finding established that mitochondrial fission is important for yeast fitness, since sporulation is an essential part of the yeast life cycle in the wild. Since *CAF4* was not analyzed in this study, I asked whether loss of *CAF4* affected sporulation efficiency and mitochondrial distribution during sporulation. *WT, caf4 null, mdv1 null* and *caf4 null mdv1 null* diploids were sporulated in liquid cultures and the number of asci with four, three or two spores was scored. In strains lacking *MDV1* or both of the adaptors, production of four-spored asci was reduced from 35% in WT to 21% (mdv1 null) and 26% (caf4 null mdv1 null) of the population, respectively (Figure 4.5). On the other hand, removing *CAF4* from the diploid genome did not seem to change the overall sporulation efficiency (34 % four spored asci, caf4 null) compared to WT (35%). Interestingly, the number of four-spored asci containing GFP-labeled mitochondria in all four tetrads is slightly different. In WT tetrads, ~69% of four-spored asci contained mitochondria in all four spores. By contrast, when Caf4 is the only adaptor (mdv1 null), there were actually more four-spored asci with mitochondria in all four spores (77%). This percentage decreased to 66% when Mdv1 was the only adaptor present (caf4 null). While the latter result suggests that Caf4 may slightly enhance mitochondrial partitioning during sporulation, further studies are required to test this model.

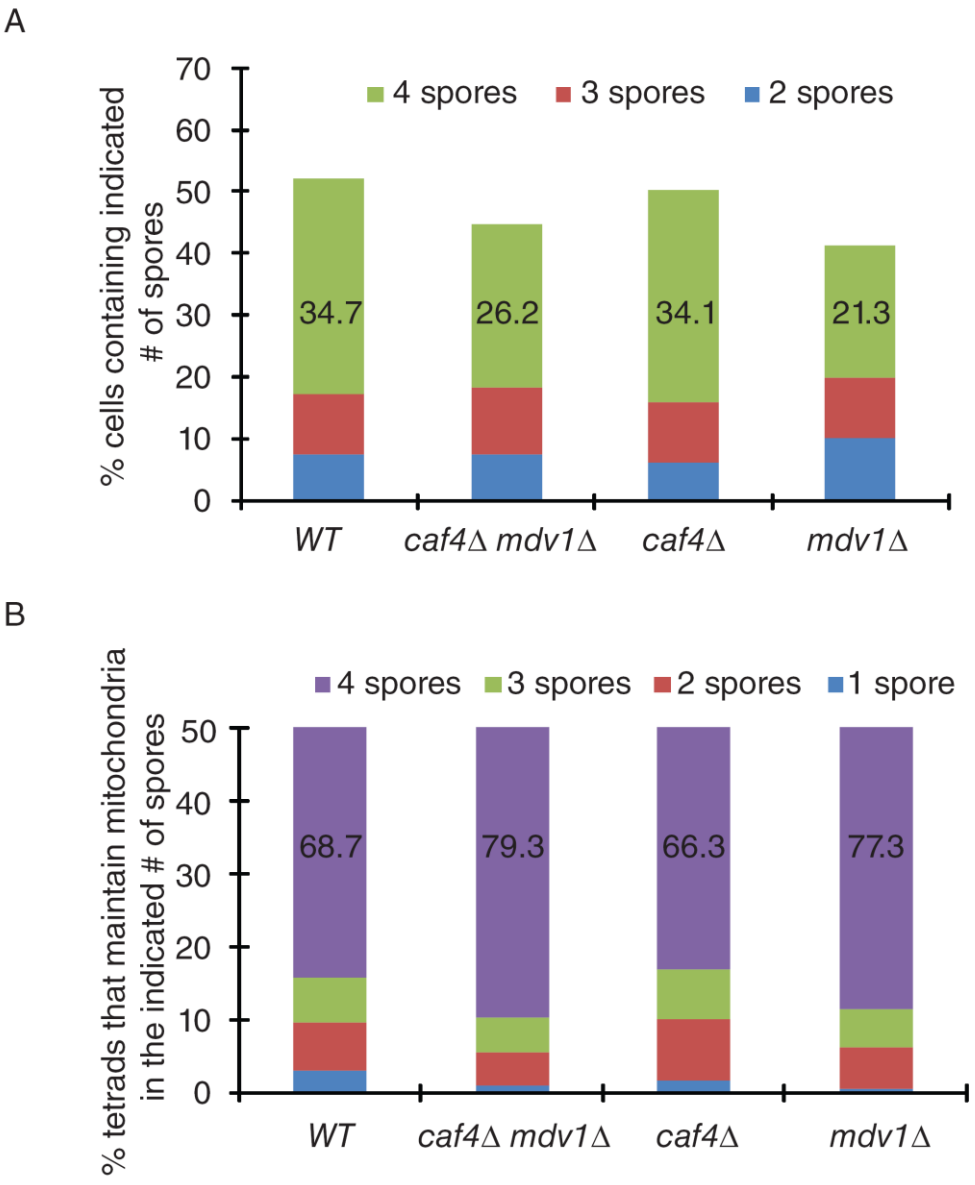

Figure 4.5. Role of Caf4 and Mdv1 in mitochondrial inheritance during sporulation. (A) Quantification of spores per ascus in the indicated strains. n=1600 (WT), 1501 (*caf4*Δ *mdv1*Δ) and 1500 (*caf4*Δ or *mdv1*Δ). (B) Quantification of mitochondrial inheritance by spores in the indicated strains. n=100. Bars represent the mean of the three independent experiments.

I also carried out a head-to-head competition study to ask whether the loss of *CAF4* lowered the fitness of yeast relative to WT. To test this, the genomic *CAF4* coding region was replaced by the *URA3* selectable marker to create *caf4::URA3*. Equal amounts of *caf4::URA3* cells were mixed with an isogenic WT strain (containing an intact *CAF4* gene and a *URA3* gene at a separate locus). With regular dilution to keep cells healthy and in log phase growth, the culture was sampled every two days. The amount of eachstrain was measured by PCR amplification at the *CAF4* locus. Over time, the strain that holds the fitness advantage (grows faster) will become the dominant strain in the culture. As shown in Figure 4.6C, I did not observe a dramatic change in the ratio of the two strains in the culture over a 15-day period of continuous culture. Based on these data, it is unlikely that *CAF4* provides a significant fitness advantage to yeast grown under these conditions.

Mammalian fission adaptors

The lack of obvious Caf4 and Mdv1 homologs in mammals initially led some researchers to suggest that Drp1 bound directly to Fis1 on the membrane in this system. However, others believed this scenario was unlikely, given the fact that Fis1 and Drp1 did not appear to interact directly using any of the available assays. The recent discovery of Mff and MiD49/MiD51 resolves this debate. These adaptors independently bind Drp1 and contain a transmembrane domain, which enables them to be anchored to the outer mitochondrial membrane without Fis1 (Otera et al., 2010; Palmer et al., 2011; Zhao et al., 2011). Interestingly, in yeast, Fis1 is only needed to direct Caf4/Mdv1 and Dnm1 to the mitochondrial membrane (Chapter 3). When Mdv1 is artificially embedded in the outer

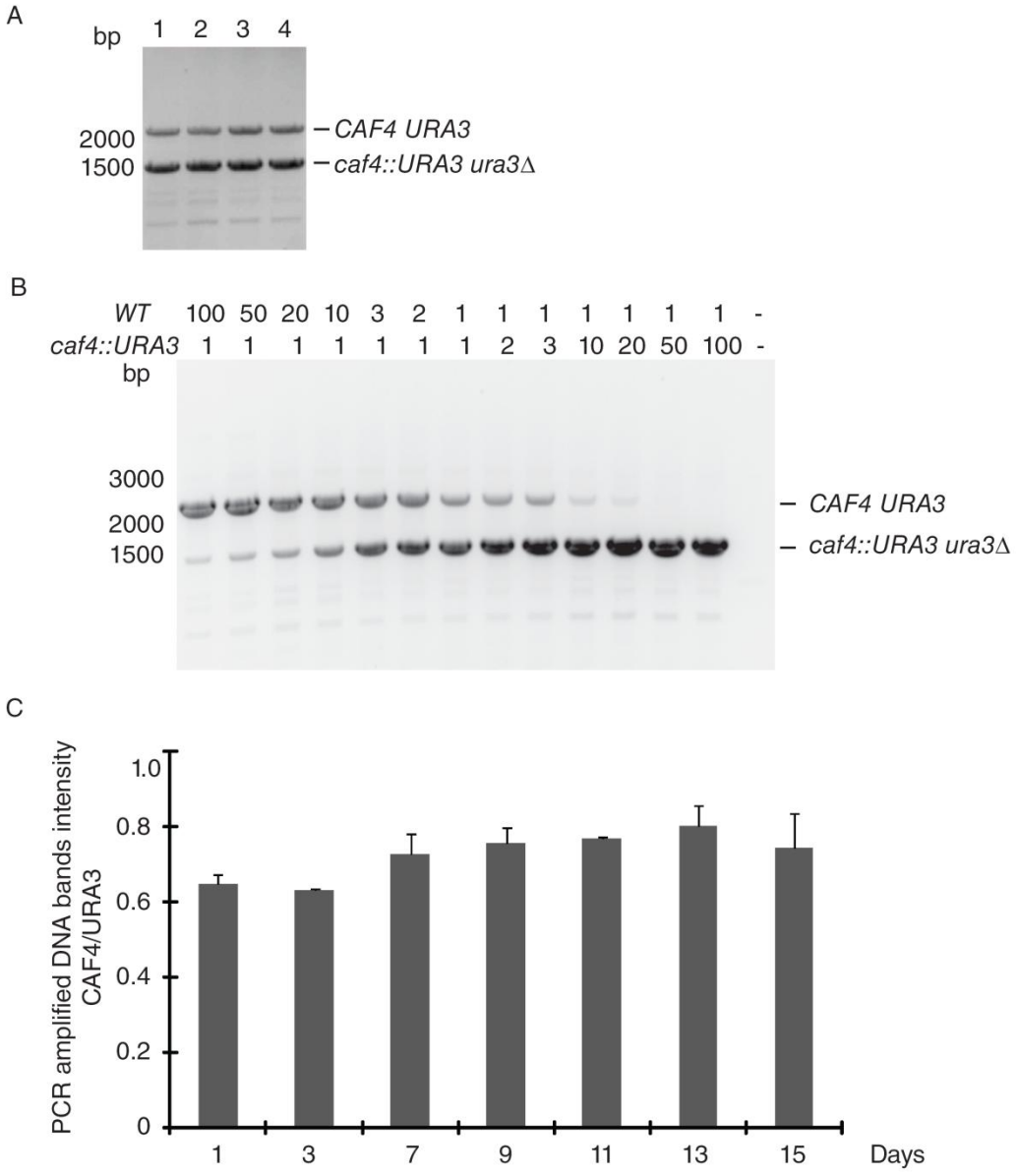

Figure 4.6. Competition between isogenic *CAF4* and *caf4*Δ strains in liquid culture. (A) PCR amplification of quadruplicate genomic samples of 1:1 *CAF4 URA3* and *caf4::URA3 ura3*Δ mixed cultures. The intensities of DNA fragment bands are comparable across samples. (B) PCR amplification of genomic samples from *CAF4 URA3* and *caf4::URA3 ura3*Δ mixed cultures. The ratios of the mixed cultures are indicated. Both CAF4 and URA3 band intensities correspond to the mixed culture ratio. (C) PCR amplification at the *CAF4* locus followed by densitometry was used to calculate the fraction of each strain (*CAF4*/*URA3*) in a mixed culture grown as described in supplemental materials and methods for 15 days. Bars and error bars are the mean and s.d. of three independent experiments.

membrane, mitochondrial fission can occur in the absence of Fis1. In this respect, mitochondrial fission in yeast and humans is more similar than we previously appreciated. The fact that Fis1 has been conserved during evolution suggests that it does have some important cellular or tissue-specific function that has not yet been discovered.

The role of MiD51/Mief1 remains controversial. Zhao et al. reported that MiD51 recruits Drp1 to mitochondria but inhibit Drp1 function in fission, while Palmer et al. reported that MiD51, as well as MiD49, promote mitochondrial fission (Palmer et al., 2011; Zhao et al., 2011). The time-lapse imaging studies and mitochondrial morphology quantification results shown in Chapter 3 of this thesis support the model that MiD49 and MiD51 both facilitate fission. It is therefore possible that these mammalian fission adaptors function similarly to yeast fission adaptor protein Mdv1. Lackner et al. reported that Mdv1 stimulate Dnm1 self-assembly and, as a consequence, indirectly stimulates Dnm1 GTP hydrolysis (Lackner and Nunnari, 2009). However, TEM analysis did not reveal an effect of Mdv1 on Dnm1 assembly. By contrast, the studies in Chapter 3 indicate that the mammalian MiD49 adaptor only modestly stimulated Drp1 GTP hydrolysis. Instead, coassembly of MiD51 with Drp1 decreases the polymer diameter and perhaps the basic structure of the Drp1 polymer formed.

Maintenance of yeast mitochondrial morphology requires a balance between fission and fusion (Okamoto and Shaw, 2005). Prior to our studies, it was not known whether this coordination required direct communication between the fission and fusion molecules of a particular organism. Surprisingly, this does not appear to be the case. When the yeast fission machinery is replaced by the mammalian fission machinery, fission and fusion remain balanced. As in WT yeast cells, time-lapse studies showed that

new fission events generated tips that quickly fused with nearby tubules shortly after fission. If active mechanisms exist to coordinate fission and fusion in yeast, they do not appear to distinguish between the yeast and mammalian fission components.

Adaptors in yeast and mammalian mitochondrial fission: Open questions

In yeast, the exact role of Caf4 is still not clear. In a proteasome study, a strain lacking Caf4 but expressing a temperature-sensitive form of a proteasomal protein (Rpn11) grown in oleate-containing medium exhibited severe growth abnormalities including giant cell size, elongated cell shape and multiple buds (Hofmann et al., 2009). If Mdv1 rather than Caf4 is absent in this strain background, these phenotypes are not observed. This result, while puzzling, suggests that Caf4 and Mdv1 are not identical, and that there may be additional functions of Caf4 to be discovered.

Unlike classical dynamin, the mitochondrial dynamin-related proteins Dnm1 and Drp1 are not able to directly contact the lipids in the membrane that they remodel. Instead, they require the assistance of adaptor proteins. The adaptor proteins not only bind and target Dnm1 and Drp1 to the membrane, they also affect the activity and assembly of these GTPases. In the case of yeast Mdv1, the adaptor may stimulate Dnm1 self-assembly and (indirectly) GTP hydrolysis but does not have an effect on the structure of Dnm1 assemblies. By contrast, MiD49 likely stimulates Drp1 assembly once it reaches the membrane but has little effect on Drp1 GTP hydrolysis activity. Importantly, MiD49 is the first adaptor shown to alter the structure of the assemblies formed by a dynamin-related protein. In the future, it will be important to determine whether these copolymers

assemble on and constrict liposomes. In addition, solution of the cryo-EM structure will answer important questions about the potential effects of MiD49 and other adaptors on lipid remodeling and Drp1-mediated GTP hydrolysis. Finally, the effects of Mff and MiD51 on Drp1 assembly and lipid remodeling must also be tested.

The additional experimental data discussed in this chapter were performed as described in Appendix.

References

Baudin-Baillieu, A., Tollervey, D., Cullin, C., and Lacroute, F. (1997). Functional analysis of Rrp7p, an essential yeast protein involved in pre-rRNA processing and ribosome assembly. Mol Cell Biol *17*, 5023-5032.

Cerveny, K. L., McCaffery, J. M., and Jensen, R. E. (2001). Division of mitochondria requires a novel DMN1-interacting protein, Net2p. Mol Biol Cell *12*, 309-321.

Goffeau, A., Barrell, B. G., Bussey, H., Davis, R. W., Dujon, B., Feldmann, H., Galibert, F., Hoheisel, J. D., Jacq, C., Johnston, M., *et al.* (1996). Life with 6000 genes. Science *274*, 546, 563-547.

Gorsich, S. W., and Shaw, J. M. (2004). Importance of mitochondrial dynamics during meiosis and sporulation. Mol Biol Cell *15*, 4369-4381.

Griffin, E. E., Graumann, J., and Chan, D. C. (2005). The WD40 protein Caf4p is a component of the mitochondrial fission machinery and recruits Dnm1p to mitochondria. J Cell Biol *170*, 237-248.

Hofmann, L., Saunier, R., Cossard, R., Esposito, M., Rinaldi, T., and Delahodde, A. (2009). A nonproteolytic proteasome activity controls organelle fission in yeast. J Cell Sci *122*, 3673-3683.

Kellis, M., Birren, B. W., and Lander, E. S. (2004). Proof and evolutionary analysis of ancient genome duplication in the yeast Saccharomyces cerevisiae. Nature *428*, 617-624.

Koirala, S., Bui, H. T., Schubert, H. L., Eckert, D. M., Hill, C. P., Kay, M. S., and Shaw, J. M. (2010). Molecular architecture of a dynamin adaptor: implications for assembly of mitochondrial fission complexes. J Cell Biol *191*, 1127-1139.

Lackner, L. L., and Nunnari, J. M. (2009). The molecular mechanism and cellular functions of mitochondrial division. Biochim Biophys Acta *1792*, 1138-1144.

Larkin, M. A., Blackshields, G., Brown, N. P., Chenna, R., McGettigan, P. A., McWilliam, H., Valentin, F., Wallace, I. M., Wilm, A., Lopez, R., *et al.* (2007). Clustal W and Clustal X version 2.0. Bioinformatics *23*, 2947-2948.

Motley, A. M., Ward, G. P., and Hettema, E. H. (2008). Dnm1p-dependent peroxisome fission requires Caf4p, Mdv1p and Fis1p. J Cell Sci *121*, 1633-1640.

Mozdy, A. D., McCaffery, J. M., and Shaw, J. M. (2000). Dnm1p GTPase-mediated mitochondrial fission is a multi-step process requiring the novel integral membrane component Fis1p. J Cell Biol *151*, 367-380.

Musso, G., Zhang, Z., and Emili, A. (2007). Retention of protein complex membership by ancient duplicated gene products in budding yeast. Trends Genet *23*, 266-269.

Okamoto, K., and Shaw, J. M. (2005). Mitochondrial morphology and dynamics in yeast and multicellular eukaryotes. Annu Rev Genet *39*, 503-536.

Otera, H., Wang, C., Cleland, M. M., Setoguchi, K., Yokota, S., Youle, R. J., and Mihara, K. (2010). Mff is an essential factor for mitochondrial recruitment of Drp1 during mitochondrial fission in mammalian cells. J Cell Biol *191*, 1141-1158.

Palmer, C. S., Osellame, L. D., Laine, D., Koutsopoulos, O. S., Frazier, A. E., and Ryan, M. T. (2011). MiD49 and MiD51, new components of the mitochondrial fission machinery. EMBO Rep *12*, 565-573.

Schauss, A. C., Bewersdorf, J., and Jakobs, S. (2006). Fis1p and Caf4p, but not Mdv1p, determine the polar localization of Dnm1p clusters on the mitochondrial surface. J Cell Sci *119*, 3098-3106.

Tieu, Q., and Nunnari, J. (2000). Mdv1p is a WD repeat protein that interacts with the dynamin-related GTPase, Dnm1p, to trigger mitochondrial division. J Cell Biol *151*, 353-366.

Wolf, E., Kim, P. S., and Berger, B. (1997). MultiCoil: a program for predicting two- and three-stranded coiled coils. Protein Sci *6*, 1179-1189.

Zhang, Y., and Chan, D. C. (2007). Structural basis for recruitment of mitochondrial fission complexes by Fis1. Proc Natl Acad Sci U S A *104*, 18526-18530.

Zhao, J., Liu, T., Jin, S., Wang, X., Qu, M., Uhlen, P., Tomilin, N., Shupliakov, O., Lendahl, U., and Nister, M. (2011). Human MIEF1 recruits Drp1 to mitochondrial

outer membranes and promotes mitochondrial fusion rather than fission. Embo J *30*, 2762-2778.

APPENDIX

Materials and methods

Strains and plasmids

Yeast strains and plasmids used in this study are listed in supplementary material Table A.1 and A.2. Unless noted in the figure legend, standard rich or synthetic dropout media were used for growth, transformation and genetic manipulation of *S. cerevisiae* (Guthrie and Fink, 2002) and *E. coli* (Maniatis et al., 1982).

Plasmid pRS414-*GPD-mt-ffRFP* (Karren et al., 2005; Koirala et al., 2010) was used to visualize and score mitochondrial morphology in the chimera and sporulation studies. pRS416-*MET25-MDV1*^{NTE}*-CAF4*$^{CC+WD}$ and pRS416-*MET25-CAF4*$^{NTE+CC}$*-MDV1*^{WD} were constructed as follows. *CAF4* was PCR amplified with primers containing terminal BamHI and EagI sites and cloned between the same sites in pRS416-*MET25* to generate pRS416-*MET25-CAF4*. pRS416-*MET25-CAF4* was digested with EcoRV and XbaI (to produce a gap within the *CAF4*^{NTE}) or XhoI and SalI (to produce a gap within the *CAF4*^{WD}). Fragments containing *MDV1*$^{NTE\ (1\text{-}690NT)}$ and *MDV1*$^{WD(877\text{-}2145NT)}$ were PCR amplified and the DNA fragments were co-transformed with EcoRV and XbaI digested pRS416-*MET25-CAF4* or XhoI and SalI digested pRS416-*MET25-CAF4* to generate pRS416-*MET25-MDV1*^{NTE}*-CAF4*$^{CC+WD}$ and pRS416-*MET25-CAF4*$^{NTE+CC}$*-MDV1*^{WD}, respectively, by gap repair. pRS416-*MET25-CAF4*^{NTE}*-MDV1*^{CC}*-CAF4*^{NTE} was constructed by altering the *CAF4* sequence T^{754}TGGAA^{759} in pRS416-*MET25-CAF4* to C^{754}TCGAG^{759} by site-directed mutagenesis. This mutagenesis introduced an XhoI site but did not alter the amino acid sequence of the encoded protein. The resulting construct

Table A.1 Plasmids used in additional yeast adaptors study

Strain ID	Plasmid	Protein Expressed	Reference
B494	pRS416-*MET25*	None	ATCC 87324
B1642	pRS414-*GPD-mt-ffRFP*	*N. crassa* ATP9(1-69) + fast folding DsRed (RFP)	Karren et al., 2005
B2053	pRS416-*MET25-MDV1*	Mdv1	Karren et al., 2005
B2212	pRS416-*MET25-CAF4*	Caf4	This Study
B3174	pRS416-*MET25-CAF4*^{NTE}-*MDV1*$^{CC+WD}$	Caf4^{NTE}-Mdv1^{CC+WD}	This Study
B3175	pRS416-*MET25-MDV1*^{NTE}-*CAF4*^{CC}-*MDV1*^{NTE}	Mdv1^{NTE}-Caf4^{CC}-Mdv1^{NTE}	This Study
B3176	pRS416-*MET25-MDV1*$^{NTE+CC}$-*CAF4*^{WD}	Mdv1^{NTE+CC}-Caf4^{WD}	This Study
B3177	pRS416-*MET25-MDV1*^{NTE}-*CAF4*$^{CC+WD}$	Mdv1^{NTE}-Caf4^{CC+WD}	This Study
B3178	pRS416-*MET25-CAF4*^{NTE}-*MDV1*^{CC}-*CAF4*^{NTE}	Caf4^{NTE}-Mdv1^{CC}-Caf4^{NTE}	This Study
B3179	pRS416-*MET25-CAF4*$^{NTE+CC}$-*MDV1*^{WD}	Caf4^{NTE+CC}-Mdv1^{WD}	This Study

Table A.2 Yeast strains used in additional yeast adaptor study

Strain ID	Mating type	Genotype	Reference
JSY5740	*MAT**a***	*ura3-52, leu2Δ1, his3Δ200, trp1Δ63*	Koirala et al., 2010
JSY5750	*MATα*	*ura3-52, leu2Δ1, his3Δ200, trp1Δ63*	This Study
JSY8612	*MAT**a***	*ura3-52, leu2Δ1, his3Δ200, trp1Δ63, caf4::KanMx, mdv1::HIS3*	Koirala et al., 2010
JSY8613	*MATα*	*ura3-52, leu2Δ1, his3Δ200, trp1Δ63, mdv1::HIS3*	This Study
JSY8614	*MAT**a***	*ura3-52, leu2Δ1, his3Δ200, trp1Δ63, caf4::KanMx*	This Study
JSY8615	*MATα*	*ura3-52, leu2Δ1, his3Δ200, trp1Δ63, lys2Δ202, caf4::KanMx*	This Study
JSY8616	*MAT**a***	*ura3-52, leu2Δ1, his3Δ200, trp1Δ63, mdv1::HIS3*	This Study
JSY8618	*MATα*	*ura3-52, leu2Δ1, his3Δ200, trp1Δ63, caf4::KanMx, mdv1::HIS3*	This Study
JSY9642	*MATα*	*ura3-0 or 52, leu2Δ0 or 1, his3Δ1 or 200, trp1Δ63, mdv1::MDV1-3xHA/pRS406 +URA3*	This Study
JSY9644	*MATα*	*ura3-0 or 52, leu2Δ0 or 1, his3Δ1 or 200, trp1Δ63, caf4::CAF4-3xHA/pRS406 +URA3*	This Study
JSY9870	*MATα*	*ura3-52, leu2Δ1, his3Δ200, trp1Δ63, lys2Δ200, caf4::URA3*	This Study
JSY9938	*MATα*	*URA3, leu2Δ1, his3Δ200, trp1Δ63, lys2Δ200, CAF4*	This Study

was digested with XhoI and XbaI to remove *CAF4*$^{CC(517\text{-}759NT)}$, and PCR amplified *MDV1*$^{CC(691\text{-}876NT)}$ was cloned between these sites. To construct pRS416-*MET25*-*CAF4*^{NTE}-*MDV1*$^{CC+WD}$ and pRS416-*MET25*-*MDV1*$^{NTE+CC}$-*CAF4*^{WD}, *MDV1* was PCR amplified with primers containing terminal BamHI and SalI sites and cloned between the same sites of pRS416-*MET25*. pRS416-*MET25*-*MDV1* was digested with BamHI and XmaI (to generate a gap within the *MDV1*^{NTE}) or XhoI and SalI (to generate a gap within the MDV1^{WD}) and cotransformed with PCR amplified *CAF4*$^{NTE\ (1\text{-}516NT)}$ and *CAF4*$^{WD40\ (760\text{-}1980NT)}$ into JSY8612 to generate pRS416-*MET25*-*CAF4*^{NTE}-*MDV1*$^{CC+WD}$ and pRS416-*MET25*-*MDV1*$^{NTE+CC}$-*CAF4*^{WD}, respectively, by gap repair. pRS416-*MET25*-*MDV1*^{NTE}-*CAF4*^{CC}-*MDV1*^{NTE} was constructed by digesting pRS416-*MET25*-*MDV1* with XmaI and XhoI to remove *MDV1*$^{CC(691\text{-}876NT)}$. *CAF4*$^{CC(517\text{-}759NT)}$ was then PCR amplified and cloned into the XmaI and XhoI sites.

Western blots and protein quantification

Protein expression and abundance was analyzed in yeast whole cell extracts prepared by the alkaline extraction method (Kushnirov, 2000). Overnight cultures of JSY9642 and JSY9644 were harvested, washed and diluted in synthetic medium containing one of the following carbon source: 2% Dextrose, 3% Ethanol, 2% Galactose, 3% Glycerol, 2% Lactate (Na^+) or 2% Raffinose. The two cultures were also harvested, washed and diluted in SD media contain one of the following chemicals: Antimycin A (10µM, Alfa Aesar), CCCP (10µM, Tocris Cookson), FCCP (10µM, Tocris Cookson), H_2O_2 (3mM, Arcos), NaAc (3%, Mallinckrodt), Oligomycin (10µM, EMD Millipore), Paraquat (500mM, EMD Millipore), rapamycin (200ng/ml, EMD Millipore), $CaCl_2$ (50,

200, 500 and 1000mM, Mallinckrodt) and LiCl (50, 200, 500 and 1000mM, Mallinckrodt). 0.25 OD_{600} equivalents of extract was separated by SDS-PAGE and analyzed by Western blotting using the following primary antibodies: anti-yeast actin (1:5000, J. Cooper, Washington University Saint Louis) and anti-HA (1:2000, Core facility, University of Utah). Primary antibodies were detected using fluorescent secondary anti-goat or anti-mouse IRDye 800 (LiCor). Fluorescent signals were quantified using an Odyssey scanner and Odyssey 3.0 analysis software (LiCor). In Figure 4.3, anti-HA signals were normalized to anti-actin signals.

Growth assays

For growth curves measured in oleate medium, overnight cultures of JSY5740 *CAF4 MDV1*, JSY8612 *caf4*Δ *mdv1*Δ, JSY8614 *caf4*Δ *MDV1* and JSY8616 *CAF4* *mdv1*Δ were diluted to ~0.5 OD in oleate medium (YNB 0.67%, $(NH4)_2SO_4$ 1.97%, glucose 0.1%, tween40 0.05%, yeast extract 0.1% oleate acid 0.1% and pH 6.0). Cell densities (absorbance at 600 nm) were measured over the indicated time course.

For serial dilutions, strains JSY5740, JSY8612, JSY8614 and JSY8616 were grown in SD medium to early log phase (OD_{600} 0.5–1.0), pelleted, and resuspended at 0.5 OD_{600}. Aliquots of 1:10 serial dilutions were spotted onto synthetic media with the indicated carbon sources or SD plates containing one of the following chemicals, DMSO (28, 56, 112, 280 and 560 ppm, Mallinckrodt), Antimycin A (0.5, 1, 5, 10µM, Sigma Aldrich), CCCP (1, 5, 10µM, Sigma Aldrich), FCCP (1, 5, 10µM, Sigma Aldrich), Oligomycin (0.5, 1, 5, 10µM, Sigma Aldrich) and Rapamycin (20ng/ml, Sigma Aldrich). The strains were grown for 3 days at 30^{o}C.

For the head-to-head competition assays, overnight cultures of JSY9824 and JSY8667 were mixed (final concentration 0.02 OD_{600} units of each strain) in SD medium and grow at 30^{o}C with agitation. 4.0 OD_{600} cell equivalents from the mixed culture was harvested every two days followed by dilution of the culture to 0.02 OD_{600} in fresh medium. The genomic samples were extracted from cell pellets using a MasterPure^{TM} yeast DNA purification kit (Epicentre Biotechnologies). Genes at the *CAF4* locus from both strains were PCR amplified and separated by DNA agarose electrophoresis. The abundance of DNA fragments specific for each strain at this locus were imaged and analyzed using a ChemiDoc™ MP System and Quantity One V4.6.6 software (Bio-Rad). The data are represented as the average and SD of three independent experiments.

Quantification of mitochondrial morphology

Mitochondrial morphology was scored in JSY8612 *caf4*Δ *mdv1*Δ cells expressing fast folding matrix-targeted red fluorescent protein (mt-ffRFP) and the indicated Caf4 or Mdv1 constructs. Strains were grown at 30°C in selective dextrose synthetic medium and scored in log phase (0.2-0.8 OD_{600}). Mitochondrial phenotypes were scored in 100 cells as described previously (Koirala et al., 2010), and data are represented as the average and SD of three independent experiments.

Quantification of sporulation and mitochondrial distribution in spores

Overnight cultures of WT and fission mutant diploid strains, JSY5740 x JSY5750 (WT/WT), JSY8612 x JSY8618 (*caf4*Δ *mdv1*Δ/*caf4*Δ *mdv1*Δ), JSY8614 x JSY8615

(*caf4*Δ *MDV1*/*caf4*Δ *MDV1*) and JSY8616 x JSY8617 (*CAF4 mdv1*Δ/*CAF4 mdv1*Δ), expressing fast folding matrix-targeted red fluorescent protein (mt-ffRFP) were harvested, washed three times and diluted to ~0.2 OD_{600} in sporulation medium (1% KAc, 20% raffinose, 10μm of Adenine, arginine, histidine, isolucine, leucine, lysine, methionine, phenylalanine, threonine, uracil, and valine). The cultures were incubated at 25^{o}C for 14 days with agitation after which sporulation efficiency and mitochondrial distribution were scored.

References

Guthrie, C., and Fink, G. (2002). Guide to Yeast Genetics and Molecular Biology, Vol 194).

Karren, M. A., Coonrod, E. M., Anderson, T. K., and Shaw, J. M. (2005). The role of Fis1p-Mdv1p interactions in mitochondrial fission complex assembly. J Cell Biol *171*, 291-301.

Koirala, S., Bui, H. T., Schubert, H. L., Eckert, D. M., Hill, C. P., Kay, M. S., and Shaw, J. M. (2010). Molecular architecture of a dynamin adaptor: implications for assembly of mitochondrial fission complexes. J Cell Biol *191*, 1127-1139.

Kushnirov, V. V. (2000). Rapid and reliable protein extraction from yeast. Yeast *16*, 857-860.

Maniatis, T., Fritsch, E. F., and Sambrook, J. (1982). Molecular Cloning: A Laboratory Manual (Cold Spring Harbor, NY: Cold Spring Harbor Laboratory Press).